

IMAGE CODING AND TRANSMISSION
IN WIRELESS MULTIMEDIA SENSOR NETWORKS

by
Kerem Irgan

Submitted to the Institute of Graduate Studies in
Science and Engineering in partial fulfillment of
the requirements for the degree of
Master of Science
in
Computer Engineering

Yeditepe University
2010

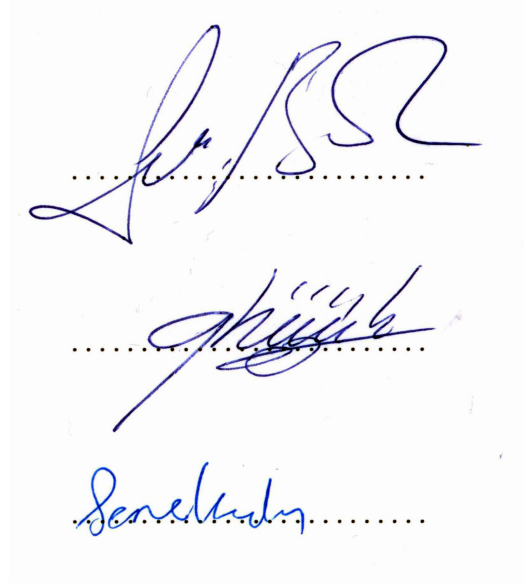
IMAGE CODING AND TRANSMISSION
IN WIRELESS MULTIMEDIA SENSOR NETWORKS

APPROVED BY:

Prof. Dr. Şebnem BAYDERE
(Thesis Supervisor)

Assist. Prof. Dr. Gürhan KÜÇÜK

Assist. Prof. Dr. Sanem KABADAYI
(Istanbul Technical University)



The image shows three handwritten signatures in blue ink, each positioned above a horizontal dotted line. The top signature is the most stylized, the middle one is more legible, and the bottom one is written in a cursive style.

DATE OF APPROVAL:/..../2010

ACKNOWLEDGEMENTS

I wish to express my sincere gratitude to Prof. Dr. Şebnem Baydere for her excellent mentorship. Her felicitous steering and wisdom make me find the way whenever I have been lost. It was a great opportunity and honor for me to work with her.

I would like to thank Assoc. Prof. Dr. Cem Ünsalan, Dr. Mustafa Mutluođlu and Pınar Sarısaray for their ideas and helps in several parts of this study.

I would also like to thank Assist. Prof. Dr. Sanem Kabadayı and Assist. Prof. Dr. Gürhan Küçük for serving on my thesis committee and their valuable advises and corrections to make this thesis better.

I am indebted to my colleagues Bilgin Koşucu and Okan Türkeş for standing by me whenever i need, and Nazlı Nakeeb for her encouragement. I also thank to Özgür Altun for being “wired” to Matlab for me.

I am also grateful to my parents and sisters for their support and encouragement through all of my life. I wish to thank my working partner Ayhan Selmo for making this study possible by taking all the load and responsibility of our business. Last, but certainly not least, I wish to convey my cordial gratitude to my wife for her patience and encouragement during my M.Sc. study, and becoming a great mother.

To my precious children, Oğuz and Sezgi.

ABSTRACT

IMAGE CODING AND TRANSMISSION IN WIRELESS MULTIMEDIA SENSOR NETWORKS

Multimedia data is a versatile tool for any kind of application which aims to collect and extract information from a phenomenon. It can be ubiquitously available by the utilization of Wireless Sensor Networks (WSNs). Wireless Multimedia Sensor Networks (WMSNs) have come into existence as a result of this idea. However, handling this combination is a challenging task.

This thesis focuses on image coding and transmission in WMSNs. Existing coding and transmission schemes are examined and considering the requirements of multimedia transmission together with the constraints of WSN, several contributions are made: A priority based encoding scheme for self-adaptive prioritization of image partitions is proposed, with novel priority measures. The superior performance of this scheme, especially in terms of resources required for it, is shown via experiments and sensor node implementations. A real testbed environment has been set up to observe the effect of channel conditions on transmitted images. By utilizing this testbed, the robustness of an existing coding technique, i.e. error concealment is also validated with over 30,000 transmissions. Hybrid usage of these two schemes is also examined, and a considerable performance gain is achieved. Moreover, an image transmission framework (ITF) is suggested to be coupled with the priority based encoding scheme. ITF is based on bursty and regulated transmission of large image partitions with prioritization via multiple paths. With these attributes, ITF is a promising candidate to satisfy Quality of Service requirements of multimedia applications.

ÖZET

KABLOSUZ ÇOKLU ORTAM DUYARGA AĞLARDA İMGE KODLAMASI VE İLETİMİ

Çokluortam verileri, olgular hakkında bilgi toplamayı amaçlayan her tür uygulama tarafından kullanılabilir çok yönlü ve çok amaçlı bir araçtır. Kablosuz Duyarga Ağlar'ın (KDA) kullanımı ile, bu veriler her yerden eşzamanlı ulaşılabilir hale getirilebilir. Kablosuz Çokluortam Duyarga Ağlar (KÇDA) bu fikrin sonucu olarak ortaya çıkmışlardır. Bununla birlikte, bu birleşimi istenilen şekilde yönetmek pek çok zorluğu da beraberinde getirmektedir.

Bu çalışma KÇDA' da imge kodlaması ve iletimi üzerine yoğunlaşmıştır. Var olan kodlama ve iletim teknikleri incelenmiş, KDA' da çokluortam verilerinin iletim gereksinimleri de göz önüne alınarak birçok katkıda bulunulmuştur: Özgün öncelik ölçüleri kullanan, önceliğe dayalı, özuyarlanan bir kodlama sistemi önerilmiştir. Bu sistemin üstün başarısı, özellikle gereksinim duyulan kaynaklar açısından, deneyler ve duyarga gerçekleştirmeleriyle ortaya konmuştur. Kanal koşullarının iletilen imgeler üzerindeki etkisinin incelenmesi için gerçek bir sına ortamı oluşturulmuştur. Bu sına ortamı üzerinde, var olan bir kodlama tekniğinin (hata gizleme) dayanıklılığı da 30,000 iletim ile doğrulanmıştır. Söz konusu imge gizleme algoritmasının ve bu çalışmada önerilen kodlama sisteminin birlikte kullanılması da incelenmiş ve bu hibrit sistemin dikkate değer performans artışı sağladığı gösterilmiştir. Bunların yanısıra, önceliğe dayalı kodlama sistemi ile birlikte kullanılmak üzere bir İmge İletimi Çerçevesi (İİÇ) de ortaya konmuştur. İİÇ, büyük imge kesimlerinin birçok yoldan öncelikli olarak çoğuşmalı ve kararlı veri iletimi üzerine kuruludur. Bu özellikleri sayesinde İİÇ, çokluortam uygulamalarındaki hizmet niteliği gereksinimlerinin karşılanması için uygun bir aday olarak ileri çıkmaktadır.

TABLE OF CONTENTS

ACKNOWLEDGEMENTS	iv
ABSTRACT	vi
ÖZET	vii
LIST OF FIGURES	x
LIST OF TABLES	xiv
LIST OF SYMBOLS/ABBREVIATIONS	xv
1. INTRODUCTION	1
1.1. PROBLEM DEFINITION	2
1.2. MOTIVATION	4
1.3. CONTRIBUTIONS	5
1.4. ORGANIZATION OF THE THESIS	6
2. RELATED WORK	7
2.1. IMAGE CODING AND COMPRESSION	7
2.2. IMAGE TRANSMISSION	9
2.2.1. Prioritized Transmission	10
2.3. TESTBEDS	11
2.4. IMAGE QUALITY ASSESSMENT	13
2.4.1. The Structural SIMilarity (SSIM) Index	15
2.4.2. Objective Picture Quality Scale (PQS)	16
2.4.3. Peak Signal To Noise Ratio (PSNR)	17
3. IMAGE CODING AND TRANSMISSION	18
3.1. MACRO-BLOCK BASED PRIORITY ENCODING (MBPE)	18
3.1.1. Priority Measures	20
3.1.1.1. Entropy Measure	20
3.1.1.2. Edge Measure	22
3.1.1.3. Reproducibility Measure	22
3.1.1.4. Hybrid Measures	24
3.1.2. Priority Levels And Thresholds	25
3.2. ERROR CONCEALMENT (EC)	27

3.2.1. The EC Algorithm.....	28
3.3. ERROR CONCEALMENT with PRIORITY ENCODING (ECPE).....	29
3.4. IMAGE TRANSMISSION FRAMEWORK.....	30
4. EXPERIMENTS.....	36
4.1. IMAGE QUALITY METRICS.....	36
4.1.1. Object Transmission Rate (OTR).....	36
4.2. MBPE EVALUATION.....	37
4.2.1. System Model.....	37
4.2.2. Methodology.....	40
4.2.3. Performance Analysis.....	46
4.2.3.1. Monte Carlo Simulations.....	46
4.2.3.2. Object Transmission Index.....	46
4.2.3.3. Implementation Cost.....	49
4.2.3.4. JPEG Comparison.....	50
4.2.4. Discussion.....	51
4.3. REAL TESTBED.....	52
4.3.1. System Model.....	52
4.3.2. Methodology.....	54
4.3.3. Testbed Setup.....	57
4.3.3.1. Node Deployment.....	57
4.3.3.2. Transmission Scheme.....	58
4.3.4. Testbed Results and Analysis.....	60
4.3.5. Discussion.....	66
4.4. ECPE EVALUATION.....	66
4.4.1. Methodology.....	66
4.4.2. ECPE Results.....	67
4.4.3. Discussion.....	71
5. CONCLUSION AND FUTURE WORK.....	72
REFERENCES.....	75

LIST OF FIGURES

Figure 2.1.	JPEG compression algorithm	8
Figure 2.2.	Distributed compression of two statistically dependent random processes.	9
Figure 2.3.	Current sensor platforms and cameras	12
Figure 2.4.	A water counter from an example application	13
Figure 2.5.	Usage of RR IQA in a wireless imaging system.....	15
Figure 3.1.	The mountain test image and its 8×8 macro-blocks	19
Figure 3.2.	MBPE system model.....	20
Figure 3.3.	Entropy based measure of macro-blocks in the mountain test image.....	21
Figure 3.4.	Edge based measure of macro-blocks in the mountain test image	22
Figure 3.5.	Reproducibility operation.....	23
Figure 3.6.	Reproducibility based measure of macro-blocks in the mountain test image	24
Figure 3.7.	Delta-entropy operation.....	25
Figure 3.8.	Delta-edge operation	26
Figure 3.9.	Delta-entropy based measure of macro-blocks in the mountain test image	26
Figure 3.10.	Delta-edge based measure of macro-blocks in the mountain test image ...	27

Figure 3.11. Source Node	31
Figure 3.12. Source node algorithm	32
Figure 3.13. State diagram of an image transmission.....	33
Figure 3.14. Router node algorithm	34
Figure 3.15. The illustration of an example transmission	35
Figure 4.1. Comparison of OTR and PSNR values on a test image	38
Figure 4.2. WMSN scenario for border surveillance	39
Figure 4.3. Transmission scheme used in MBPE experiments	40
Figure 4.4. Sample test images used in MBPE experiments	41
Figure 4.5. CDFs with group thresholds and histograms of each measure (Part 1 of 2)	42
Figure 4.6. CDFs with group thresholds and histograms of each measure (Part 2 of 2)	43
Figure 4.7. PPR values for all measures (Part 1 of 2)	44
Figure 4.8. PPR values for all measures (Part 2 of 2)	45
Figure 4.9. OTR values for all measures and corresponding simulations (Part 1 of 2).	47
Figure 4.10. OTR values for all measures and corresponding simulations (Part 2 of 2).	48
Figure 4.11. Testbed WMSN scenario	53

Figure 4.12. An illustration of ECDP	54
Figure 4.13. Testbed software diagram	55
Figure 4.14. Projecting image loss patterns to different images	56
Figure 4.15. Test images used in EC tests	56
Figure 4.16. A view from testbed area	57
Figure 4.17. Node Group 0	58
Figure 4.18. Testbed Diagram	59
Figure 4.19. The result of a one day long test for <i>five</i> hops	59
Figure 4.20. Example results for <i>1,3,5,7 hops</i> tests without using the backchannel	61
Figure 4.21. The result of a <i>1-to-8 hops</i> test using the backchannel	62
Figure 4.22. Scatter plot of PSNR vs. PRR for each scheme including 30,000 transmissions	63
Figure 4.23. The received EC coded images at different PRRs	64
Figure 4.24. PSNR vs. Number of Hops for all schemes.....	65
Figure 4.25. PRR vs. Average LQI	65
Figure 4.26. Operations to compare ECPE with EC	68
Figure 4.27. EC vs. ECPE	68

Figure 4.28. PSNR values for all measures, for EC and ECPE schemes (Part 1 of 2) ... 69

Figure 4.29. PSNR values for all measures, for EC and ECPE schemes (Part 2 of 2) ... 70

LIST OF TABLES

Table 2.1. An overview of the current hardware platforms	11
Table 2.2. An overview of the current testbeds	11
Table 4.1. Object transmission index values	49
Table 4.2. Implementation costs of the measures for a macro-block	50
Table 4.3. JPEG comparison	51
Table 4.4. ECPE analysis.....	71

LIST OF SYMBOLS/ABBREVIATIONS

b_j	Partial regression coefficients in PQS
C_h	Channel with a transmission probability $p=1$
C_l	Channel with a transmission probability $p=0$
$C_{1,2}$	SSIM constants
F_i	Disturbance factors
I_{ext}	Extracted image
I_{healed}	Healed image
I_j	Test images
I_{rec}	Received image
k	Graylevel value of a pixel
$K_{1,2}$	SSIM constants
L	The maximum number of pixel values
LL	Low-low sub-band
m	Macro-block size
M	Macro-block size in EC
m^i	Set of the medians of weight matrices
M_j^i	Weight matrices for each measure-image pair
n_p	Number of disjoint paths
N_1	Image dimension
N_2	Image dimension
P	Probability
pL_i	Priority levels
Q_{tab}	JPEG quality scaling factor
R_i	Relay nodes
R_{ij}	Routing nodes
S_i	Snooping nodes
t^i	Group thresholds for the priority measures
V_i	Camera nodes
W_p^{ent}	Entropy weight of the macro-block p

W_p^{edg}	Edge weight of the macro-block p
W_p^{rep}	Reproducibility weight of the macro-block p
W_p^{dedg}	Delta-edge weight of the macro-block p
W_p^{dent}	Delta-entropy weight of the macro-block p
x	Non-negative image signal
y	Non-negative image signal
Z_j	Principal components of F_i
$\mu_{x,y}$	the mean intensity of the image signals
$\sigma_{x,y}$	the mean contrast of the image signals
ARQ	Automated Repeat Request
CDF	Cumulative Distribution Function
CM	Control Message
COTS	Commercial Off-The-Shelf
CPU	Central Processing Unit
DCT	Discrete Cosine Transform
DSC	Distributed Source Coding
DWT	Discrete Wavelet Transform
EC	Error Concealment
ECDP	Error Concealment with Disjoint Multipath
ECPE	Error Concealment with Priority Encoding
FEC	Forward Error Correction
FR	Full-Reference
HVS	Human Visual System
IDWT	Inverse Discrete Wavelet Transform
IQA	Image Quality Assessment
IQM	Image Quality Metric
IWM	IDWT of the watermarked image
JPEG	Joint Photographic Experts Group
LBT	Lapped Biorthogonal Transform

LQI	Link Quality Indicator
MBPE	Macro-block Based Priority Encoding
MEMS	Micro-Electro-Mechanical Systems
MOS	Mean Opinion Score
MSE	Mean Squared Error
NC	No Concealment
NR	No-Reference
OTI	Object Transmission Index
OTR	Object Transmission Rate
PIR	Passive InfraRed
PPR	Prioritized Packet Rate
PQS	Picture Quality Scale
PRR	Packet Reception Rate
PSNR	Peak Signal to Noise Ratio
QoS	Quality of Service
ROI	Region Of Interest
RR	Reduced-Reference
RSSI	Received Signal Strength Indicator
SIEC	Sub-bands based Image Error Concealment
SPIHT	Set Partitioning In Hierarchical Trees
SSIM	Structural SIMilarity
USB	Universal Serial Bus
WSN	Wireless Sensor Network
WMSN	Wireless Multimedia Sensor Network

1. INTRODUCTION

Wireless Sensor Networks (WSNs) consist of intentionally resource-constrained sensing, processing and communicating devices, i.e. sensor nodes. Sensor nodes are densely distributed over an area of interest to cooperatively sense physical phenomena and act accordingly. WSNs are used in several application areas such as environmental and industrial monitoring, biomedical health monitoring, vehicle tracking, military target tracking and surveillance [1,2]. Since WSN nodes are supposed to work autonomously and unattended for long periods of time without any maintenance, their components are designed to consume relatively low power when compared to traditional sensors. This scheme, together with the defects inherited from the nature of wireless medium, poses some challenges specific to WSNs: high transmission error-rate, limited network lifetime, node failures, mobility, network partitioning, scalability issues and end-to-end delay.

The advances in the micro-electro-mechanical systems (MEMS), especially in the image sensor technology, have triggered the era of Wireless Multimedia Sensor Networks (WMSNs) [3–5]. The possibility to process audio and video streams and still images together with scalar data provides additional flexibility, accuracy and high quality services to the applications in WSN. In consequence of these benefits, the nature of multimedia delivery introduces more demand in processing and energy resources together with stringent Quality of Service (QoS) requirements. These requirements necessitate to revise the knowledge gained from WSNs to manage resources much more efficiently.

Still-image coding and transmission is an essential part of multimedia applications. Images are good representatives of multimedia data. Furthermore, gathering images from an event area helps to identify and quantify the detected event more accurately and descriptively. For instance, in a border surveillance application, even though it may be sufficient to detect an intrusion via Passive InfraRed (PIR) sensors, only a snapshot of the area could reveal the source of the intrusion and the identity of the intruder. In this way, false positives could be avoided.

Main challenges in WMSNs can be addressed by extensive researches on the coding and transmission of images. In this thesis, a coding scheme based on *adaptive prioritization* of image partitions is proposed and examined in detail. Besides, the effect of channel conditions on transmitted images is observed with a real testbed, and the performance of a well-known technique, i.e. *error concealment*, is evaluated on this testbed. Hybrid utilization of our proposed method with error concealment is also studied and its performance is revealed. Moreover, an image transmission framework is proposed to address the requirements of multimedia transmission in WSNs.

1.1. PROBLEM DEFINITION

In WMSN applications, it is required to get images within accepted quality and time. To achieve expected lifetime for the application, energy efficiency is an inevitable issue when satisfying these requirements. There is always a trade-off between delay, energy consumption, bandwidth usage and image quality.

Fulfilling stringent QoS requirements of multimedia data is a nontrivial process, even in resourceful traditional networks. Static resource reservation based methods are mostly used in those networks. WMSNs are erratic, and it is not possible to guarantee the quality of links and the aliveness of nodes throughout an image transmission. Therefore, static resource allocation methods are not convenient.

For handling the vast amount of image data with tiny sensors nodes, it is necessary to use tailored source and channel coding techniques which are efficient in terms of processing power and required memory. At first sight, it may be thought that compression at the source eliminates delay by reducing the data size radically. It is not always operative in WMSNs because of the delay introduced by the computation time [6]. Another intuitive reasoning may be compressing images prior to transmission is more energy efficient than direct transmission of uncompressed bigger images. This reasoning comes from the general situation in WSN, in which the power requirement of transmission is generally greater than computation. There is not enough study in the literature to enlighten this hypothesis for WMSNs quantitatively [7]. This hypothesis may not be valid because of the complexity of

the compression algorithms.

To make use of compression in WMSNs, the traditional complex encoder, simple decoder approach in source coding should be reversed [5]. Distributed source coding is a favorable solution specifically when a spatial and/or temporal correlation between camera nodes exist. Temporal correlation is mainly related to video streams. Spatial correlation in images may exist when the viewing area of the nodes partially or completely overlaps. In this case, defining correlating areas is extremely hard especially when the network topology is unknown, so an initial training phase and in-network processing are mandatory [8].

Another aspect of compression is that in case of packet loss, much more information is lost because each packet includes much more information than raw transmission of images. Packet loss tolerance of an image coded with classical compression algorithms (e.g., JPEG [9], JPEG2000 [10], SPIHT [11]) is very low [12]. Error resilient robust source coding schemes or extensions to current schemes are required.

To avoid exponential loss of information and to achieve required perceptual quality, channel coding and error correction techniques must be employed in compressed image transmission such as Automated Repeat Request (ARQ) [13] or Forward Error Correction (FEC) [14]. However, these transport schemes may not be suitable for WMSNs. ARQ scheme achieves efficient bandwidth usage but due to packet retransmissions, it cannot satisfy strict delay constraints. FEC is based on imposing redundant packets or appending erasure codes to the packets and so comes up with increased bandwidth which is already limited in WMSNs [3, 15].

On the other hand, images contain redundant and correlated data, therefore they are open to diverse error correction and image reconstruction techniques. In this respect, error concealment (EC) approach has received particular attention as an effective mechanism that reconstructs the distorted image data as closely as the original one without increasing the bandwidth demand as well as avoiding the burden of retransmissions and consequent delay [16]. Consequently, EC algorithms are promising candidates to alleviate packet losses due to errors and failures in WMSNs.

Another considerable attribute of image data is unequal importance of pixels to reconstruct lost parts [5]. Methods that exploit relatively important part of images can be used to adaptively adjust image coding and transmission strategies to application and network requirements. Prioritization is one of the fundamental parts of QoS support mechanisms.

Image quality assessment is another issue when devising image transmission schemes for every level of communication stack. The purpose of quality assessment is objective evaluation of encoded and/or transmitted images [17]. This evaluation helps us to ascertain error tolerance of our methods quantitatively, and consequently to find optimal trade-offs among resource utilization and application specific QoS requirements.

1.2. MOTIVATION

Even the algorithms known as lightweight in traditional systems are generally not applicable to resource-poor sensor nodes. Many of the solutions proposed for image transmission in this field of research do not properly consider the facts of WMSNs. Most of the time, they include several assumptions and cannot go beyond a theoretical basis. In order to validate and advance these theoretical solutions, exhaustive experiments including real testbed implementations must be conducted [18].

The challenges in WMSNs can be overcome by interdisciplinary approaches. Images include redundant and correlated data. Besides, the pixels in images have unequal importance for perceptual reconstruction. This attribute makes it possible to assign different priorities to different parts of data to satisfy expected QoS. These inherent properties of image data can be the key instruments in WMSN solutions.

Multipath transmission is another promising method to overcome bandwidth deficiencies, overloaded buffers, node and link failures.

Image coding techniques are at the heart of any solution in WMSNs. Performance evaluation of these techniques helps to check their validity and feasibility. By this way,

the parameters in these techniques can be tuned and their effect is observed in different circumstances. Moreover, findings acquired from the evaluation of existing methods would be inspiring when devising new ones.

With the motivation above, we aim to put forward an adaptive and resource aware image coding and transmission scheme that gracefully adapts itself to applications' quality requirements.

1.3. CONTRIBUTIONS

In addressing the challenges outlined above, the following contributions are made:

- 1) A simple encoding scheme that dynamically (on-the-fly) prioritizes image partitions is proposed. In this method, data blocks are prioritized at the source, based on the information they contain and labeled accordingly.
 - a) To extract the information, different packet priority measures are considered: entropy, edge detection, reproducibility and hybrid measures, i.e. delta-entropy and delta-edge. These measures are applicable to image partitions rather than the full image.
 - b) To quantitatively evaluate the performance of the measures in prioritization, a new metric called *Object Transmission Rate* (OTR) is proposed and used in comparisons. The case of transmissions over lossy links without any encoding is used as the baseline for the comparisons.
 - c) Finally, the proposed priority measures are implemented on Telos [19] equivalent Tmote Sky nodes and their implementation costs are evaluated, and compared to JPEG image compression algorithm.

This contribution is accepted for publication as a research paper [20].

- 2) A real multi-hop testbed is established with Tmote Sky sensor nodes. The testbed is used to examine the effect of channel conditions on both raw images without encoding and images encoded with an existing error concealment (EC) algorithm [15]. The EC algorithm used is a modified version of Sub-bands based Image Error Concealment (SIEC) [21] algorithm. A series of exhaustive tests including 30,000 transmissions are

conducted for single-path and disjoint multipath transmission scenarios. This study is submitted as a research paper [22] and it is under review.

- 3) Hybrid usage of EC with the proposed priority-based encoding scheme is analyzed and compared to the real testbed results obtained in EC tests.
- 4) An image transmission framework is proposed to be coupled with priority-based encoding. This framework includes a regulated buffer transmission mechanism which transmits buffers in a bursty manner. In this scalable framework, fine-grained adjustment of the transmission parameters helps to satisfy the application's QoS requirements. It achieves adaptiveness in routing by the included link checking state.

1.4. ORGANIZATION OF THE THESIS

The remainder of this thesis organized as follows. Chapter 2 gives a literature review about the current research on the subject. Chapter 3 explains the coding schemes, algorithms and the transmission framework proposed in this study. Chapter 4 discusses the contributed methods and their experimental evaluations, including the testbed architecture. Chapter 5 concludes the thesis and points out future research directions.

2. RELATED WORK

Comprehensive surveys of WSNs can be found in [1, 2]. With the integration of the multimedia data to WSNs, together with its benefits, new challenges arose. [3] covers new applications, challenges, proposed solutions and open research issues. A comprehensive survey of WMSNs is given in [5]. Other surveys focus on different aspects of WMSNs. In [23], the authors examine multimedia streaming in WMSNs. [8] is a survey about visual sensor networks. In this work, the authors stated:

Future directions in visual sensor networks research should be aimed at exploring the following interdisciplinary problems.

- (i) How should vision processing tasks depend on the underlying network conditions, such as limited bandwidth, limited (and potentially time-varying) connectivity between camera nodes or data loss due to varying channel conditions?
- (ii) How should the design of network communication protocols be influenced by the vision tasks? For example, how should different priorities be assigned to data flows to dynamically find the smallest delay route or to find the best fusion center?
- (iii) How should camera nodes be managed, considering the limited network resources as well as both the vision processing and networking tasks, in order to achieve application-specific QoS requirements, such as those related to the quality of the collected visual data or coverage of the monitored area?

2.1. IMAGE CODING AND COMPRESSION

Image coding is the fundamental part of visual data handling in WMSNs. There are several researches about different aspects of image coding in WMSNs. One of the main concerns of these researches is about compression. Compressing relatively large image data for WSN significantly reduces required bandwidth. However, compressing images is a costly operation in terms of energy consumption. For the limited processors of tiny sensor nodes, computations included in compression are time-consuming operations, hence they pose undesirable delay during transmission in multimedia applications. In Figure 2.1, the operations included in one of the remarkable compression technique (JPEG) are given from [7]. Moreover, compression is sometimes not possible for the methods that require full image, such as JPEG 2000 [10], because of the limited available memory of sensor nodes. In these circumstances, optimizing compression for WMSNs and fine-tuning

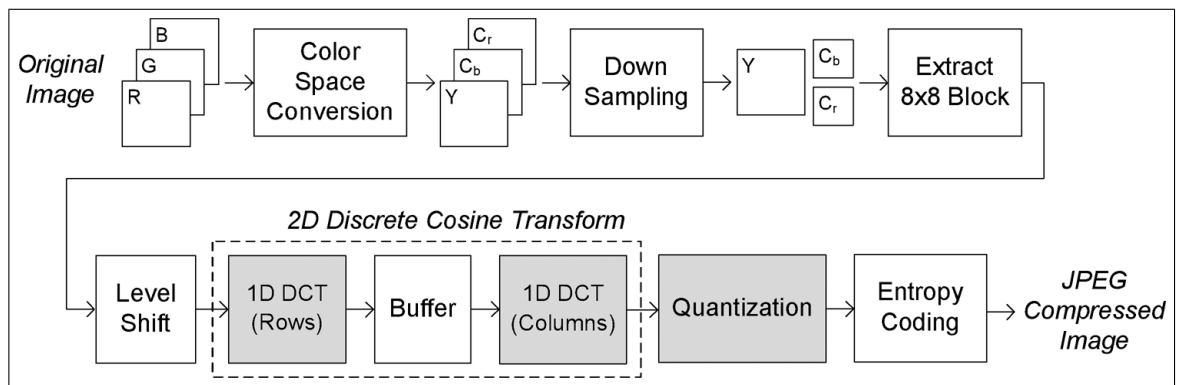


Figure 2.1. JPEG compression algorithm

the parameters of it are necessary. In this context, Lee et.al have studied trade-offs in compression parameters in terms of computational cost, energy consumption, speed and image quality in [7]. They also proposed optimization methods. For testing the methods on different hardware platforms, they have utilized a framework which automatically generate C codes for the platforms. Their findings are used for JPEG comparisons in our work. In [24], Lu et.al. proposed a low-complexity and energy efficient image compression scheme designed especially for WMSNs and based on Lapped Biorthogonal Transform (LBT) [25].

Another drawback of compression is its fragility to packet losses. In the real tests of the work [12] 14 per cent of the JPEG 2000 coded images are unrecoverable in a 2-hop transmission. Error recovery mechanism should be used to overcome the fragility of the compressed images. However, employing these mechanisms in the network introduces either additional delay [26] or increased bandwidth demand.

Another coding method is distributed source coding (DSC) [27] to balance the computational load on sensor nodes. There are many studies in the literature about DSC [28–31]. A diagram of DSC, taken from [31], is depicted in Figure 2.2. They are mostly based on Slepian and Wolf’s and Wyner and Ziv’s information-theoretic works [32, 33]. However, there must be a spatial or temporal correlation between the images taken from different sensor nodes. With regard to still-images, it is only possible when the field of views of more than one camera overlaps. Since we are not focused on multiple-camera scenarios in this study, this method is not further discussed.

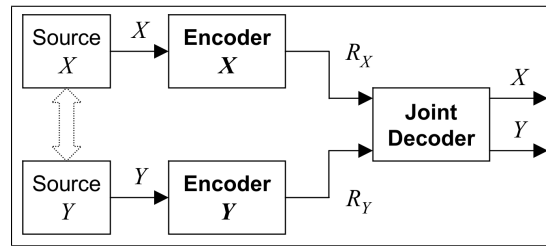


Figure 2.2. Distributed compression of two statistically dependent random processes

2.2. IMAGE TRANSMISSION

To increase robustness of the transmitted images in WMSN, the redundancy naturally included in them can be used. In the well-known and pioneer work [34] of Shannon, he states that:

The redundancy must be introduced in the proper way to combat the particular noise structure involved. However, any redundancy in the source will usually help if it is utilized at the receiving point. In particular, if the source already has a certain redundancy and no attempt is made to eliminate it in matching to the channel, this redundancy will help combat noise.

In the light of this theory, instead of removing the redundancy with compression, we should make use of it. Error concealment is a method that increases redundancy of data for error recovery. Error concealment techniques are well-studied in [35]. Error concealment techniques that increase redundancy without increasing image size [15, 36–38] should be preferred in WMSNs.

The redundancy in image data is benefited by image reconstruction techniques [39,40]. The authors in [41] separate image data into two different sets as structure and texture and propose different reconstruction techniques for them. This is a good example of classified treatment of image data.

Image transmission is one of the main concerns of WMSN researches. Transmitting relatively big data in the poor conditions of WSN is a complicated operation. The problem is not only the amount of data but also tight QoS requirements of the application. Therefore,

many of the studies in this field are about providing QoS support to applications in WMSN [42–47].

The bandwidth requirements in image transmission can be satisfied by using multiple paths [48]. Multipath transmission also helps to overcome congestion problem in WMSNs [49]. By using multiple paths, that naturally occur in WMSNs, error resilience is also achieved [50]. Another benefit of multipath transmission is in timeliness domain, thus it helps to minimize delay in transmission. MMSPEED [44] is the one of the representative of using multiple paths to achieve QoS in both timeliness and reliability domain.

2.2.1. Prioritized Transmission

Prioritized transmission of different services is a commonly used technique in any kind of networks. The theoretical study [51] of Albanese et.al. shows the basis of priority encoding transmission. This paper is probably the most related one to our study. However, the authors focused on priority encoding transmission of data in a general manner and they did not offer any priority measure for images. The studies about prioritization are mostly related to inter-prioritization of different data types, i.e. scalar data, audio, video etc. [52]. On the contrary, we offer intra-image prioritization and measures to weigh the importance of image partitions. Image data consist of different partitions which have different perceptual, semantical and structural importance. In [53], authors propose prioritization of image data in wavelet domain. They assign different priorities to different subbands with a semi-reliable transmission scheme based on priority-based packet discarding. In that scheme, intermediate nodes intentionally drop lower priority packets according to their battery's state-of-charge.

Several studies in the literature insist on the valuable information extracted from the images. In [54], authors point out the importance of object recognition. Background subtraction is a mainly used method for this purpose [55, 56]. However, it is a costly method for tiny sensor nodes.

Table 2.1. An overview of the current hardware platforms

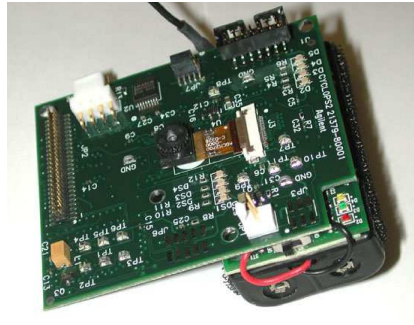
Device Name	Manufacturer	Processor	Memory	Multimedia Support	Wireless
Stargate	Crossbow	Intel PXA-255 Xscale processor at 400 MHz	32 MByte Flash 64 MByte RAM	High computation power, embedded linux OS	802.11 Compact Flash, 802.15.4 through MICA2/z interface
Imote2	Intel	32 – bit PXA271 Marvell processor at 13 – 416 MHz	32 KByte Flash 64 KByte RAM	MMX co-processor for audio/video imaging acceleration	Integrated 802.15.4
CMUcam3	CMU	32 – bit NXP LPC2106 microcontroller at 60 MHz	128 KByte Flash 64 KByte RAM	On-board cc3-open source image processing library	–
MeshEye	Stanford Univ.	32 – bit ARM7TDMI RISC processor at 55 MHz	128 KByte Flash 64 KByte RAM	Multiple resolution support	–
WiCa	XNP and Philips Research	IC3D Xetal II processor at 84 MHz	10 Mbit RAM	Dedicated parallel processor, multiple camera modules	–
Cyclops	Agilent Technologies	8 – bit ATMEL ATmega128L microcontroller	512 KByte Flash 512 KByte RAM	On-board image processing, low power, cost and size	–

Table 2.2. An overview of the current testbeds

Testbed Name	Imaging Device	Pixels	Interfacing Mote	Additional Features
Meerkats	Logitech Quick Cam Pro 4000	640 × 480	Stargate	Camera on-off switching for energy conservation
Explorebots2	XCam2	320 × 240	MICA2	Mobile robots Sonic sensors
Mobile Emulab	Overhead Hitachi KP-D20A	768 × 494	Stargate MICA2	Mobile robot Remote Reconfiguration
IrisNet	Logitech Quick Cam Pro 3000	640 × 480	Stargate	Network animator Highly scalable
SensEye	Cyclops, CMUcam pan-tilt-zoom webcams	352 × 288	Stargate MICA2	3-4 camera tiers Boundary/motion detection and tracking
BWN Lab Testbed	Logitech Quick Cam Pro 4000	640 × 480	Stargate MICA2	Mobile robot

2.3. TESTBEDS

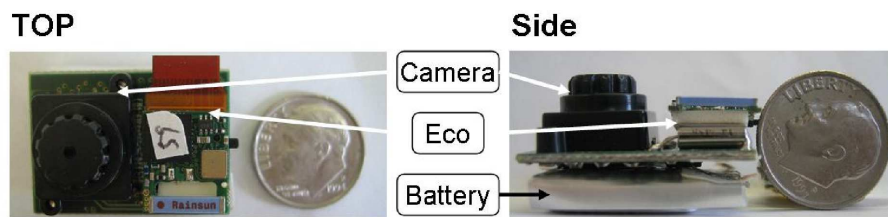
Although the studies mentioned above include notable theoretical solutions, many of them are not validated by real testbed experiments. It is important to test the effectiveness and the feasibility of algorithms and protocols in a controlled environment. Recent testbeds on WMSNs are exposed, and current applications and hardware platforms are revealed in [18]. An overview of the features of the platforms and recent testbed studies mentioned in [18] are given in Table 2.1 and Table 2.2 respectively. Some of the camera platforms, i.e. Cyclops [55], ALOHA [57], eCAM [58], CMUcam3 [59], are illustrated in Figure 2.3.



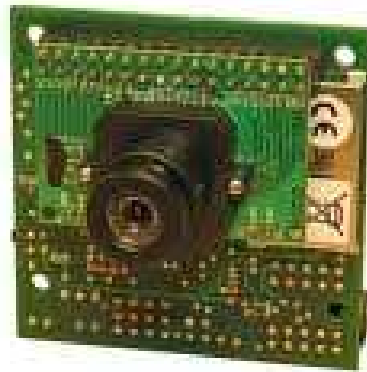
a. Cyclops with Mica2



b. ALOHA platform



c. eCAM platform



d. CMUcam3 camera

Figure 2.3. Current sensor platforms and cameras

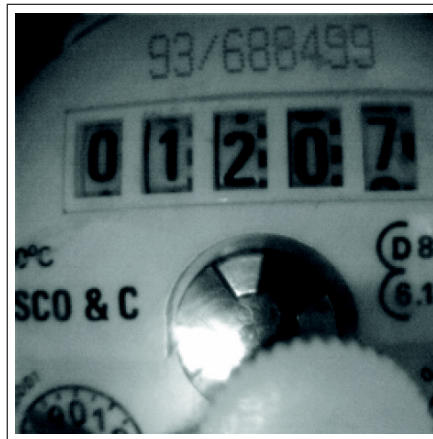


Figure 2.4. A water counter from an example application

2.4. IMAGE QUALITY ASSESSMENT

When evaluating the performance of an image coding and transmission scheme, *inter alia*, the quality of the degraded images at the receiving end has significant importance. Moreover, Image quality assessment (IQA) is utilized in quality aware transmission schemes, when making routing decisions. IQA is also beneficial for the adjustment of coding and transmission parameters. In many applications, transmission of the images in full quality is not necessary. In those cases, intentionally reducing the quality of the images extremely improves the network performance and the lifetime of the system. IQA is employed in several WMSN applications before the information extraction stage to figure out whether the received image is sufficient to extract the required information or not. For instance, in [60] authors aim to find a trade off between compression ratio, compression time, transmission time and image quality. They have applied their methodology to a case study: the use of wireless visual sensors for remote metering of water counters. A sample image from the application is given in Figure 2.4. In that application, the authors have used CW-SSIM [61] as an image quality metric (IQMs). Their success criterion is the ability of detecting the digits of the water counter with an optical character recognition (OCR) software. They have tested several images corrupted by various methods and estimated the CW-SSIM threshold value. This value have been considered as the minimum acceptable quality level of the acquired image. Then, they have adjusted the compression parameters as to satisfy this value.

Human Visual System (HVS) has a great ability to determine the quality of the image [62]. Assessing the quality of an image is most reliably done by subjective evaluation [63]. In this respect, Mean Opinion Score (MOS) is the most widely used subjective IQM. To attain the MOS values, a study group involving several individuals is formed. Each person in the group examines the images and gives scores about the quality of them. MOS is taken as the average rating of their scores. MOS is mainly used for the evaluation of objective IQMs. Objective IQMs are devised to automatically and quantitatively predict perceived image quality in a way that is consistent with subjective human evaluation [64]. Objective IQMs remove the necessity of human interaction and introduces more practical and dynamic way for IQA. The performance of objective IQMs are evaluated by following criteria [62].

- 1) Prediction Accuracy; This is revealed by MOS comparisons.
- 2) Prediction Monotonicity; The IQM values should increase and decrease monotonically with the corresponding MOS values.
- 3) Prediction Consistency; The performance of the IQM should not be affected from the characteristics of different images.

IQMs are examined in three different classes according to availability of the original image.

- 1) Full-Reference (FR) Metric; Original image is available.
- 2) No-Reference (NR) Metric; Original image is not available. It is also called as “single-ended” and “blind”.
- 3) Reduced-Reference (RR) Metric; Original image is partially available or information about the features of the image is available for IQA purposes.

FR metrics are the most commonly used metrics. They can be used for evaluating the performance of image related methods but they cannot be used dynamically in a communication system because the reference image is not available at both intermediate nodes and the sink. NR metrics may be used for this purpose but NR IQA is extremely difficult for an automated algorithm to execute [65]. Exploiting edge sharpness is a commonly used technique in NR metrics [66, 67].

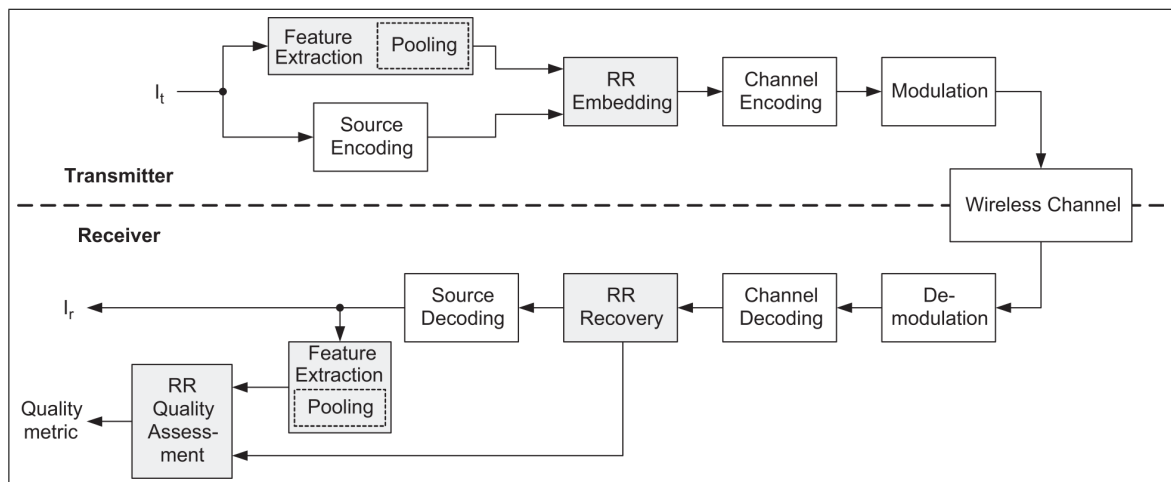


Figure 2.5. Usage of RR IQA in a wireless imaging system

RR metrics provide a good compromise between FR and NR metrics for image communication. [68] proposes a IQA method based on a natural image statistic model in the wavelet transform domain. [69] has a similar wavelet based RR approach, but instead of transmitting required information for quality assessment via an ancillary channel or piggybacking, that information is embedded to the image by watermarking. In [65], two RR metrics are proposed for wireless imaging, considering the system depicted in Figure 2.5.

IQA is a large field of research in image processing. [17, 70–72] are surveys comparing the performance of several IQMs. Although, there are lots of proposed IQMs, there is no universal IQM which can be used in all situations and all types of images. Because of this, IQMs should be chosen in accordance with the aim of the application by conducting experiments over the possible images which would be faced throughout the application. Since, we use IQMs for only the evaluation of our methods, we further focus on objective FR IQMs.

2.4.1. The Structural SIMilarity (SSIM) Index

The SSIM index is devised under the assumption that HVS is highly adapted for structural information extraction from a scene [64]. This index weighs structural distortions

in the image. This is done by utilizing simple intensity and contrast measures. SSIM index is calculated as

$$SSIM(x, y) = \frac{(2\mu_x\mu_y + C_1)(2\sigma_{xy} + C_2)}{(\mu_x^2 + \mu_y^2 + C_1)(\sigma_x^2 + \sigma_y^2 + C_2)} \quad (2.1)$$

where x and y denote two non-negative image signals. μ_x, μ_y and σ_x, σ_y represent the mean intensity and the contrast of the image signals, respectively. C_1 and C_2 are the constants used for to avoid instabilities when μ_x, μ_y and σ_x, σ_y approach to zero. They can be chosen as

$$C_{1,2} = (K_{1,2}L)^2 \quad (2.2)$$

where L is the maximum number of pixel values (255 for 8-bit grayscale images), and $K_{1,2} \ll 1$ are small constants.

2.4.2. Objective Picture Quality Scale (PQS)

In [73], a methodology is given for the determination of an objective IQM. As an application of this methodology, PQS is presented. It is based on the properties of visual perception for both global features and localized impairments caused by image coding. In this method, source of disturbances are considered as effect of noise, luminance coding mistakes, end of block disturbances, correlated errors and problems near high contrast changes. To quantify these factors, they are modeled by five distortion factors, $F_i=1, \dots, 5$. Some of these factors are correlated. Principal component analysis is utilized to obtain the correlation between the factors. And PQS is the linear combination of the principal components $Z_j=1, \dots, 5$:

$$PQS = b_0 + \sum_{j=1}^J b_j Z_j \quad (2.3)$$

where b_j is the partial regression coefficients computed using multiple regression analysis of PQS from MOSs obtained experimentally.

2.4.3. Peak Signal To Noise Ratio (PSNR)

PSNR is a general quality metric which weighs differences in signals with a logarithmic base. It is used mainly to assess distortions of the signals caused by external sources. It is commonly used in image processing especially for comparing the performance of compression algorithms.

PSNR is based on the Mean Squared Error (MSE) value which is defined as

$$MSE = \frac{1}{N_1 \times N_2} \sum_i^{N_1} \sum_i^{N_2} [I(i, j) - \hat{I}(i, j)]^2 \quad (2.4)$$

where $I(i, j)$ and $\hat{I}(i, j)$ are the pixel values of the original and reconstructed images respectively. And MSE is used to calculate PSNR as,

$$PSNR(dB) = 20 \log_{10} \frac{2^n - 1}{\sqrt{MSE}} \quad (2.5)$$

where $n = 8$ for 8-bit grayscale images and $(2^n - 1)$ is the largest possible value of the signal.

3. IMAGE CODING AND TRANSMISSION

In WMSN, image coding and transmission are tightly connected to each other. Their interaction is important to provide QoS support to the applications. Any transmission scheme should be aware of the coding mechanisms, and the attributes of the images encoded with that. A coding scheme may result in images that are not robust to packet losses, such as compressed images. In this case, a transmission scheme which provides reliability should be employed. On the other hand, a coding scheme can introduce additional error correction codes to increase the robustness of the images. In such a case, more bandwidth is required, and the transmission scheme should handle this additional bandwidth requirement. Some coding methods are designed to make use of multiple paths. In this situation, the transmission scheme should extract and manage available paths effectively. In this study, coding and transmission of images are treated together.

In this chapter, a priority encoding scheme is proposed with novel priority measures. After that an error concealment technique which improves the robustness of the images is examined. Hybrid usage of error concealment with priority encoding is also discussed. Finally, an image transmission framework, which is designed to be coupled with priority encoding, is proposed and explained in detail.

3.1. MACRO-BLOCK BASED PRIORITY ENCODING (MBPE)

Prioritization of packets for different kind of network traffics and services is a frequently used method for QoS support [52, 74]. Prioritization of image data is beneficial for resource utilization and data-centric transmission schemes. However, image data are not homogeneous. The spatial relation in image data makes some partitions of the image more valuable in terms of reconstruction and information extraction. Main reason for gathering images from an environment is to get usable information about the subject of the application. Therefore, the partitions of an image that include structural information is more useful.

Image macro-blocks are $m \times m$ pixel image partitions which can be fit into one

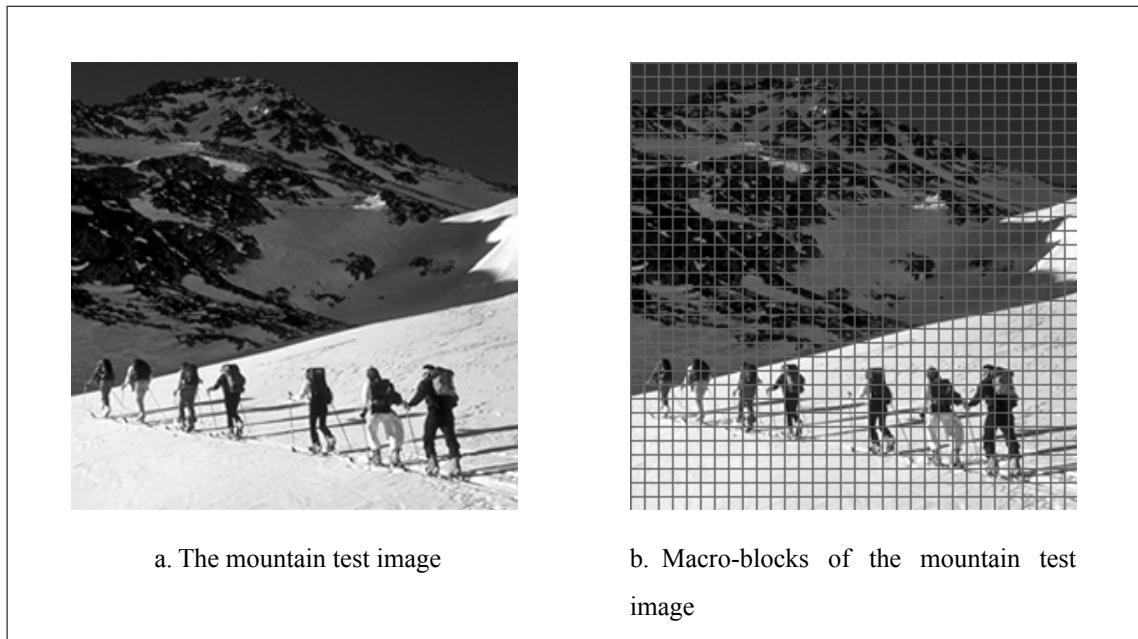


Figure 3.1. The mountain test image and its 8×8 macro-blocks

transmission data packet. A 256×256 test image and its 8×8 macro-blocks are depicted in Figure 3.1.

The proposed coding method, called *Macro-block Based Priority Encoding (MBPE)*, is based on prioritization of image macro-blocks on-the-fly according to the information they contain. In this method, priority level of the macro-blocks is intended to be used for data-driven transmission schemes. Links between a sensor node and its neighbors have different and temporarily changing qualities. Transmitting macro-blocks via these links in accordance with their priority levels is the basis of this scheme. An illustration of the considered system is given in Figure 3.2. Adaptively matching the quality of the link and the importance of the macro-blocks increases the possibility of valuable image data to arrive the sink. By this way, load-balancing is also achieved and energy burden on static paths is avoided. This situation increases overall network lifetime. Using multiple paths prevents congestion arising from overloaded buffers.

To decide the priority of a macro-block, the importance of it should be evaluated quantitatively. Since, most of the commercial off-the-shelf (COTS) sensors have not enough

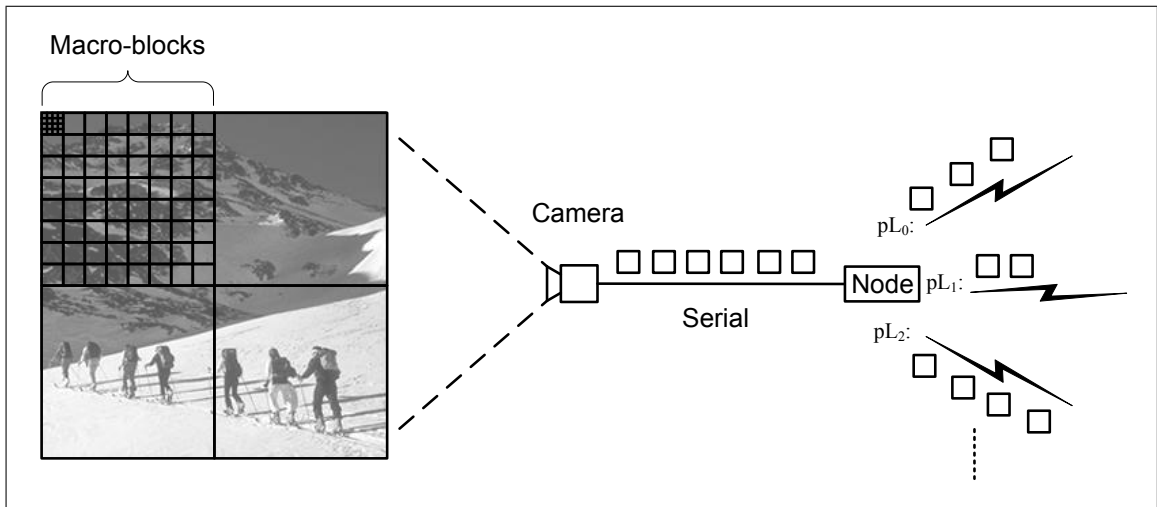


Figure 3.2. MBPE system model

memory and processing power to handle full image data, the evaluation process should be done without acquiring the whole image. In this study, several *priority measures* are proposed to weigh the importance of macro-blocks. In the proposed measures, full image data are not required. The required data change according to the measures. It is either only the macro-block itself or the neighboring macro-blocks together it. The details of the measures are presented in Section 3.1.1.

At the source node, we classify image data to *priority levels* by applying thresholds to the weights attained from the measures. At each node, the priority levels are assigned to available links prior to transmission. Determining the priority levels and corresponding threshold values should be adaptive based on the setup of the sensor nodes and the application's requirements. This subject is discussed in Section 3.1.2.

3.1.1. Priority Measures

3.1.1.1. Entropy Measure

The first measure proposed for image packet prioritization is based on Shannon-entropy [34]. Shannon-entropy defines a quantity that measures the amount of information included in a dataset, in other words the rate of the information included in it. With regard to image data, conceptually, it reflects the redundancy in the image. If the

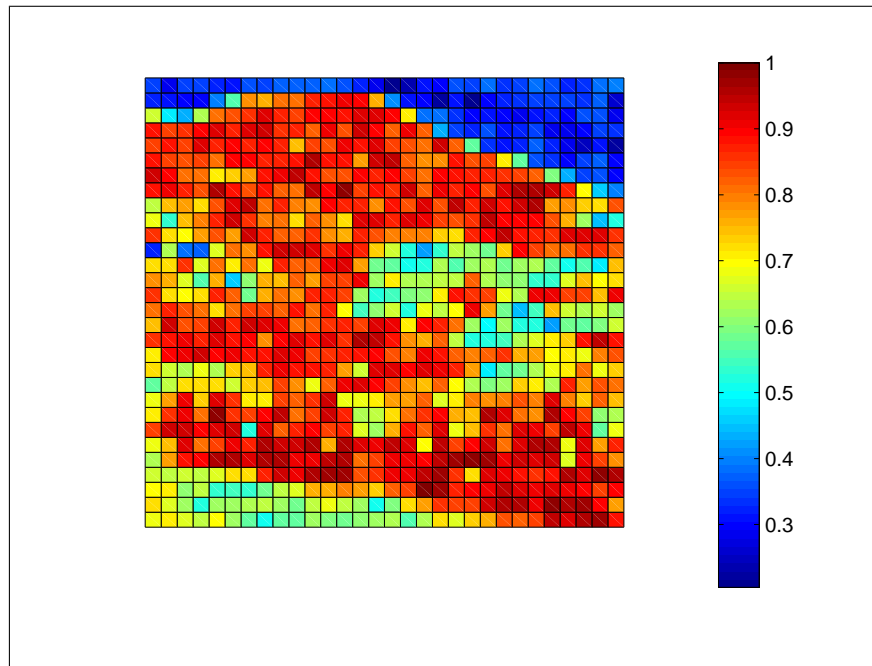


Figure 3.3. Entropy based measure of macro-blocks in the mountain test image

entropy of a macro-block is relatively low, the redundancy included in it is high and the importance of the macro-block is low. For a macro-block in which all the pixels have the same value, entropy is *zero*. On the other hand, for a 8×8 pixels macro-block in which all the pixels have different values, entropy is *six*.

Entropy can be taken as the probabilistic information measure of a given macro-block [75]. For each image macro-block, entropy is calculated by its normalized grayscale intensity histogram. This is actually the sample probability mass function, $P(k)$, of the packet. The entropy for a 256 level grayscale image is calculated by

$$W_p^{ent} = - \sum_{k=1}^{256} P(k) \log_2(P(k)) \quad (3.1)$$

The entropy is calculated for all macro-blocks. For the mountain test image in Figure 3.1, the entropy measures of 8×8 macro-blocks are given in Figure 3.3. The macro-blocks are prioritized and transmitted via appropriate channels based on these values. As can be seen, the macro-blocks corresponding to the background have lower entropy values. The other sections of the image have relatively higher entropy measures.

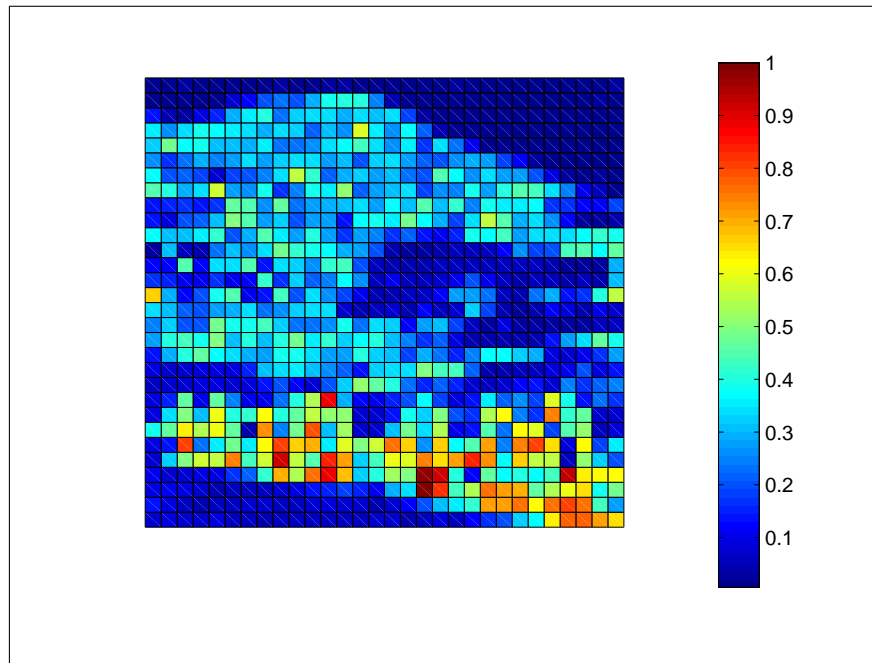


Figure 3.4. Edge based measure of macro-blocks in the mountain test image

3.1.1.2. Edge Measure

The second packet priority measure is based on edge information. In the image, structured data correspond to edges [41]. Therefore, if a priority measure can be developed based on the edge information, then it can also increase aliveness of structure of the subject. There is a vast amount of literature on edge detection [76]. In this study, the simplest edge detection method based on Haar filter (with coefficients $\{+1, -1\}$) is used without direction selectivity. The absolute values of these edge filter responses in the image macro-block are summed and taken as the edge measure.

The edge measure of the macro-blocks in the mountain test image is given in Figure 3.4. As can be seen in this figure, the macro-blocks corresponding to the skaters have the highest edge measures. The other macro-blocks have fairly low edge measures. It can be deduced that this measure hints on the possible objects in the macro-block.

3.1.1.3. Reproducibility Measure

The last “pure” packet priority measure is based on image reproducibility. The idea for developing this measure is as follows. If a macro-block is lost, can it be reproduced

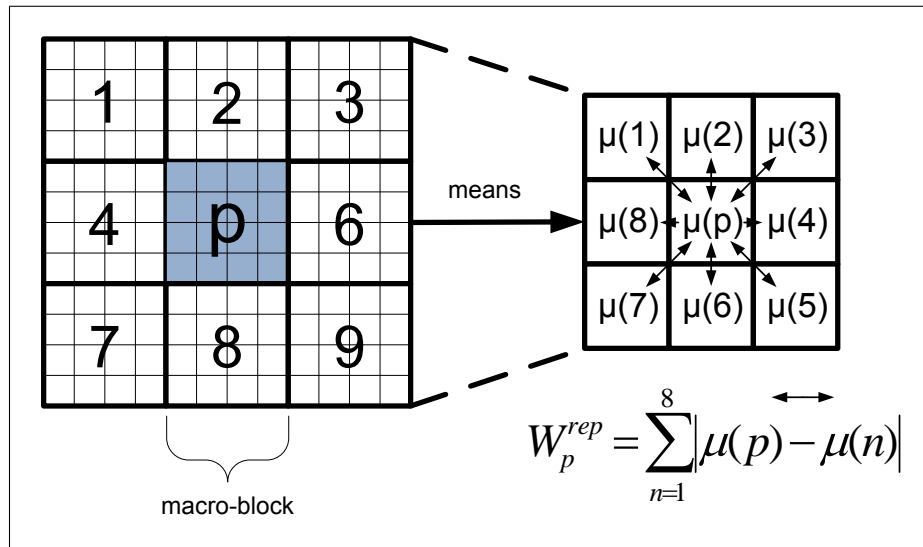


Figure 3.5. Reproducibility operation

easily by its neighbors? This is in fact a simple form of the well-known technique in image processing called as *image inpainting* [77]. Reproducibility measure depends on this idea. Each macro-block is represented by the mean value of its grayscale pixel values. If the mean value of a macro-block is close to the mean values of its neighboring macro-blocks, in general terms it resembles its neighbors. Hence, it is possible to reproduce it. If the mean values are different, then the macro-block differs from its neighbors and it may not be easy to reproduce it. Here, it is important to mention that the present study does not focus on reproduction. Only the basic idea is used for packet prioritization. Based on these definitions, the weight for the macro-block p is calculated as

$$W_p^{rep} = \sum_{n=1}^8 |\mu(p) - \mu(n)| \quad (3.2)$$

where $\mu(p)$ is the mean value of the macro-block p . In the summation, $n = 1, \dots, 8$ are the *eight neighbors* of the macro-block p . The diagram of this operation is depicted in Figure 3.5.

Reproducibility measure differs from the previous measures in terms of used data. In the previous measures only intra macro-block information is used, but here, this measure makes use of inter macro-block information. This approach improves the efficiency of the measure with a tolerable memory overhead.

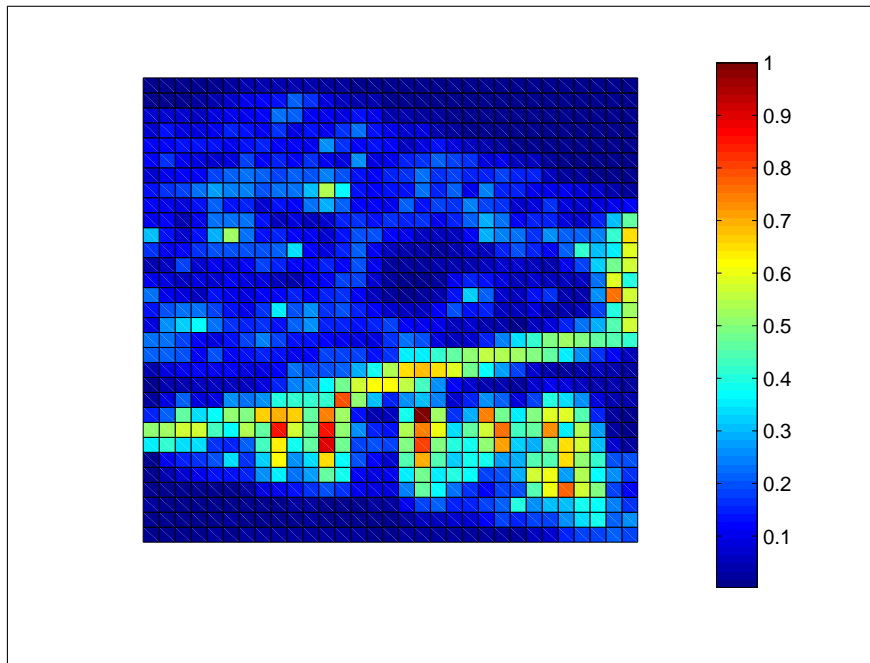


Figure 3.6. Reproducibility based measure of macro-blocks in the mountain test image

This measure is applied on the mountain test image. Macro-block weights can be seen in Figure 3.6. As can be seen, image macro-blocks containing objects have higher weights compared to the rest of the macro-blocks. This indicates that the reproducibility measure may be of use for packet prioritization.

3.1.1.4. Hybrid Measures

In this class of measures, edge and entropy measures are combined with reproducibility measure separately. As mentioned before, reproducibility measure is based on mean grayscale values of macro-blocks and their differentiations. It tries to extract representability of a macro-block by its neighbours in terms of mean grayscale values. By using edge and entropy values, instead of mean grayscale values of macro-blocks, and applying the same differentiation, some performance gain can be obtained. These hybrid measures i.e. delta-entropy and delta-edge are calculated for entropy and edge values respectively as

$$W_p^{Dent} = \sum_{n=1}^8 |W_p^{ent} - W_n^{ent}| \quad (3.3)$$

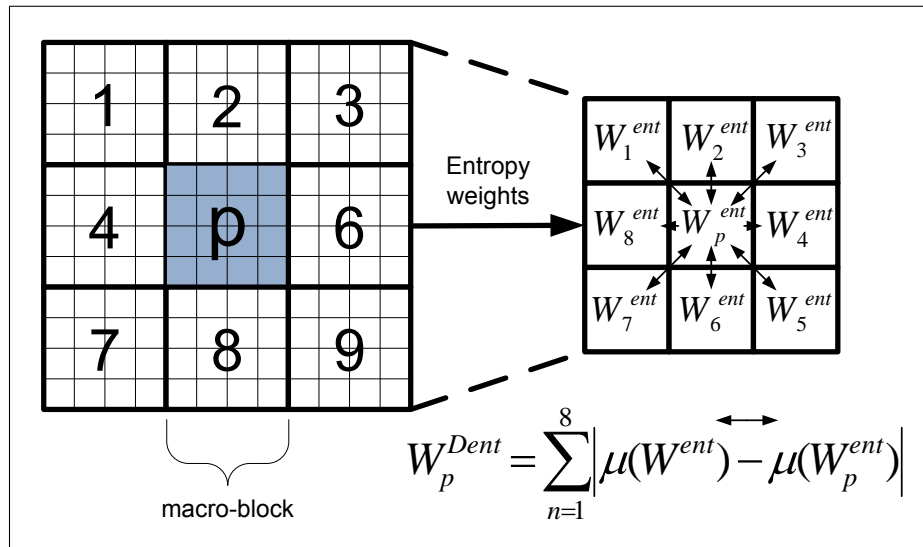


Figure 3.7. Delta-entropy operation

$$W_p^{Dedg} = \sum_{n=1}^8 |W_p^{edg} - W_n^{edg}| \quad (3.4)$$

The diagrams of these operations are depicted in Figure 3.7 and Figure 3.8.

Example results for the hybrid measures in the mountain test image is given for entropy and edge are depicted in Figure 3.9 and Figure 3.10 respectively. As can be seen, the performance of delta-entropy measure is worse than the “pure” entropy approach but delta-edge measure results show some performance gain.

3.1.2. Priority Levels And Thresholds

In a prioritization scheme, priority levels and the corresponding thresholds should be determined. These are critical parameters which must be defined prior to network deployment. The priority levels depend on the network architecture and the application’s subjects and requirements. With regard to network architecture, the density of the network, available links between nodes and environmental conditions that effect the channels are determinant. On the other hand, applications’ considerations are different. Here, the possible images that would be encountered in the field of application are decisive. The complexity and the structure of the images must be considered. From the application’s point of view,

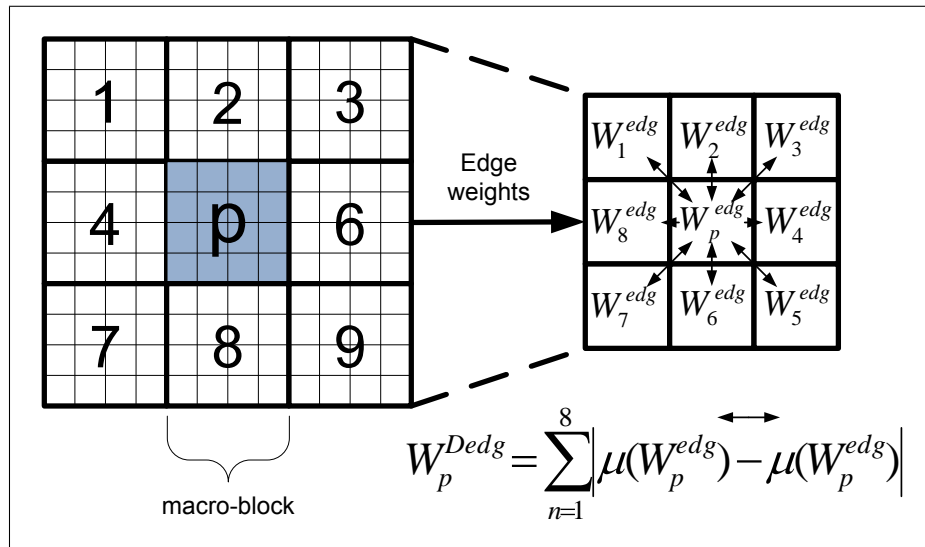


Figure 3.8. Delta-edge operation

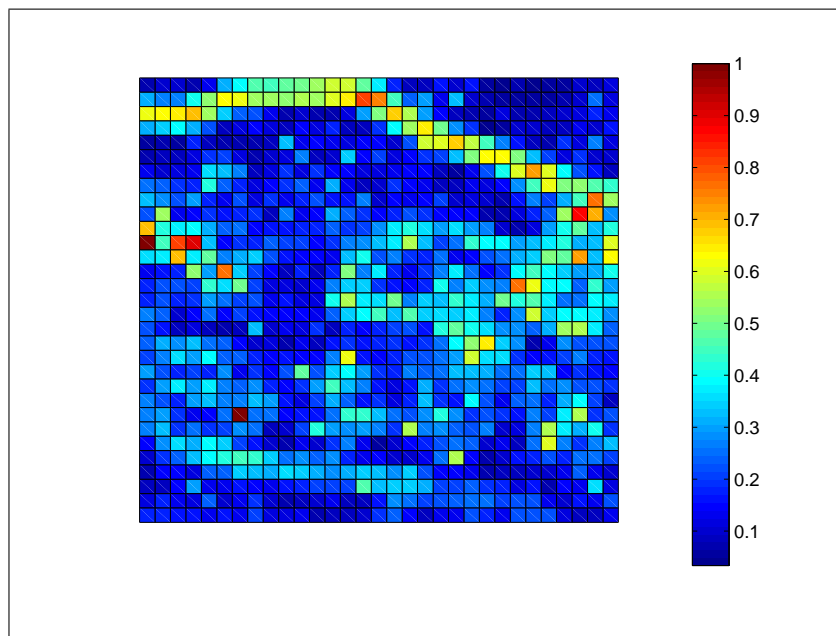


Figure 3.9. Delta-entropy based measure of macro-blocks in the mountain test image

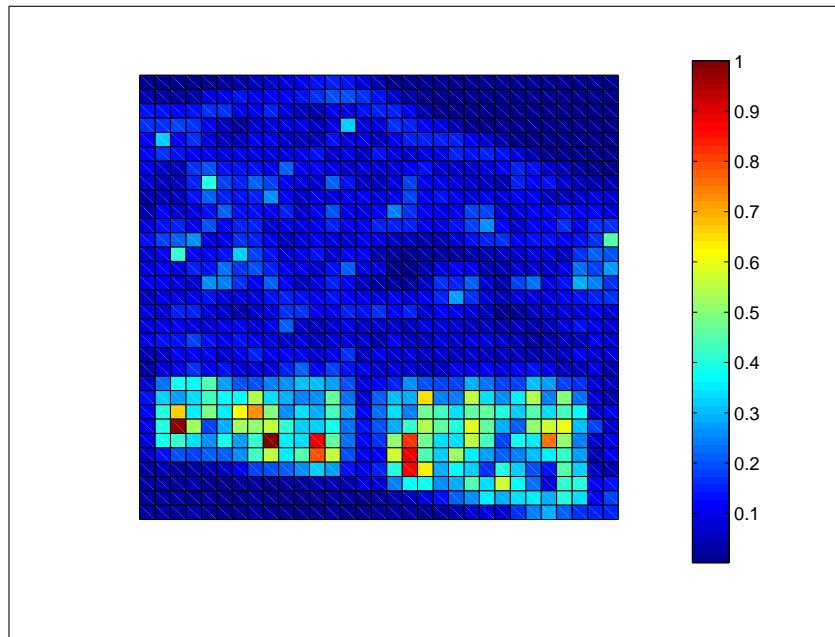


Figure 3.10. Delta-edge based measure of macro-blocks in the mountain test image

the most significant factor is the information that to be exploited from the image. Another issue is determining the threshold values for associating macro-blocks with the priority levels. The distribution of the macro-block values for each image varies dramatically. These issues are already research topics in the field of image processing. Determining the levels and thresholds is not trivial and therefore exhaustive tests on the possible images for the application are required. An example of this operation is done in our experiments. It can be examined in Section 4.2.2.

3.2. ERROR CONCEALMENT (EC)

Error concealment is the one of the favorable methods for robust image transmission. Main idea behind it is using inherently redundant and correlated image data for reconstruction of lost image partitions. One of the benefits of EC is achieving error robustness without increasing required bandwidth. When using EC the necessity of using reliable transmission is removed to some extent, and so no additional delay is introduced. As a part of this study, we focused on the EC algorithm that is modified and evaluated by Sarisaray et. al. [15]. They have examined several aspects of the EC algorithm by comparing

with FEC and no error concealment on different transmission schemes with simulations. On the other hand, in this study, the performance of the EC algorithm on real devices and environmental conditions is evaluated.

3.2.1. The EC Algorithm

The EC algorithm realized in this study is a modified version of Sub-bands based Image Error Concealment (SIEC) [21] algorithm. The algorithm employs a modified Discrete Wavelet Transform (DWT) for embedding downsized replicas of original image into itself, thereby mitigating degradations in a backward-compatible scheme without increasing the total size of the data to be transmitted. It corrects pixel and block losses due to transmissions using the embedded replicas. The replicas of the original image's $M \times M$ macro-blocks are embedded in the sub-bands of the to-be-transmitted image, excluding LL (low-low) sub-bands, in order to limit the visual degradation. The host macro-blocks where replicas are embedded are chosen by using a shared-key-dependent pseudo-random sequence, so the extraction of the replicas is blind. If all of the replicas embedded in the sub-bands are lost, then each pixel in the lost macro-block is replaced by the median value of the sequence composed of non-zero values of neighboring macro-blocks' corresponding pixel. The detailed algorithm can be described as follows:

At the Source Nodes C_j ,

1. Capture the original image, I , with size of $N_1 \times N_2$ pixels.
2. If there are macro-blocks consisting of all 0's, then replace a pixel value in each of these macro-blocks with 1. This step facilitates fragile watermarking for error detection, and is inspired by work of Kundur et al [78].
3. Take l^{th} level pyramid-structured DWT of the original image I . Note that $k \geq l$, where k is the number of levels of the tree structured DWT.
4. Store each $(M/2^k) \times (M/2^k)$ macro-block of the tree structured DWT of the original image, namely replicas. Note that there are $(N_1 \times N_2/M^2)$ macro-blocks.
5. Scale each replica by the designated coefficient, then embed that scaled replica in each pyramid-structured wavelet sub-band, excluding LL ones, by using shared-key

dependent sequence for each individual sub-band. Note that step 4 to 6 actualizes robust watermarking schema, which uses repeated watermark technique which is a modified version of the method studied by Kundur et al. [79].

6. Take inverse DWT (IDWT) of the watermarked image, namely IWM, and round the floating-point pixel values to the corresponding integer values.

At the Sink,

1. Read the received image, I_{rec} , and determine the lost pixels by searching blocks consisting of 0's. Thus, we utilize fragile watermarks in this step for error-detection.
2. Take l^{th} level pyramid-structured DWT of the received image I_{rec} .
3. By generating shared-key dependent random sequence, which was also used in the encoder, determine the location of lost pixels' replicas for each individual sub-band.
4. Multiply each replica with the known scaling coefficient used in encoder and take k^{th} level IDWT of the extracted replicas.
5. If there is more than one non-zero extracted pixels, take average of all those non-zero values, then place that average into the received image, I_{rec} , as the lost pixels. After this process is finished, the extracted image, I_{ext} is constructed.
6. Scan I_{ext} for lost blocks, which could not be healed. If there are still blocks consisting of all 0's, then replace them with the median value of the neighboring healthy blocks. After this process, the healed image I_{healed} is constructed in the sink.

3.3. ERROR CONCEALMENT WITH PRIORITY ENCODING (ECPE)

In the previous chapters, the advantages of error concealment and priority encoding are mentioned. Their advantages are in different aspects; EC increases the error robustness of image data whereas MBPE offers a lightweight infrastructure for prioritized transmission of favorable parts of the data. Here, *Error Concealment with Priority Encoding (ECPE)* is proposed as a combination of these two orthogonal approaches. EC is based on reconstruction of lost data. In conjunction with this, priority measures proposed for MBPE increase reconstruction performance. Combining these methods improves the perceptual quality of the received image along with an increased network lifetime.

In this method, first EC is applied to the images. Then, the images are priority encoded. By this means, embedded replicas are prioritized as well as other valuable parts of the image, so error robustness of the image is increased.

3.4. IMAGE TRANSMISSION FRAMEWORK

Image transmission is crucial in WMSN. Any approach suggested for image transmission should take several aspects of WMSNs and the nature of image data into account. First of all, WSNs are erratic and the links have very poor qualities than traditional networks. On the other hand, broadcast nature of WSN should be utilized. With the addition of multimedia data, new factors which influence the design of transmission schemes are emerged, such as delay, delay-jitter, additional bandwidth requirement, congestions caused by streaming data and QoS support.

With the considerations above, a new image transmission framework, to be coupled with MBPE, is devised. It is based on the bursty transmission of large image partitions with prioritization via multiple paths.

This framework is scalable in terms of required memory and bandwidth. It gives opportunity for fine-grained adjustment of the transmission parameters to satisfy the application's QoS requirements. By the regulated buffer transmission mechanism included in it, congestions at intermediate nodes are avoided. This mechanism also helps to overcome delay-jitter. With the utilization of the link checking mechanism, it also achieves adaptive routing of the data, and by-passes holes caused by failing nodes.

First phase of the transmission occurs at the source node as shown in Figure 3.11. In the majority of the hardware platforms, images do not fit into the memory of the nodes. Therefore, the images are acquired from CMOS cameras via serial bus as partitions that can fit in available memory. The partitions are to be called as *pages* in the rest of the thesis.

The page coming from the camera is prioritized according to pre-determined priority levels, discussed in Section 3.1.2. As the result of this process, the macro-blocks in the page

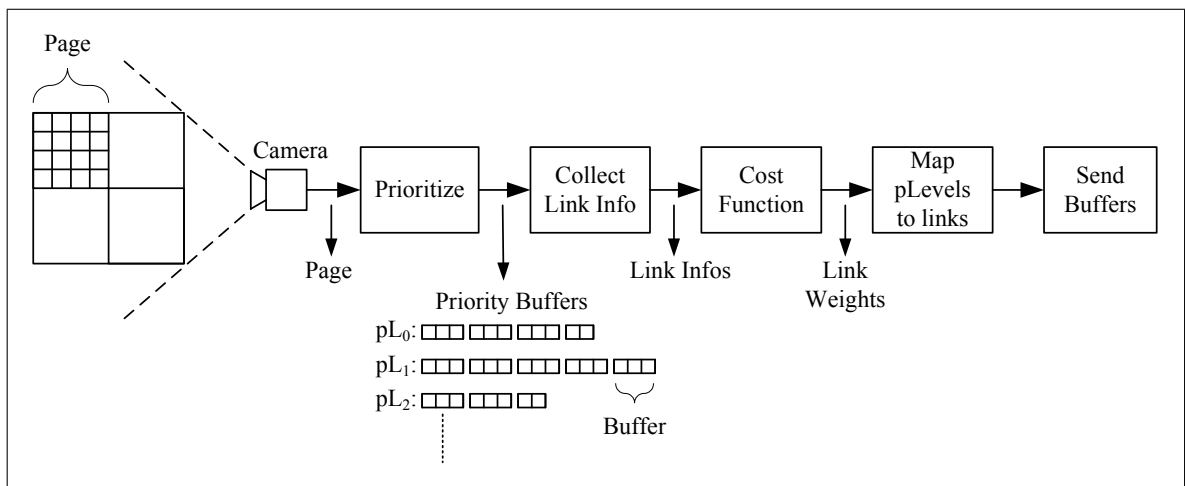


Figure 3.11. Source Node

are put into set of *buffers* according to the priority levels. Then, the information about links are gathered and fed to a *cost function* which weighs available links. The collection of the link and neighborhood information is assumed to be done by making use of the broadcast nature of the medium. With the weights calculated by the cost function, the priority levels are mapped to the available links. The highest priority buffer sets are to be sent via the best available link. When all the buffer sets in the page are transmitted, another page is taken from the camera until all the pages are completed. Figure 3.12 shows the algorithm for these operations.

So far, we explained the operations followed in the source node prior to transmission. Transmission of the pages as buffer sets also has an intrinsic mechanism. This mechanism is the most distinctive part of the proposed image transmission scheme. In this mechanism, buffer sets are transmitted in a bursty and regulated manner to avoid congestions and delay-jitter. Basically, an intermediate node receives a streaming buffer, holds it until the child node completes previous transmission, and then sends the buffer when the child node is ready. The state diagram of this mechanism is depicted in Figure 3.13.

In this mechanism, two kind of messages are used, namely *control messages (CM)* and *data messages (buffers)*. The buffers are transmitted without any reliability mechanism so no delay is introduced because of them. However, CM messages are assumed to be

```

1:  $pLevels \leftarrow PLEVELS$  {Number of priority levels.}
2: loop
3:   Wait for image query
4:    $Send(CMimageStart, camera)$ 
5:    $pageId \leftarrow 0$ 
6:   while  $pageID < numPages$  do
7:      $PAGE \leftarrow getNextPage(camera)$ 
8:      $(pBuff_1[n_1], pBuff_2[n_2] \dots pBuff_{pLevels}[n_3]) \leftarrow prioritize(PAGE)$ 
9:      $(links, linkInfos[links]) \leftarrow CollectLinkInfos()$ 
10:     $qualities[links] = CostFunction(linkInfos)$ 
11:     $children[pLevels] \leftarrow MapPlevelsToLinks(pLevels, links, qualities)$ 
12:    for  $i = 1$  to  $pLevels$  do
13:       $Send(CMpageStart, children[i])$ 
14:      for  $j = 1$  to  $n_i$  do
15:         $BUFFER \leftarrow pBuff_i[j]$ 
16:         $Send(BUFFER, children[i])$  as if RouterNode
17:      end for
18:    end for
19:     $pageId \leftarrow pageId + 1$ 
20:  end while
21: end loop

```

Figure 3.12. Source node algorithm

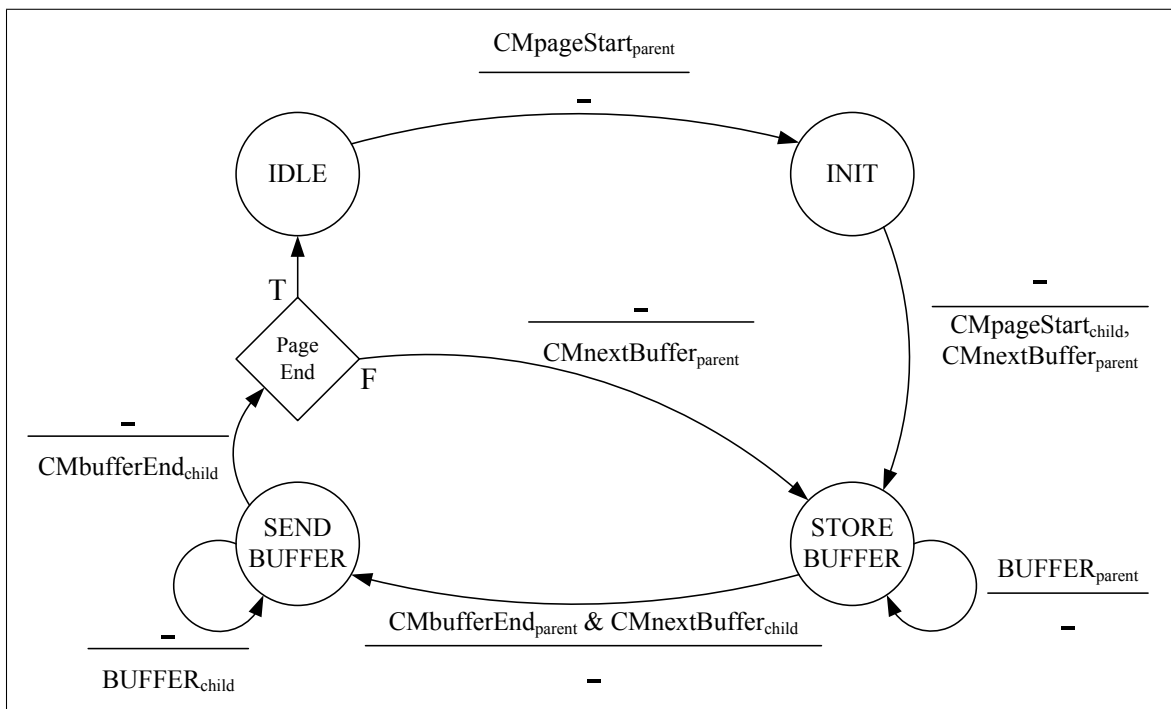


Figure 3.13. State diagram of an image transmission

transmitted reliably. Transmission of a page starts with a page start message (CMpageStart). This message includes meta information about the buffer set i.e. number of buffers and priority level. When a node gets a CMpageStart message, sends it to its child immediately, and to acquire a buffer, sends CMnextBuffer to its parent. Then the parent sends the next buffer to the node without any interruption till the end. When the buffer completes, the parent informs the node with CMbufferEnd message. The node holds the buffer until it gets both CMbufferEnd from the parent, and CMnextBuffer from his child. After it gets both of the messages, it sends the buffer to its child and so on. The steps of the algorithm are given in Figure 3.14. The illustration of an example transmission is also depicted in Figure 3.15.

```

1:  $pLevels \leftarrow PLEVELS$  {Number of priority levels.}
2: loop
3:    $bufferEnd \leftarrow \mathbf{false}$ ,  $nextBuf \leftarrow \mathbf{false}$ 
4:   while  $incomingMessage \neq CMpageStart$  do
5:      $incomingMessage \leftarrow Receive()$  {Idle state; wait for an image transmission.}
6:   end while
7:    $(numBuffers, bufferPriority) \leftarrow pageInit(CMpageStart)$ 
8:    $(links, linkInfos[links]) \leftarrow CollectLinkInfos()$ 
9:    $qualities[links] = CostFunction(linkInfos)$ 
10:   $child \leftarrow MapPriorityToLink(pLevels, bufferPriority, links, qualities)$ 
11:   $Send(CMpageStart, child)$ 
12:   $bufferId \leftarrow 0$ 
13:  while  $bufferID < numBuffers$  do
14:     $Send(CMnextBuffer, parent)$ 
15:    while  $(bufferEnd \mathbf{and} nextBuffer) = \mathbf{false}$  do
16:       $incomingMessage \leftarrow Receive()$ 
17:      if  $incomingMessage = CMbufferEnd$  then
18:         $bufferEnd \leftarrow \mathbf{true}$ 
19:      else if  $incomingMessage = CMnextBuffer$  then
20:         $nextBuffer \leftarrow \mathbf{true}$ 
21:      else
22:         $BUFFER \leftarrow incomingMessage$ 
23:      end if
24:    end while
25:     $Send(BUFFER, child)$ 
26:     $Send(CMbufferEnd, child)$ 
27:     $bufferId \leftarrow bufferId + 1$ 
28:  end while
29: end loop

```

Figure 3.14. Router node algorithm

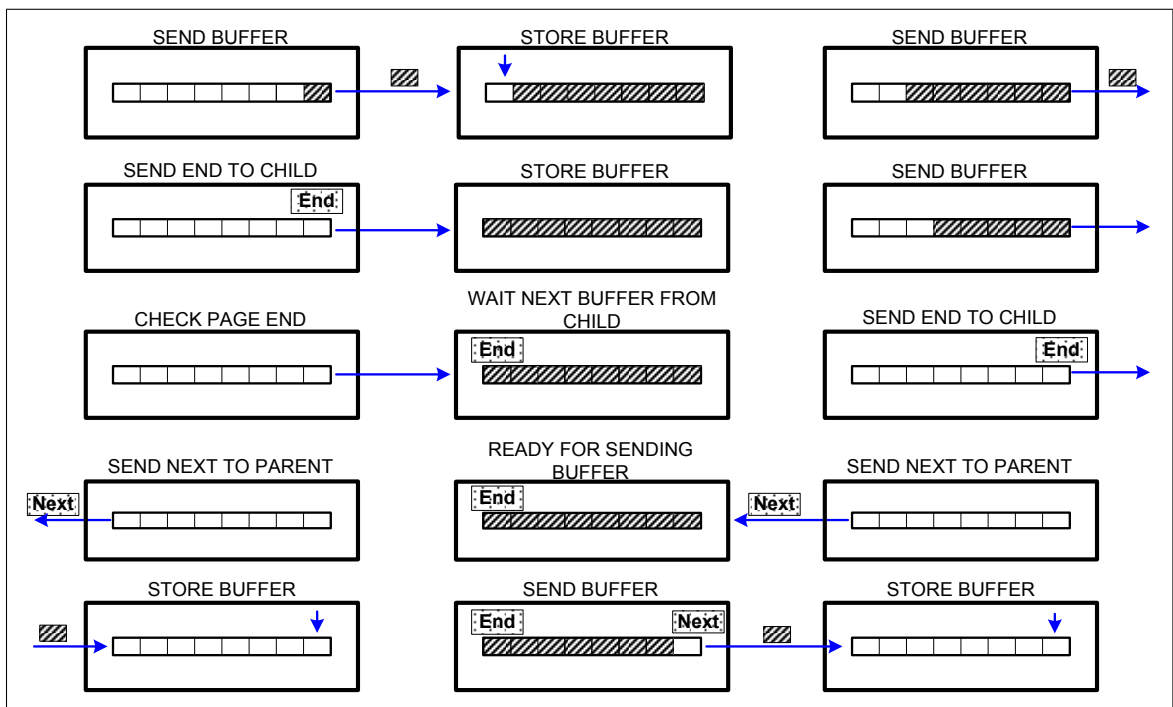


Figure 3.15. The illustration of an example transmission

4. EXPERIMENTS

In this study, the proposed methods are validated by real implementations and exhaustive tests. The real implementations help us to see applicability of the methods on COTS sensor nodes. The exhaustive tests reveal the robustness of the methods in different circumstances.

In this chapter, first, image quality metrics that are used for the evaluation of the received images in our experiments are exposed. After that, the details of the implementations and the experimental tests are given with the performance analysis and the discussions.

4.1. IMAGE QUALITY METRICS

In our study, we encountered the lack of a suitable image quality evaluation metric for packet based networks in which transmitted images are not reconstructed. Therefore, for the evaluation of MBPE, we propose an IQM called Object Transmission Rate (OTR). This IQM is explained in the following section. On the other hand, we utilize a well-known PSNR metric for the evaluation of EC coded images, since it is suitable for the situations in which any kind of reconstruction mechanism is employed after the transmission.

4.1.1. Object Transmission Rate (OTR)

In image processing, most of the evaluation metrics try to cope with some kind of distortion, i.e. change in brightness and luminance. However, in packet-based networks, image data is not distorted. Only the packets representing some part of the image are lost or not. The packets received by the sink are in full quality. Therefore, there is no widespread quality degradation. Considering this situation, we devise a new metric called *Object Transmission Rate* (OTR). OTR measures the rate of the transmitted objects which are subjects of the applications.

To compare OTR with PSNR, we performed the following experiment. We picked a test image containing objects. We labeled objects in it as given in Figure 4.1.b manually. For each image packet priority measure, we calculated the PSNR and OTR values. As shown in Figure 4.1, although the images transmitted with different measures have very close PSNR values, their OTR values differ much. Delta-edge measure is the worst one in PSNR but the most successful in OTR and the most of the objects in it (98 per cent) is transmitted. Therefore, OTR is utilized to evaluate the performance of the proposed image priority measures.

4.2. MBPE EVALUATION

We establish an experimental setup for the analysis of macro-block based priority encoding (MBPE). Border surveillance is taken into account as an example application scenario. Border surveillance is such an application, where sensor nodes equipped with low-power cameras can be utilized in an intrusion detection scenario. Critical parameters in MBPE, such as priority levels and thresholds, are determined according to requirements of this application. In order to compare the performance of the proposed priority measures, we use OTR as a performance metric. Transmissions over lossy links without any encoding case is used as the baseline for the comparisons. We also justify the feasibility of the measures by implementing them on Tmote Sky sensor nodes.

4.2.1. System Model

In this part of the study, a WMSN based border surveillance system is considered. The system consists of a set of sensors ($V_i, i=1, 2 \dots, k$) equipped with simple low power CMOS cameras such as Cyclops and CMUcam3, a set of routing sensors ($R_{ij}, i=1, 2 \dots, k_1, j=1, 2 \dots, k_2$) and a sink as given in Figure 4.2. If intruders cross the border, camera sensors capture their image and then transmit these images to the sink via routing sensors R_{ij} . Prior to transmission, the camera sensors partition the captured $N \times M$ 8-bit grayscale images into $m \times m$ pixel macro-blocks. These macro-blocks are serially passed to the network layer for encoding.

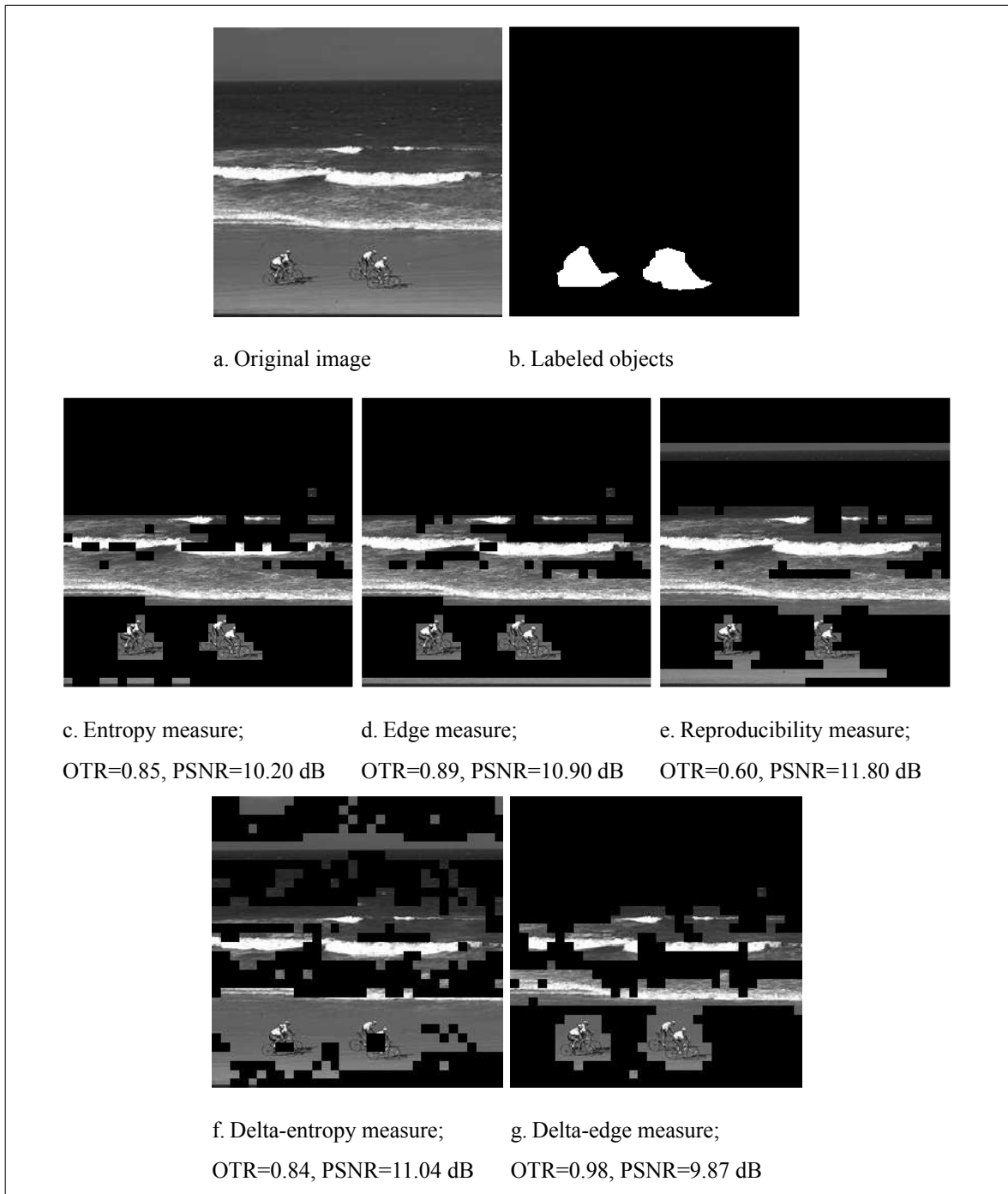


Figure 4.1. Comparison of OTR and PSNR values on a test image

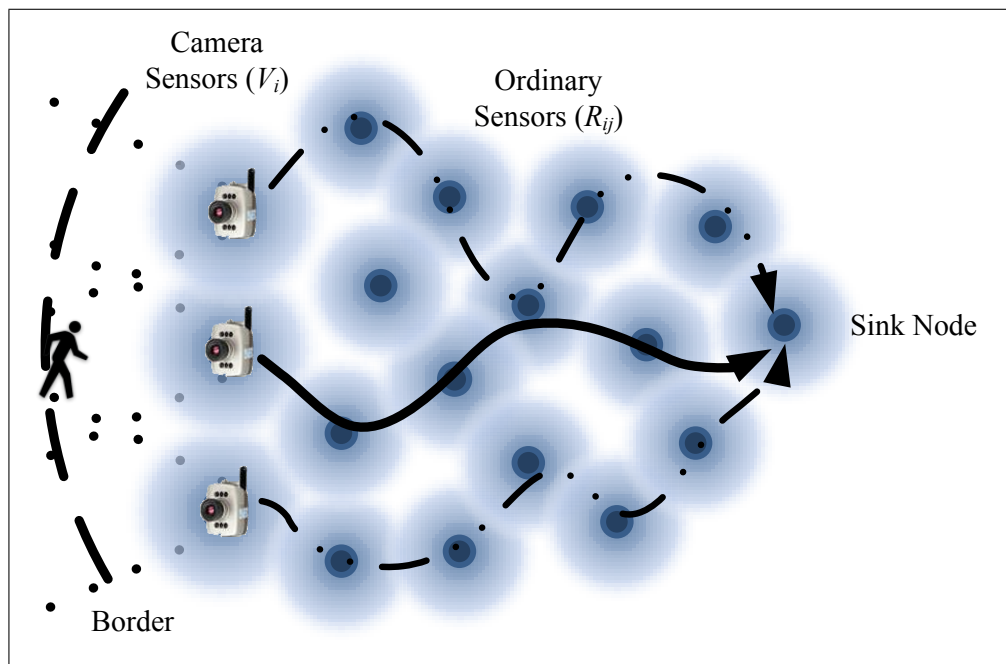


Figure 4.2. WMSN scenario for border surveillance

In the border surveillance application, the information needed to be extracted from the gathered images is intruders. The quality of the image parts containing objects is valuable. Therefore, their successful transmission to the sink node is more important than transmitting the background image. Since there are two classes of data ,i.e. objects and background in the images, for this application, it is suitable to employ two priority levels as “important” and “not-important”. The thresholds to classify macro-block weights obtained by the priority measures are determined by using possible images in such a border surveillance scenario. The packets at the network are labeled as “important” or “not-important” according to applied measures and corresponding thresholds.

In the experimental setup, it is assumed that sensor nodes do not fail during image transmission and a reliable communication path between node V_i and the sink is established prior to image transmission using a reliable transport protocol. Establishment of the reliable path is not the focus of this thesis and is not studied further.

In our transmission scheme, each macro-block labeled as “important” in accordance with the selected priority measure is transmitted as one data packet through the reliable

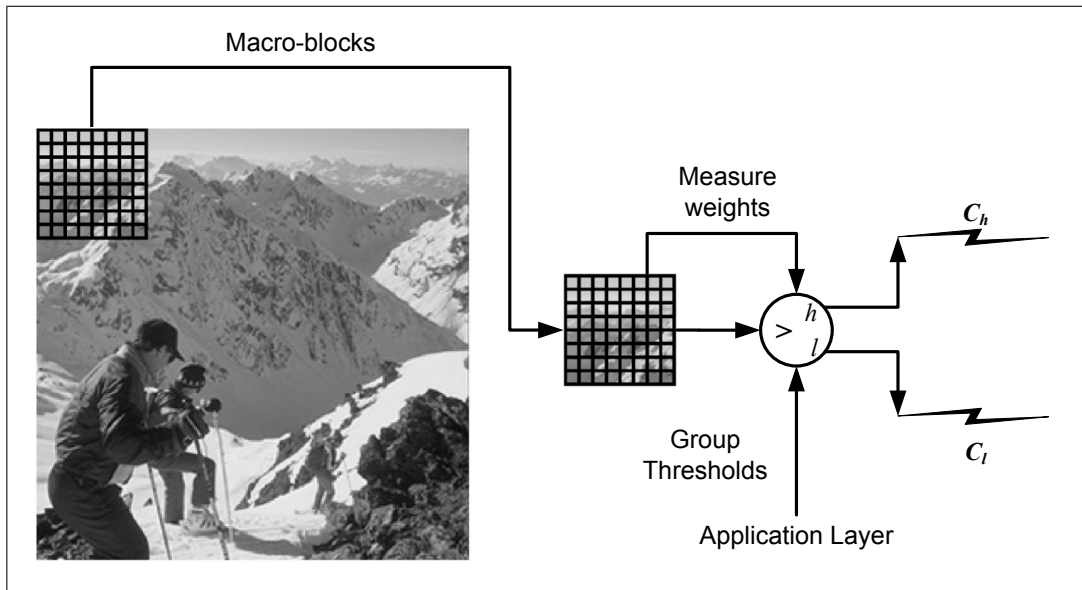


Figure 4.3. Transmission scheme used in MBPE experiments

channel C_h with a transmission probability $p = 1$ as shown in Figure 4.3. The “not-important” macro-blocks are transmitted through channel C_l with $p = 0$, i.e. these packets are dropped from the network buffer.

4.2.2. Methodology

In this study, we selected test images in accordance with their suitability to surveillance applications. For this purpose, we picked 26 images ($I_{j=[1,26]}$) from [80, 81]. Some of these test images are shown in Table 4.4. We employ the following operational steps in the experiments.

We first implemented the proposed measures under Matlab. We represented each measure by index $i = \{entropy, edge, reproducibility, delta-entropy, delta-edge\}$. Applying each measure i to test images (I_j), we obtain *macro-block weight matrices* for each measure-image pair as M_j^i . Examples are previously given in Figure 3.3, Figure 3.4 and Figure 3.6.

The distribution of macro-block weights for each image varies dramatically. On



Figure 4.4. Sample test images used in MBPE experiments

the other hand, because of the limited memory and processing capacity of sensor nodes, finding a reasonable *threshold value* on-the-fly is a non-trivial task. This situation led us to group-based thresholding. We aimed to label approximately half of the macro-blocks as “important”. To find the required threshold to achieve this ratio, for each measure, first we found the median of the macro-block weights of each image in the group (\tilde{M}_j^i). As a result, we got a set of medians ($m^i = \{\tilde{M}_1^i, \tilde{M}_2^i, \dots, \tilde{M}_{26}^i\}$) for the group. Then, we determined the group threshold (t^i) as the median of this set (\tilde{m}^i). Cumulative Distribution Functions (CDFs) and histograms of the macro-block weight matrices together with calculated t^i values for each measure are depicted as two parts in Figure 4.5 and Figure 4.6.

At this step, we applied the thresholds to macro-block weights. Since our thresholding mechanism is group and measure based, we obtained different *Prioritized Packet Rates* (PPRs) for each measure-image pair. The acquired PPRs are given in Figure 4.7 and Figure 4.8 as two parts.

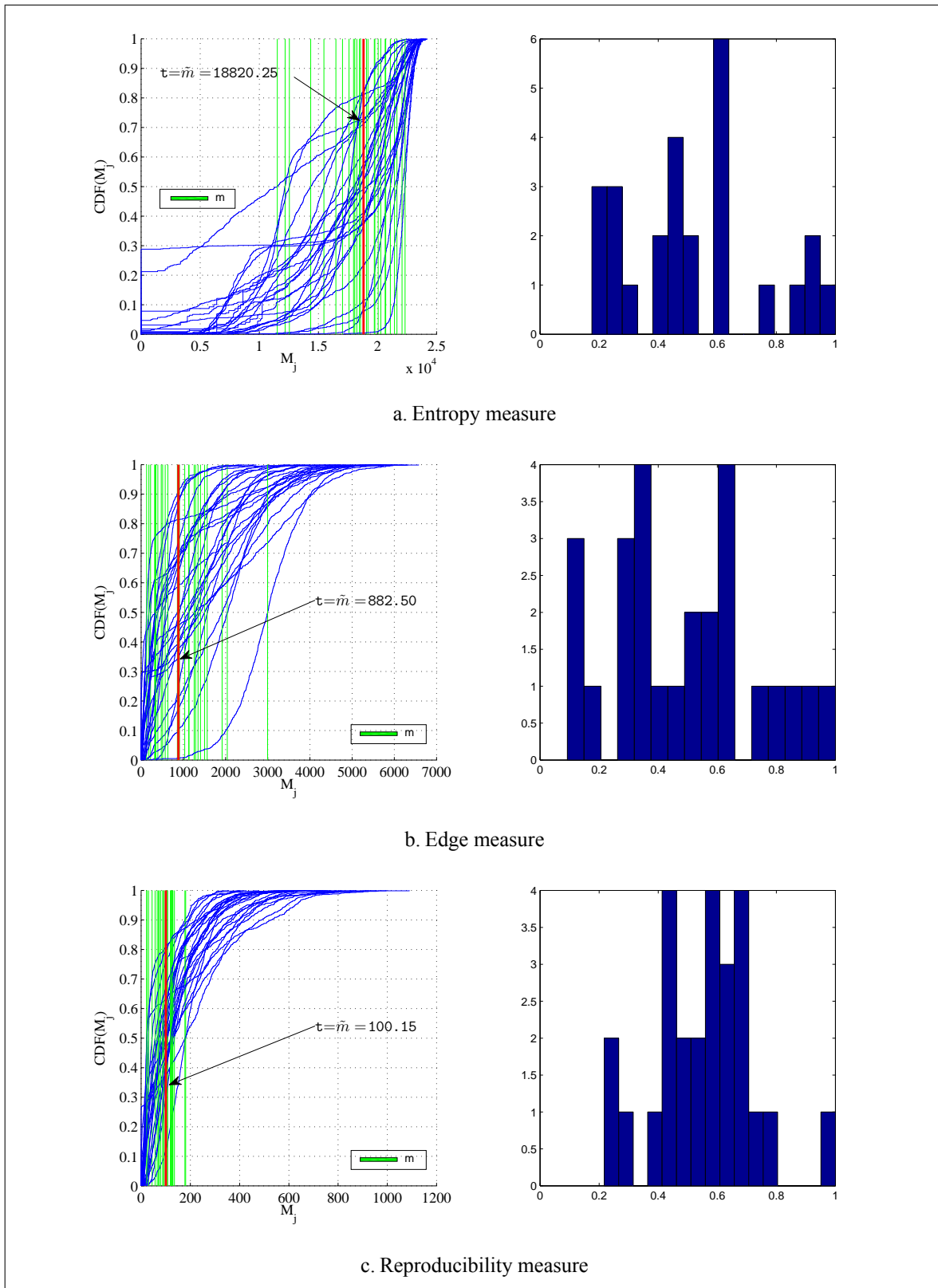


Figure 4.5. CDFs with group thresholds and histograms of each measure (Part 1 of 2)

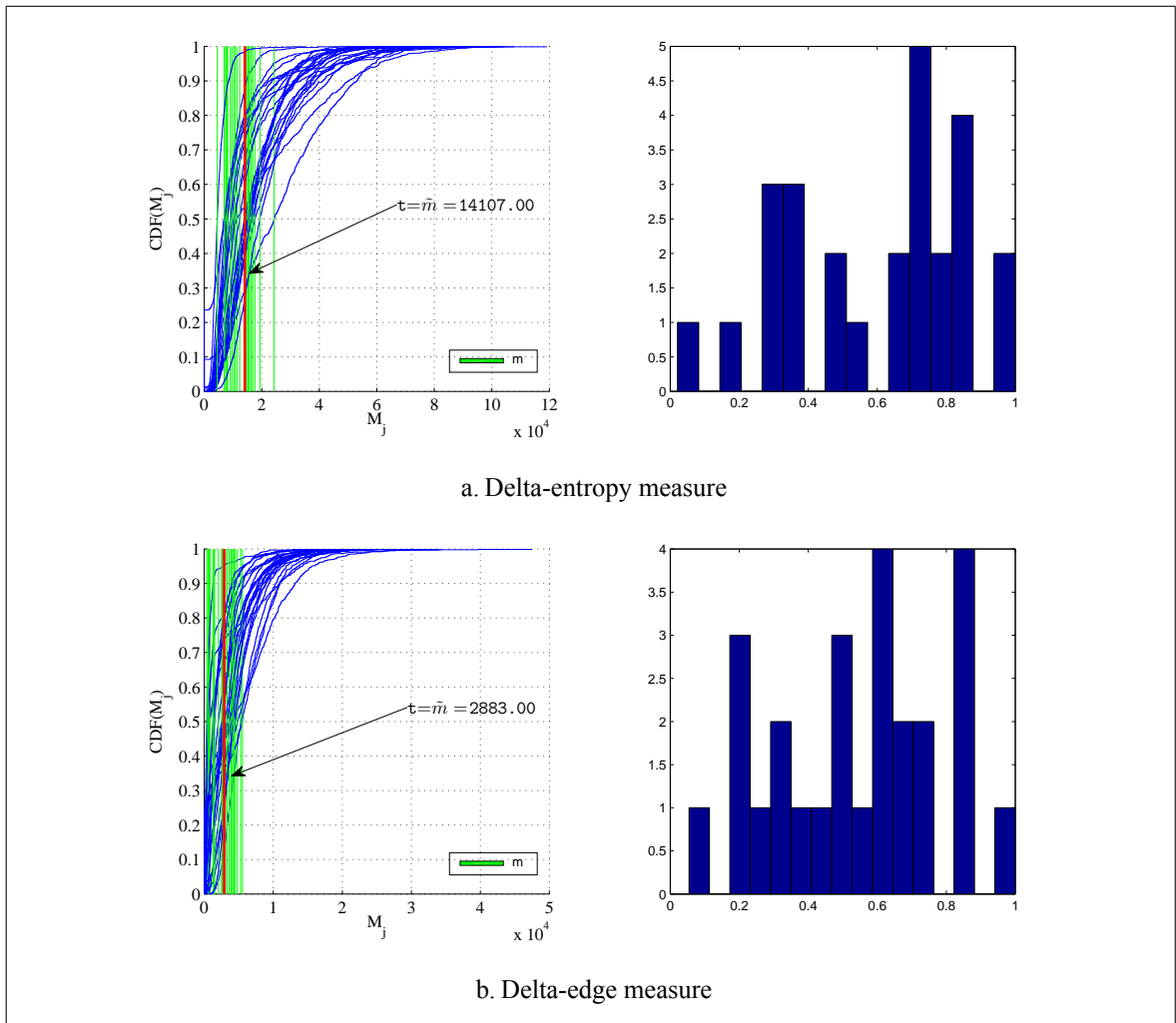


Figure 4.6. CDFs with group thresholds and histograms of each measure (Part 2 of 2)

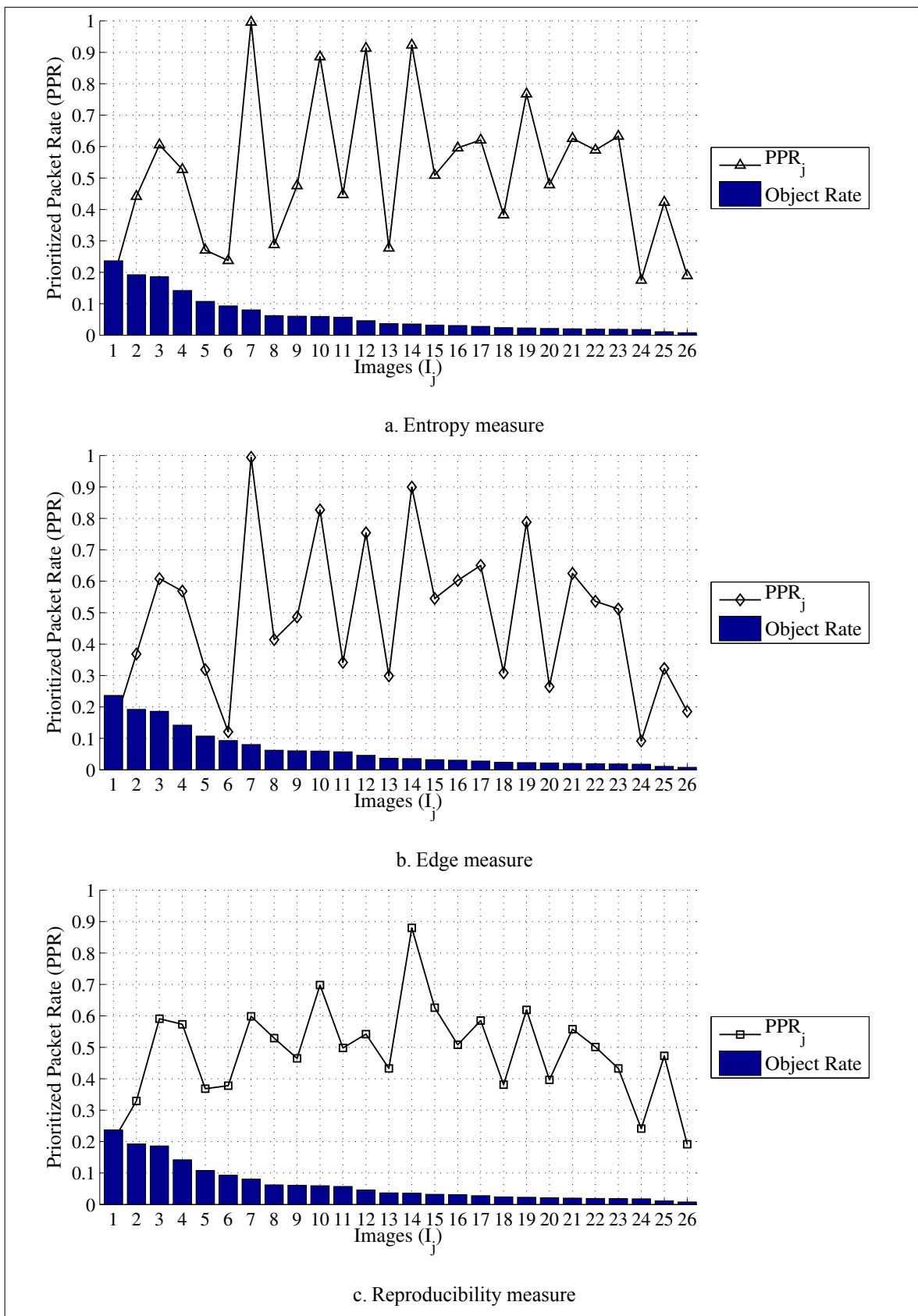


Figure 4.7. PPR values for all measures (Part 1 of 2)

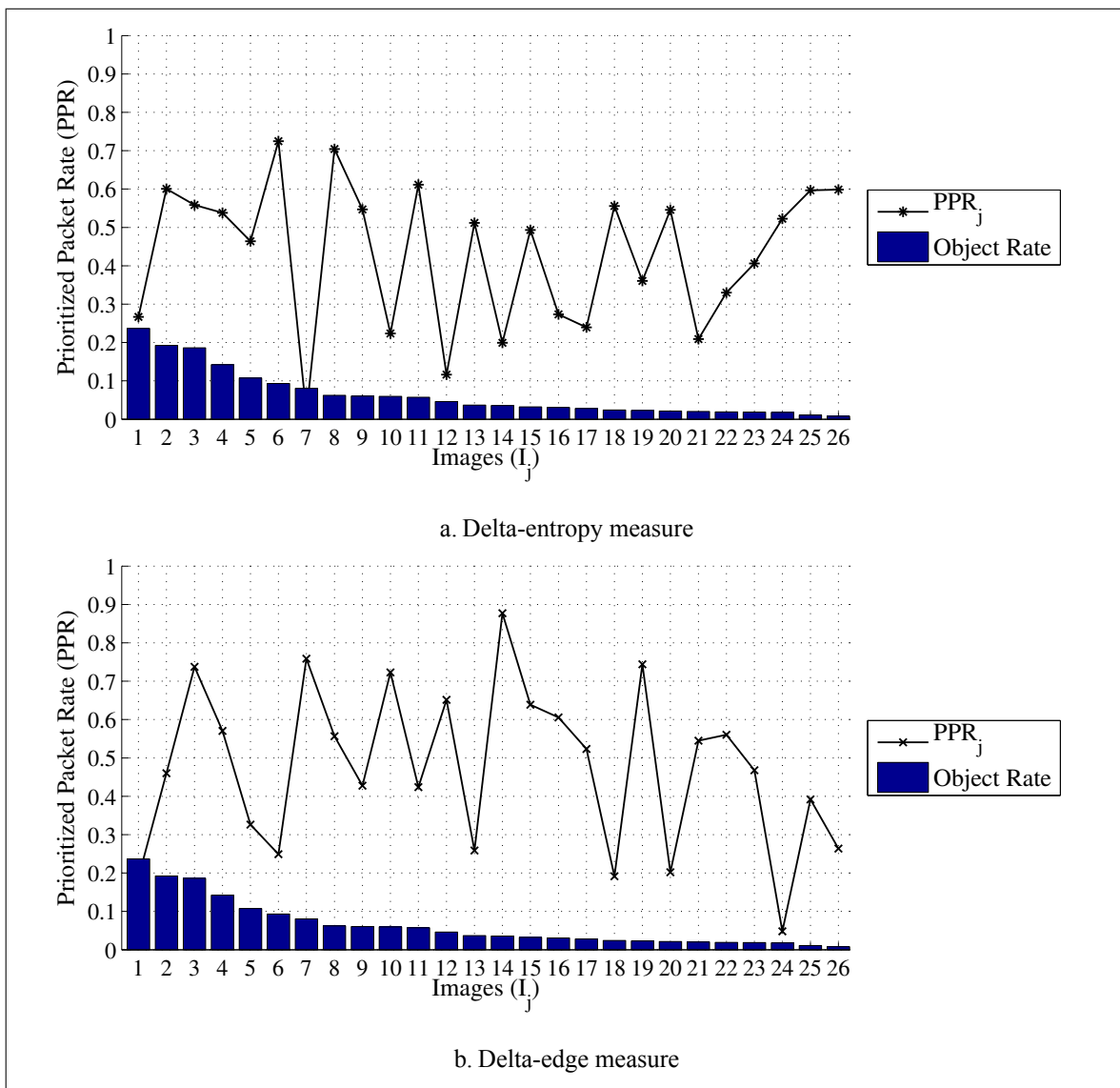


Figure 4.8. PPR values for all measures (Part 2 of 2)

According to our model, only the prioritized macro-blocks are transmitted. Thus, resulting images consist of only “important” macro-blocks. We also assumed that a network packet includes one macro-block. Therefore, the prioritized macro-blocks are equal to the transmitted packets.

4.2.3. Performance Analysis

We finally focus on the performance analysis of our measures in this section. We achieve this through several comparative tests and simulations. Moreover, implementation costs of the measures on real sensor nodes are given and compared to the JPEG compression algorithm.

4.2.3.1. Monte Carlo Simulations

We conducted a set of Monte Carlo simulations under Matlab to compare the results of the proposed measures. To make reliable comparisons, for each measure-image pair we fed the simulations with the corresponding PPRs. Running the simulations 128 times, we obtained 128 different transmitted images with uniformly distributed prioritized packets for each measure-image pair. Then, we calculated OTR values of these images and calculated the median of them as the representative of the measure-image pair ($OTRsim_j^i$). These values with the corresponding OTR_j^i values and the rate of the objects in original images are given in Figure 4.9 and Figure 4.10 as two parts.

As a success criterion of the proposed measures, the number of tests in which OTR_j^i is greater than the corresponding $OTRsim_j^i$ is considered. In this way, *entropy* and *edge* measures are unsuccessful for the images I_2 , I_7 , I_{10} and I_{12} . This yields to 85% success rate for these measures. However, *reproducibility* measure has 100% success rate.

4.2.3.2. Object Transmission Index

Another consideration points out the relation between OTR and PPR. To assess this relation, we generated the *Object Transmission Index* (OTI) which is calculated as

$$OTI = OTR/PPR \quad (4.1)$$

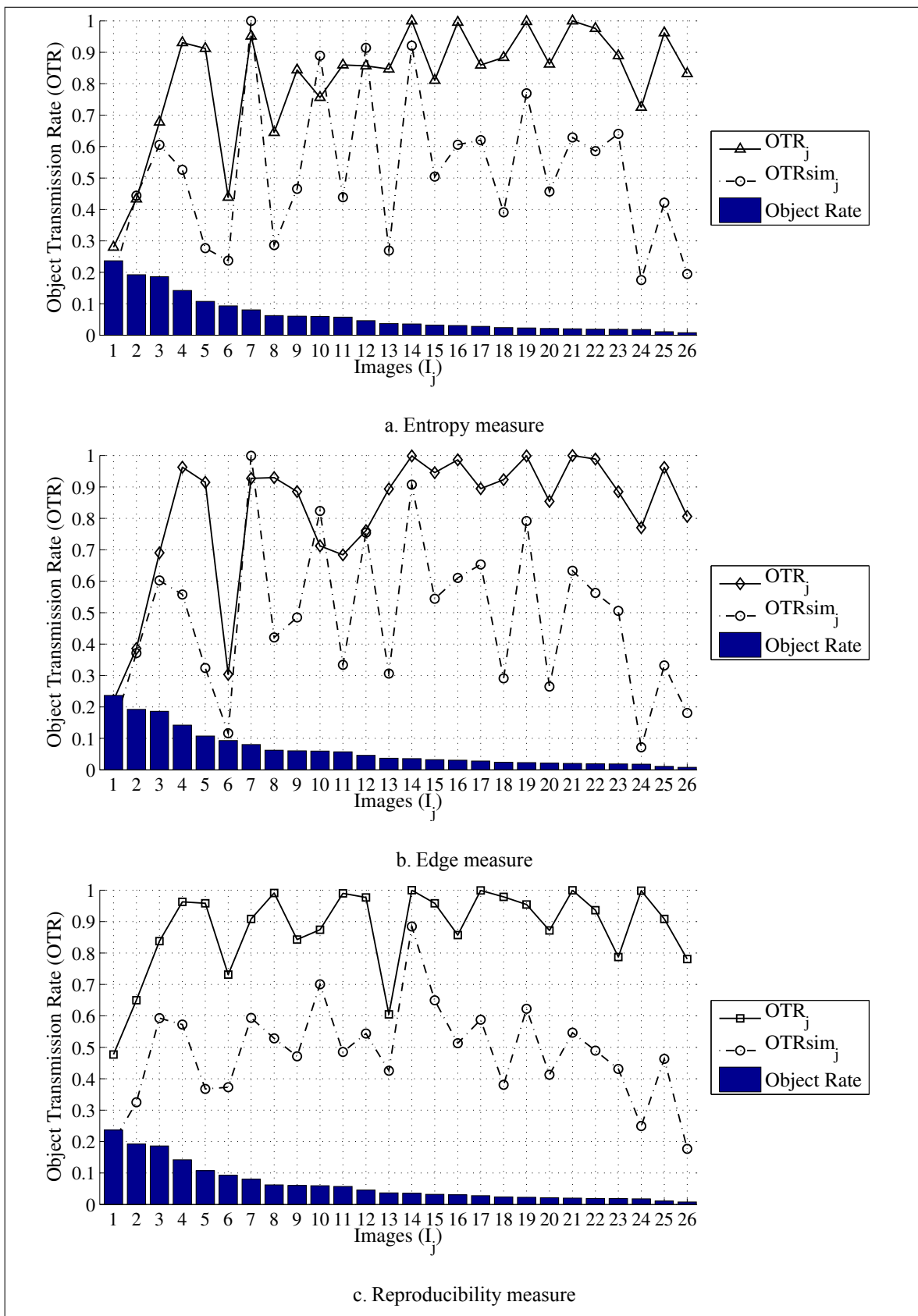


Figure 4.9. OTR values for all measures and corresponding simulations (Part 1 of 2)

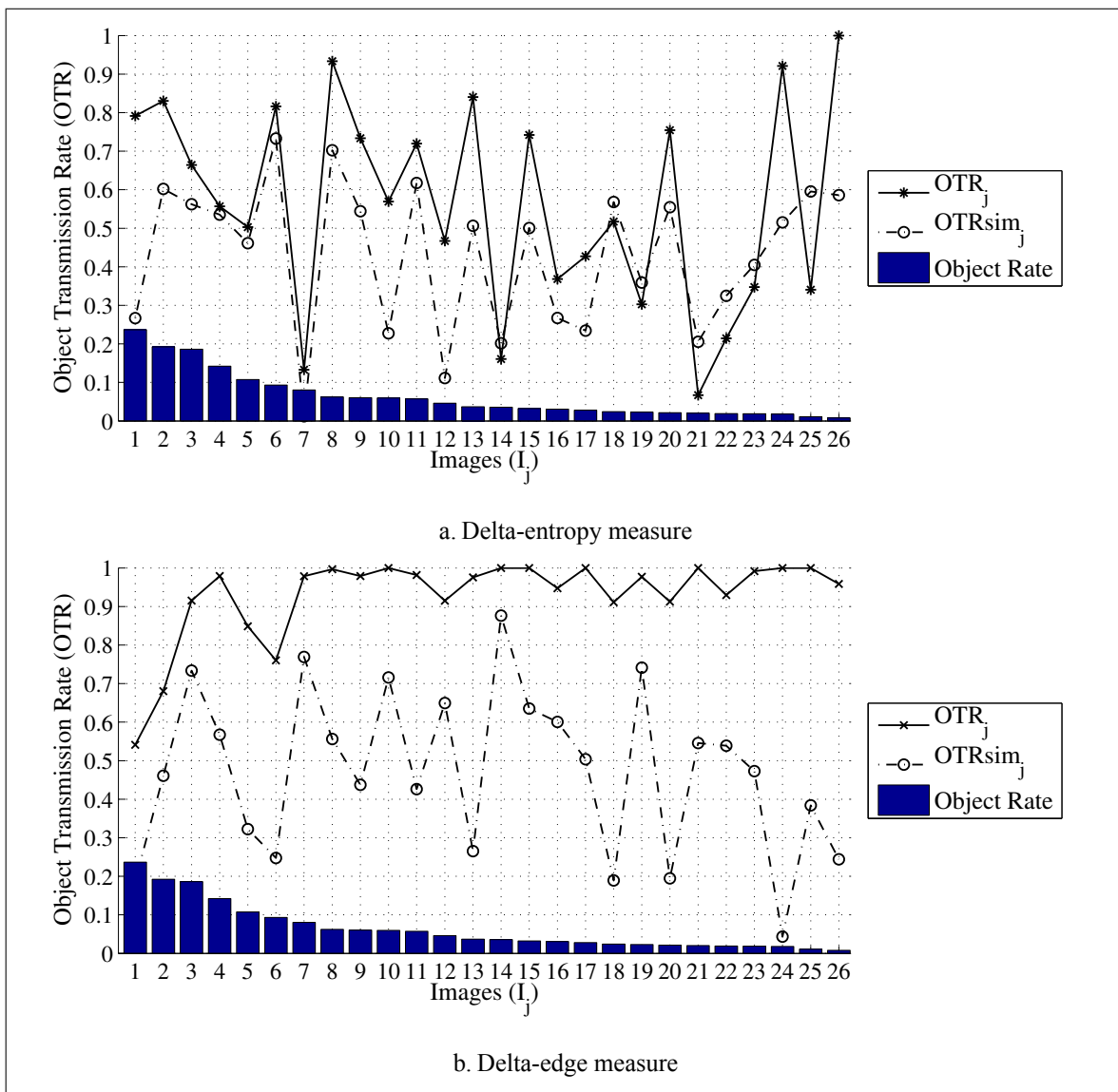


Figure 4.10. OTR values for all measures and corresponding simulations (Part 2 of 2)

Table 4.1. Object transmission index values

Measures	$\mu(OTR_j)$	$\mu(PPR_j)$	$\mu(OTI_j)$
Entropy	0.8164	0.5176	1.58
Edge	0.8186	0.4832	1.69
Reproducibility	0.8782	0.4845	1.81
Delta-edge	0.9300	0.4765	1.95
Delta-entropy	0.5662	0.4312	1.31

This index shows us the best measure in which maximum amount of objects are transmitted with minimum amount of packets. We calculated it for all images and measures by taking the mean of their OTR and PPR values. The mean OTIs for all measures are shown in Table 4.1. The results reveal that delta-edge measure is the most successful one with the highest OTI.

4.2.3.3. Implementation Cost

We examined the implementation costs of the proposed priority measures on resource-poor real WSN nodes. As WSN nodes, *Tmote sky motes* are used. We implemented each measure in TinyOS v2.1 with nesC v1.3. At this stage, the processing capability of the nodes is examined. Image data is transmitted in packets as 8×8 pixel macro-blocks from base computer to the sensor node via serial interface in a bursty manner without any delay between packets. At the reception of each packet, the corresponding priority weight for the selected measure is calculated and the packet with a weight higher than threshold is forwarded through the reliable routing path. At the first implementation, edge and reproducibility based measures succeeded by forwarding all the packets. However, in entropy based measure, some packet losses occurred. The reason for the losses were the inability of the node to process floating point calculations included in this measure at the packet transmission rate. As a solution to the computational deficiency, we transformed the floating point operations to fixed point operations by storing the terms including logarithmic expressions as tables in program memory. With this modification, entropy based measure succeeded without any packet loss. Implementation costs of each measure for a macro-block are given in Table 4.2

Table 4.2. Implementation costs of the measures for a macro-block

Measures	CPU Cycles	Program Memory (bytes)	Data Memory (bytes)	Network Buffer (bytes)
Entropy	8270	206	454	64
Edge	2800	126	72	64
Reproducibility	1820	514	154	4480
Delta-entropy	10090	720	608	4544
Delta-edge	4620	640	226	4544

in terms of memory usage and CPU cycles.

4.2.3.4. *JPEG Comparison*

To compare the implementation costs of the priority measures with the well-known compression algorithm JPEG, we use the JPEG implementation costs in [7] for two different quality levels. With regard to computational cost, three phases of JPEG compression are considerable. Those are Discrete Cosine Transform (DCT), quantization and entropy coding. In that work, the authors propose optimizations for the DCT and quantization phases. By adjusting integer and fractional bit-widths needed in view of other approximations inherent in the compression process and choice of image quality parameters, they achieve speed and energy improvements ranging from factors of 2 to 5 depending on the considered portion of the algorithm.

In JPEG compression, quantization is performed by using a quantization table. To adjust the resulting image quality and the ratio of compression, the values at the quantization table are rescaled in inverse proportion to a quality setting Q_{tab} ranging from 1 (very poor image quality) to 100 (very good image quality). $Q_{tab} = 50$ corresponds to no scaling of the quantization table. We use two Q_{tab} values 50 and 90 in our comparisons. Table 4.3 shows the execution time and energy consumption of a macro-block for the priority measures and the JPEG algorithm. As the results point out that computational costs of the proposed priority

Table 4.3. JPEG comparison

Methods	CPU Cycles	Time (ms)	Energy (mJ)
Entropy	8270	1.03	3.10
Edge	2800	0.35	1.05
Reproducibility	1820	0.23	0.68
Delta-entropy	10090	1.26	3.78
Delta-edge	4620	0.58	1.73
Fast JPEG ($Q_{tab} = 50$)	20918	2.61	7.84
Fast JPEG ($Q_{tab} = 90$)	34864	4.36	13.07

measures are far less than the traditional and mostly used compression algorithm JPEG.

4.2.4. Discussion

The results of the experiments show the performance gain in OTR and OTI, achieved by the proposed measures in MBPE. Each measure has different advantages. While edge measure has the minimum memory requirement, reproducibility measure needs least processing time. Besides, delta-edge measure is the most successful one in terms of OTI. The measures should be chosen according to the application and considering the underlying hardware. By using MBPE scheme in this scenario approximately half of the bandwidth is saved. By means of this, approximately half of the energy consumption of the whole system is reduced.

The results also indicate that adaptive labeling can successfully be done using application specific group based thresholds. Labeling the macro-blocks without acquiring full image data and computational simplicity of the proposed measures make it possible to implement this method on COTS sensor devices.

Considering the results above, MBPE is a lightweight and energy efficient method and can be adopted to different kind of application scenarios in WMSNs.

4.3. REAL TESTBED

In order to examine the effect of channel conditions on transmitted images, a real testbed is set up. Using this testbed, images are transmitted over a WSN in different channel conditions and the quality degradations caused by channel impairments are measured in terms of PSNR. Both raw images and EC coded images are considered in the testbed.

4.3.1. System Model

Figure 4.11 depicts the considered system in our experiments. This is a multi-tier system that includes two types of sensors; Type 1 $V_i, i = 1, 2 \dots w$ sensors are equipped with camera and Type 2 $R_{ij}, i = 1, 2 \dots w_1, j = 1, 2 \dots w_2$, sensors are simple routing sensors. Since the EC algorithm includes DWT, full image is necessary to realize it. Therefore, V_i 's and the sink's capabilities are higher than that of the R_{ij} 's in terms of energy, processing power and storage capacity.

In the tests, the received image quality is compared for three transport variants:

1. No error concealment (NC)
2. Error Concealment over single path (EC)
3. Error Concealment over disjoint multipath (ECDP)

In all schemes, $N_1 \times N_2$ 8-bit grayscale images are tiled into $m \times m$ pixel macro-blocks at the V_i node. Each macro-block is transmitted in a separate network packet towards the sink over a multihop WSN. So, the number of distinct data packets to be transmitted is $N = N_1 \times N_2/m^2$ per image. Scheme (1) is the simplest case, in which raw images are transmitted on a single path, selected as a baseline for performance improvement. Scheme (2) employs the error concealment algorithm on a single path. Scheme (3) employs the error concealment algorithm on two disjoint paths.

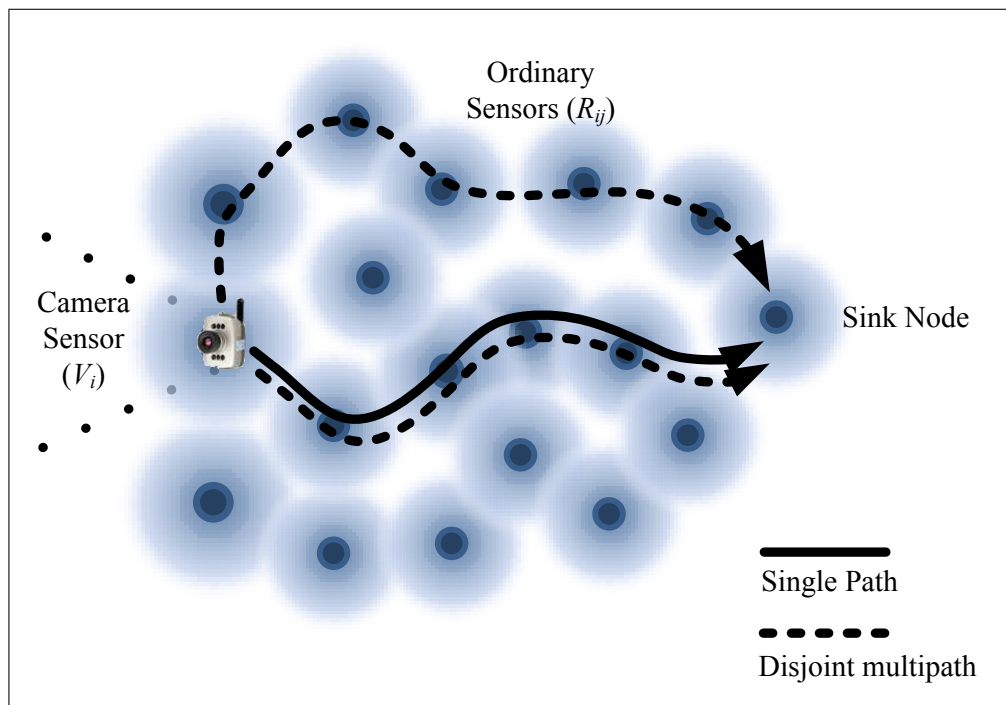


Figure 4.11. Testbed WMSN scenario

Disjoint multipath transmission is employed to provide fault tolerance at the expense of increased bandwidth usage and processing overhead. In this scheme, images are transmitted through diverse paths to improve the perceptual quality of the received image at the sink. Disjoint multipath transmission scheme constructs n_p disjoint paths ($n_p = 2$ in our case). These parallel streams may independently suffer from node failures and channel impairments. Therefore, received redundant images may include both lost and correct pixel values. However, the likelihood of simultaneous losses on all the paths is lower than losses on a single path. This probabilistic leverage facilitates an additional robustness of multipath transmission. Disjoint multipath scheme also utilizes a simple fusion algorithm, namely, *select max* on the sink. The algorithm performs fusion in the pixel value domain by selecting for each fused pixel the input coefficient with the largest absolute value. The block diagram of this operation is depicted in Figure 4.12.

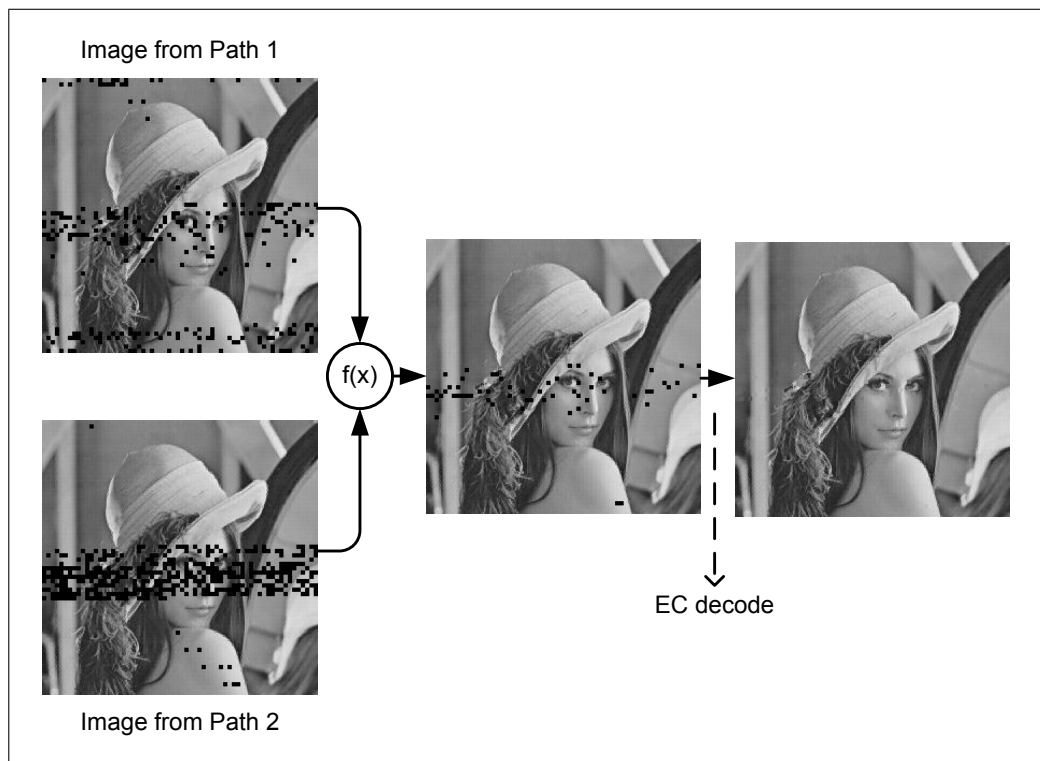


Figure 4.12. An illustration of EC DP

4.3.2. Methodology

The system modelled in Section 4.3.1 is realized as follows. Since V_i is supposed to be more capable, its role is accomplished by a computer via functions implemented under Matlab and Java. A test image, coded and tiled into macro-blocks according to the transmission scheme, is sent in data packets serially to the first node of the established WSN testbed. The testbed consists of Tmote Sky sensor nodes. The nodes are programmed using TinyOS v2.1 libraries and tool-chain [82]. In the testbed, the test image is transmitted to the sink through a chain topology. A novel backchannel mechanism is devised to collect received images at each hop concurrently in a non-intrusive manner. Quality indicators of each link are also appended to the results. Received images with the indicators are sent to the computer serially. At the computer side, for each transmission, loss patterns are extracted from the received images. Then, the patterns and transmission details such as Packet Reception Rate (PRR), hop count, quality indicators etc. are stored in a MySQL database. Overall software diagram of this setup is given in Figure 4.13.

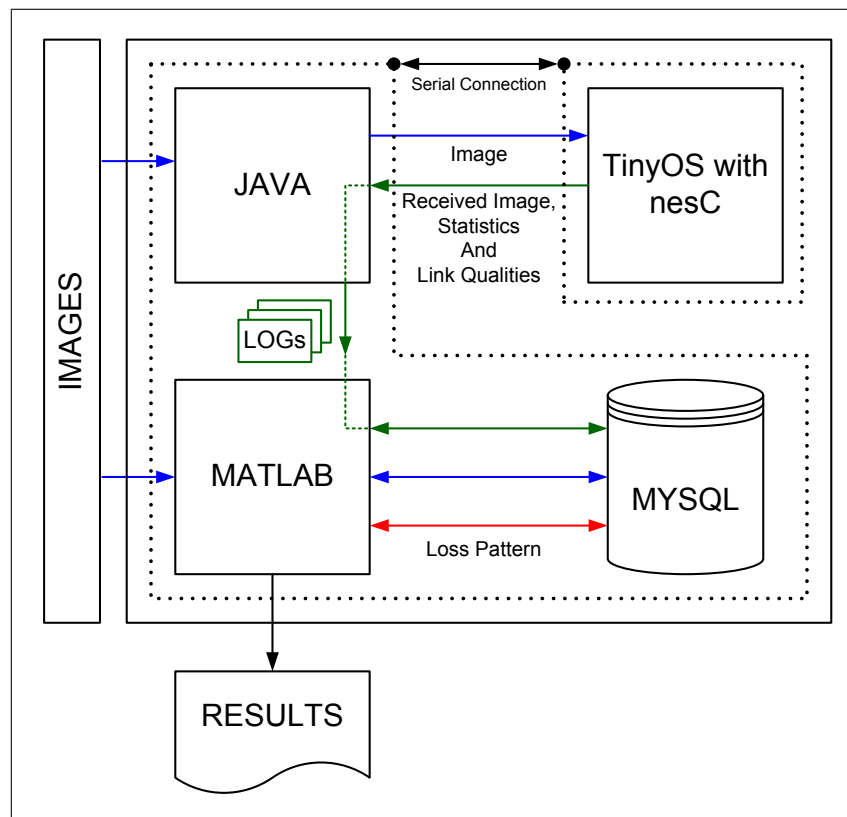


Figure 4.13. Testbed software diagram

After the transmission phase, to make more equitable comparisons of the EC algorithm on different images, instead of repeating the tests for different images, the stored image loss patterns are used as masks. These masks are projected to 30 encoded test images. Then, the images are decoded using the EC algorithm. The block diagram of this operation is given in Figure 4.14. The quality evaluations are made over the resulting images, in terms of PSNR. The results to be given at the following parts of the thesis include only five images, depicted in Figure 4.15, due to size and readability considerations in the graphics. However, the results for the other images are similar to the ones presented.

The difficulties to establish a test setup for disjoint paths in a building with the requirements above led us to use another method to realize the tests for ECDP scheme. The tests taken place at the same time of two different days are matched, the gathered image loss patterns are combined as if they are coming from disjoint paths. Again, the image loss patterns are projected as masks to the other test images.

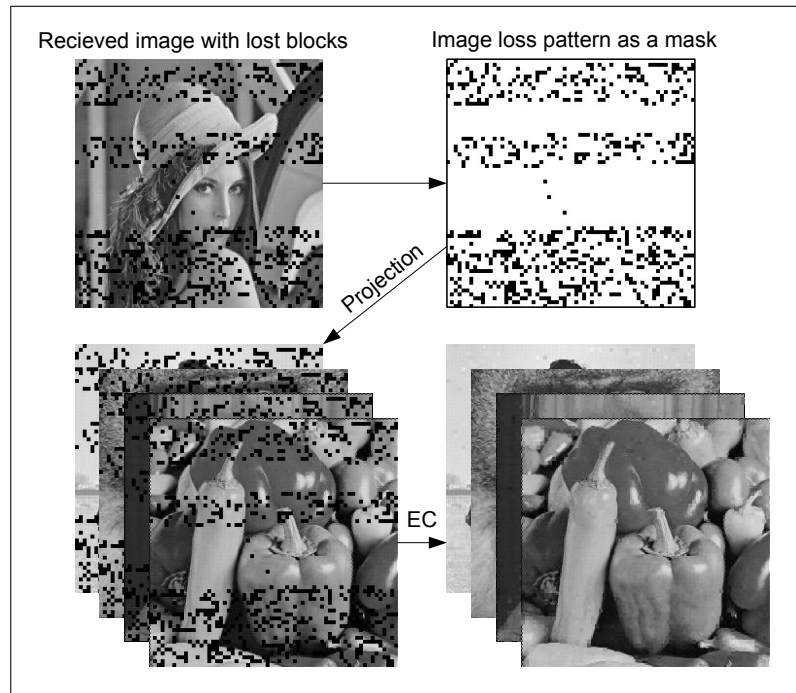


Figure 4.14. Projecting image loss patterns to different images

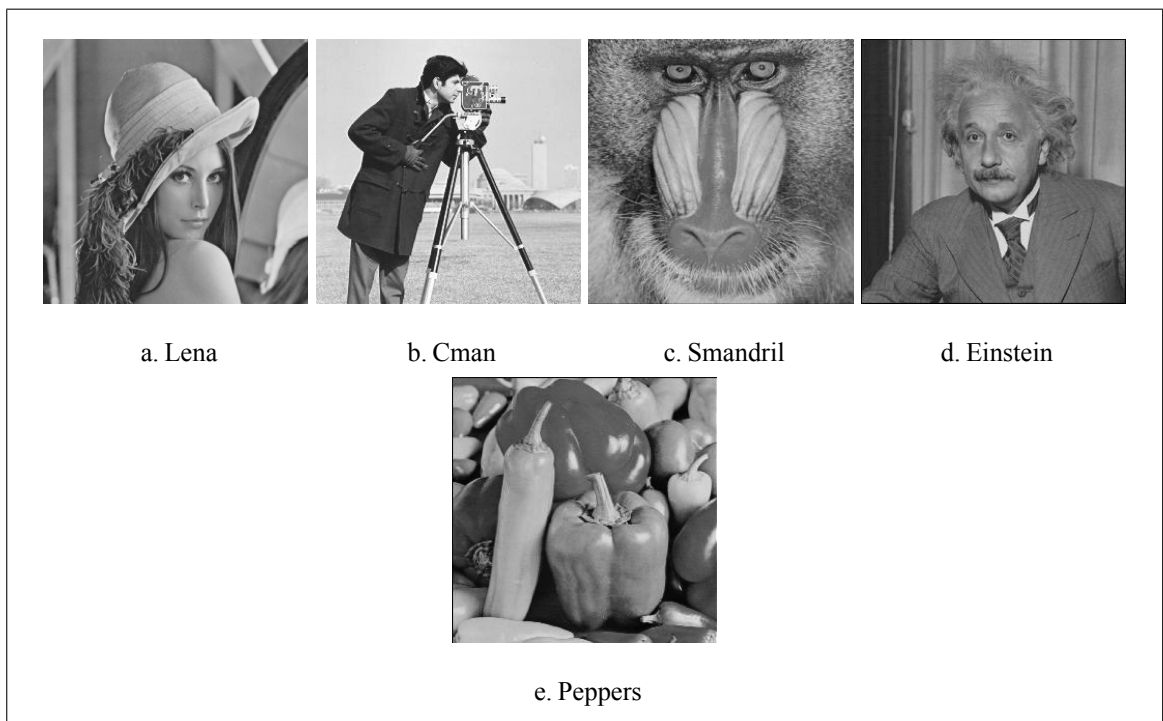


Figure 4.15. Test images used in EC tests



Figure 4.16. A view from testbed area

4.3.3. Testbed Setup

An indoor testbed is established in this study. The testbed includes 20 Tmote Sky nodes in a 10-hop chain topology. Ten of them are used for data collection as backchannel. The details of the testbed are given in the following sections.

4.3.3.1. Node Deployment

We aim to achieve a clear line of sight between nodes and make them to share the same communication medium to homogenize environmental effects on the communication channels. Therefore, the tests are conducted inside a building with a large *atrium* illustrated in Figure 4.16. Moreover, the nodes are partitioned into two groups, namely, *Group0* and *Group1*. The nodes in the groups are lined up vertically on thin linear sticks (Figure 4.17) which are horizontally pointed out from the windows on the first floor, approximately 5m above from the ground, with no obstacles between them. The distance between the groups is measured as 27m. The groups consist of five “*hop couples*” with intra and inter-couple spacings of 4 and 17cm respectively. The output power of nodes is set to -3dBm.

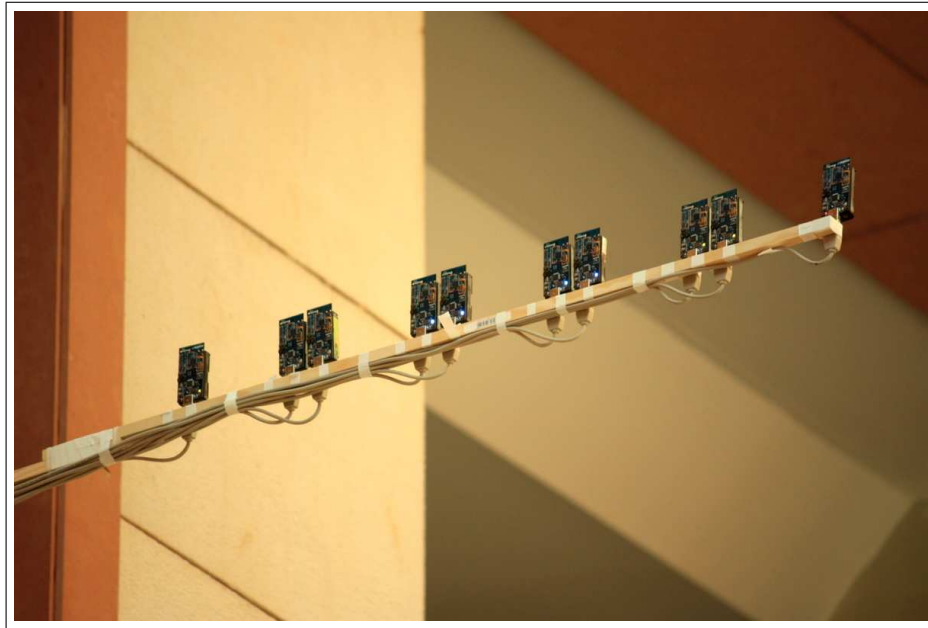


Figure 4.17. Node Group 0

As depicted in Figure 4.18, the sticks attached with the sensors nodes are positioned parallel to each other to complete a hypothetical rectangular area when looked from above. Each group is connected to a base station computer via self-powered USB hubs in order to avoid performance variation due to power differences when run on batteries.

4.3.3.2. Transmission Scheme

The actual image transfer scheme is as follows: A grayscale image of 256×256 size is partitioned into 4×4 macro-blocks at the computer. So, each packet includes 18B of data as 16B macro-block with extra 2B block offset. The packets are sent from the computer to the source node serially via USB links. Then, the source node sends the packets to the sink node over ten hops with best-effort delivery.

Conducting the tests on different time periods and consequently on different diurnal conditions causes dramatic changes in packet loss patterns. The result of a one-day-long transmission test for five hops is given in Figure 4.19 as an example of this situation. As can be seen in this figure, in the afternoon, very low PRRs occur due to the noise induced by the crowd in the atrium, but in the midnight, the PRRs are high.

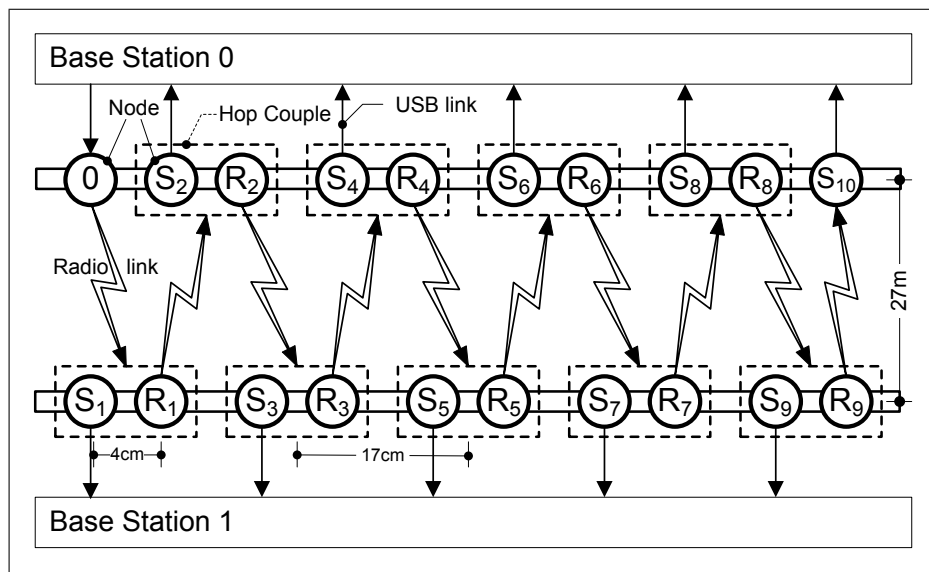
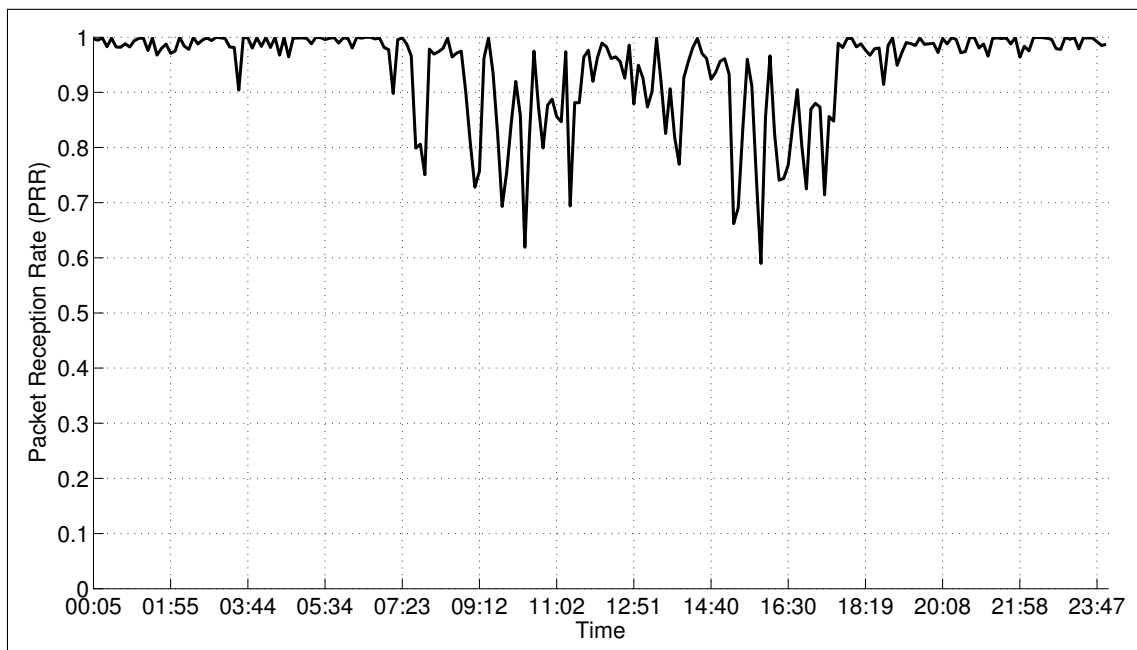


Figure 4.18. Testbed Diagram

Figure 4.19. The result of a one day long test for *five* hops

The preliminary tests had been conducted for each hop individually without using the backchannel at different days so in different channel conditions. Figure 4.20 depicts the PRR results for one, three, five and seven hops. In these tests, it was observed that circumstantially, the PRRs obtained for seven hops ($\mu\text{PRR}=0.92$) are better than five hops ($\mu\text{PRR}=0.83$), while expecting vice versa. The results have revealed that to make hop based comparisons accurately and equitably, it is necessary to get the packet loss patterns occurred in each hop at the same time. To satisfy this concurrency requirement, ten extra *snooping nodes* are used as *backchannel*. By this way, while transferring an image over ten hops, the intermediate results are recorded in each hop by using these snooping nodes. Figure 4.21 depicts the results of an example test in which the results are gathered by the backchannel.

In our image transmission scheme, each hop consists of two nodes called "*hop couple*". They have given the same node ID. In each hop couple, one of the nodes, called relay node (R_i , $i=1, 2 \dots 9$), is used to send the incoming data to the other hop couple with the consecutive node ID via radio link, while the other node, called snooping node (S_i , $i=1, 2 \dots 9$), is used to send the incoming data to the base station computer via USB link. There are only two single nodes numbered with 0 and 10, as the source and the sink node respectively. The base station computers at each side records the image data along with Received Signal Strength Indicator (RSSI) and Link Quality Indicator (LQI) values.

4.3.4. Testbed Results and Analysis

We conducted over 3,000 image transmission tests spreading approximately 15 days. We gathered over 30,000 image loss patterns via 10 hops. The graphs representing the PSNR and PRR relations for NC and EC scheme are given in Figure 4.22 including all the results projected to five different images. As can be seen in Figure 4.22.a, NC scheme is very fragile to channel impairments. The quality of the images dramatically drops even at very high PRRs for a WSN. On the other hand, The EC scheme copes with worse channel conditions robustly. Image quality slowly and linearly decreases from 30-35 dB to 20-25 dB for PRR between 1 to 0.4. Even though the quality expectations would be application specific, received image quality, even when $\text{PRR} = 0.4$, is acceptable for human visual system. The received images at different PRRs are presented as an example in Figure 4.23.

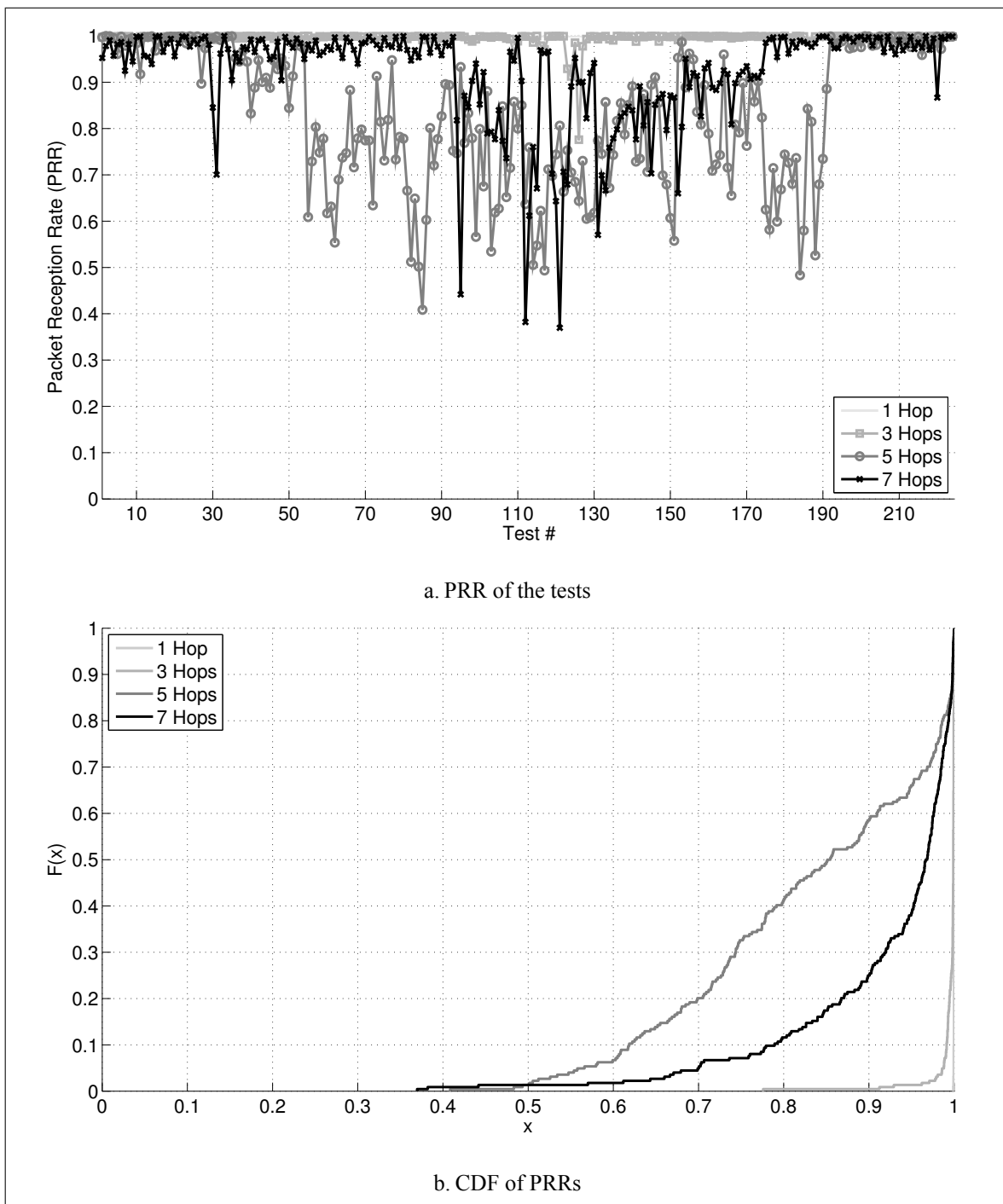


Figure 4.20. Example results for 1,3,5,7 hops tests without using the backchannel

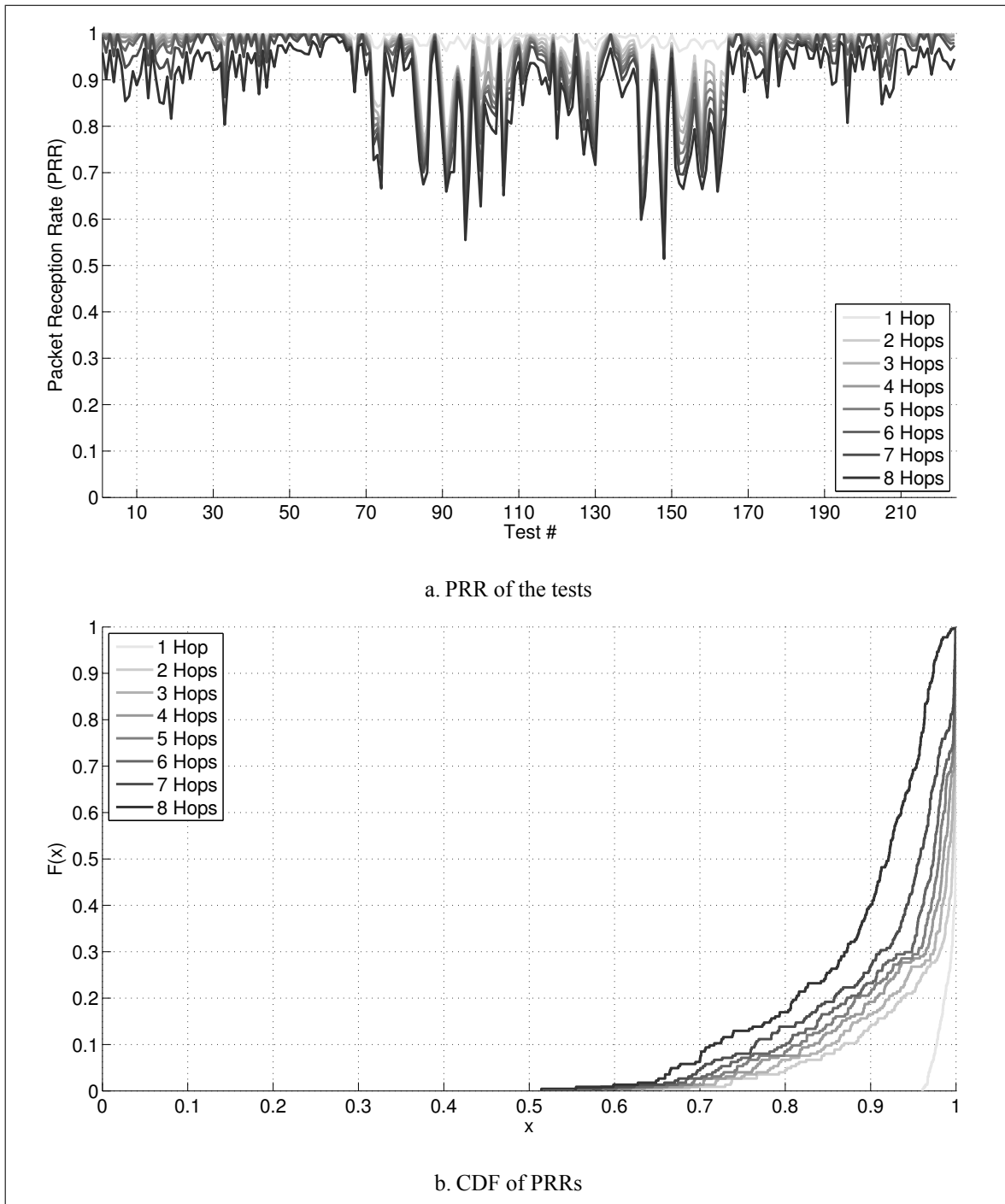


Figure 4.21. The result of a 1-to-8 hops test using the backchannel

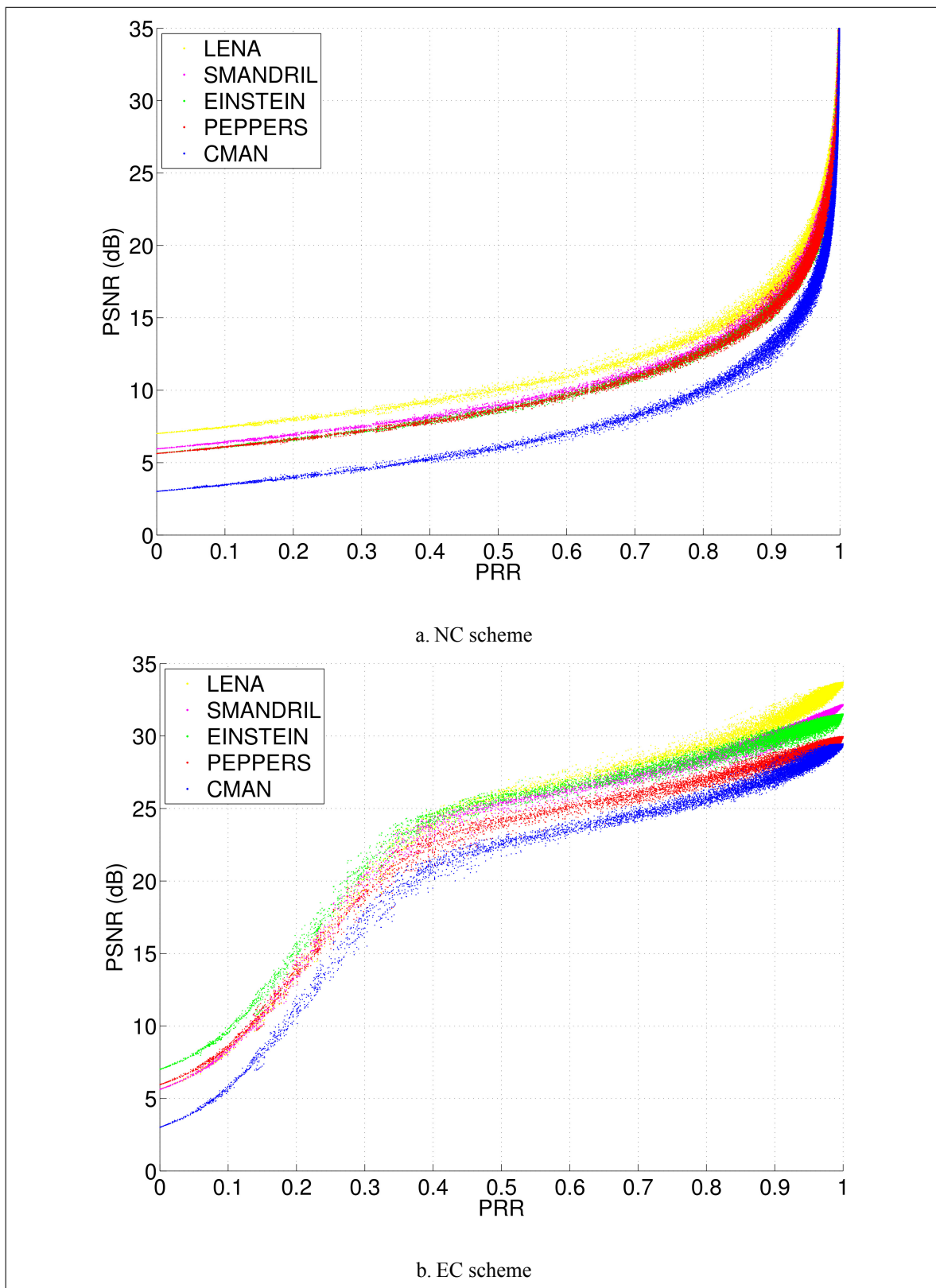


Figure 4.22. Scatter plot of PSNR vs. PRR for each scheme including 30,000 transmissions

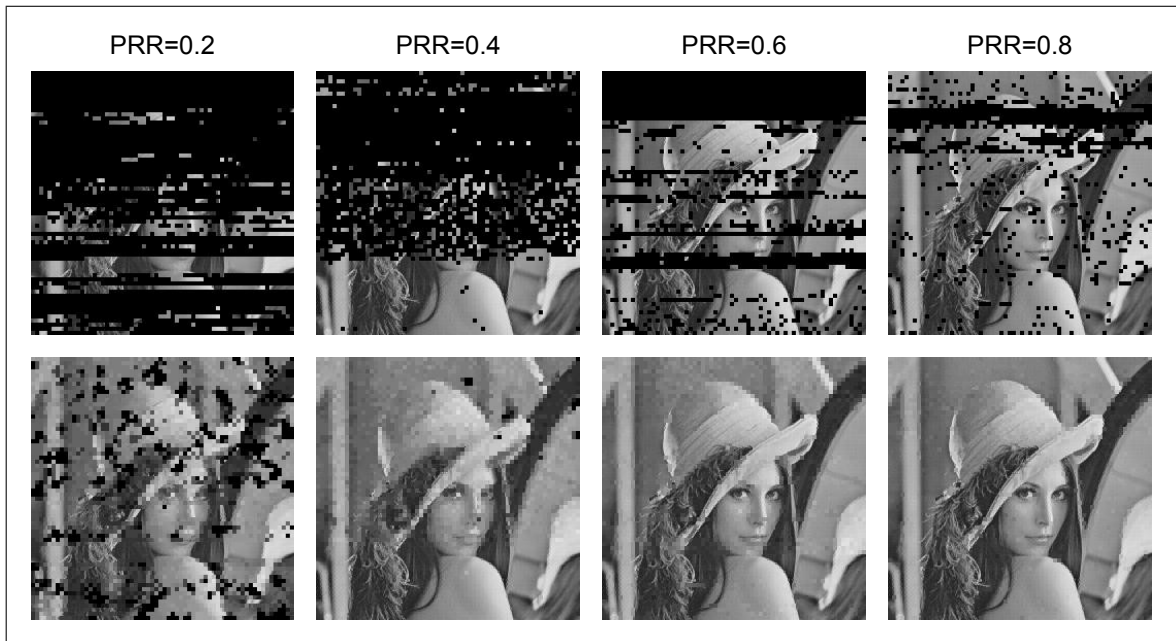


Figure 4.23. The received EC coded images at different PRRs

To evaluate the effect of the number of hops on image transmission for all schemes, one-day-long tests within our result set are used. Only the tests from weekends are used to avoid variance in packet loss patterns due to environmental changes. In the tests, PRRs vary from 0.77 to 1.00. Hop based results are depicted in Figure 4.24. The rapid fall-off in PSNR values is clearly observed in NC scheme. The images transmitted by this scheme cannot go further than six hops within an acceptable quality. As for the EC scheme, when the number of hops is increasing, PSNR values decrease very slowly and almost linearly. Even ten hops later, only 1.2 dB degradation in the received image quality is observed. ECDP scheme is the most successful one with almost no degradation caused by transmission. However, performance gain attained by integrating the EC and disjoint multipath transmission schemes is at most 1.1 dB. Hence, the performance is not profoundly improved by ECDP. The little gain achieved by this scheme is at the expense of additional energy cost.

Average LQI values and corresponding PRRs are also given in Figure 4.25 to figure out the channel conditions throughout our experiments.

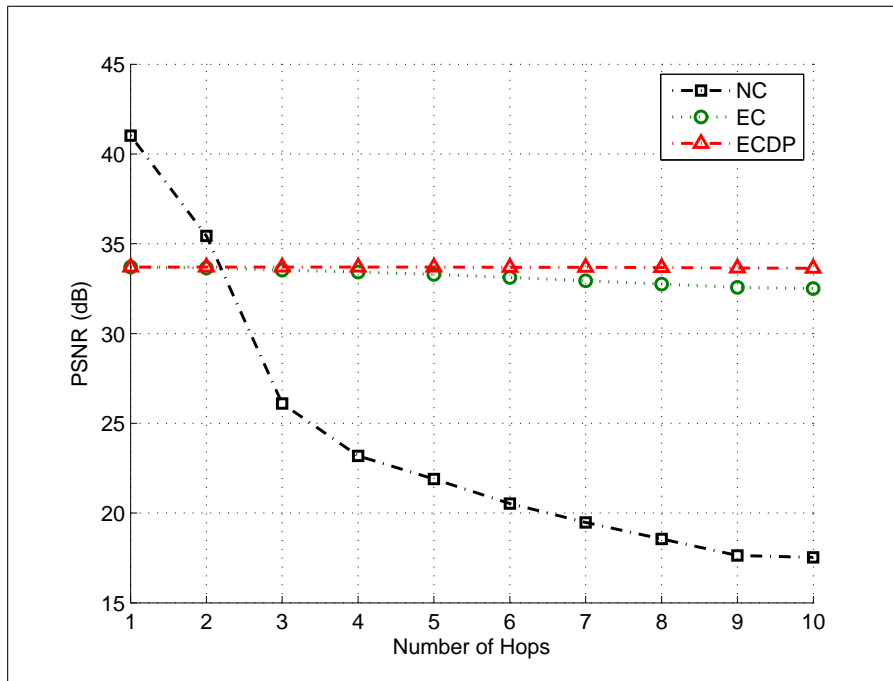


Figure 4.24. PSNR vs. Number of Hops for all schemes

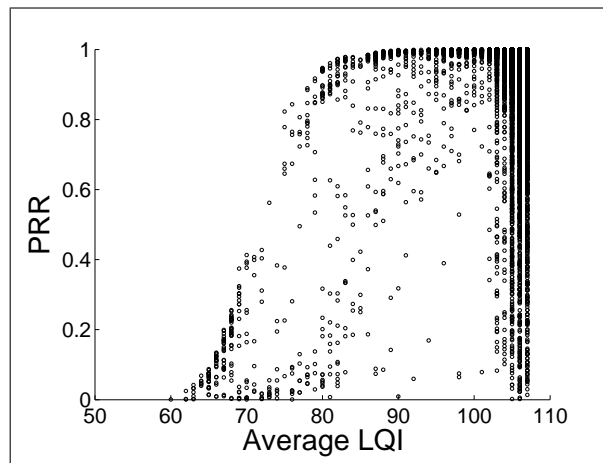


Figure 4.25. PRR vs. Average LQI

4.3.5. Discussion

The performance results attained from the tests, indicate the fragility of raw transmissions. On the contrary, error robustness of the EC algorithm is notable. With this encoding scheme we also avoid delays caused by retransmissions included in reliability mechanisms such as ARQ. We also avoid extra bandwidth required for FEC mechanisms. FEC schemes append extra data to the transmitted packets for error correction. On the contrary, in the EC scheme, the required data for correction embedded into the images. Although, this causes a little degradation in image quality prior to transmission, human visual system can easily tolerate it.

It is necessary to mention that the EC algorithm can be used in multi-tiered systems in which camera nodes have more processing and energy resources. However, by means of the multi-tiered architecture, much simpler intermediate nodes would be used and overall lifetime of the system would be increased. Therefore, the ratio of the camera nodes and the intermediate nodes is determinant to employ the EC algorithm.

4.4. ECPE EVALUATION

ECPE is a good example of a combination of two different coding schemes. This method is applied to the images by coding them with EC and MBPE consecutively. In theory, by applying MBPE over EC, we expect to achieve better image quality, as PSNR values, than using EC scheme alone. To validate this theory, we compare ECPE with the real testbed performance of EC.

4.4.1. Methodology

In order to get the results for ECPE, we use the same test images in MBPE tests. First, employing the EC algorithm on these images, we obtain EC coded images. Second, we follow all the operational steps for MBPE evaluation, declared in Section 4.2.2. Thus, we get the received EC coded images for each measure-image pair. Finally, the received images are reconstructed with the EC algorithm and PSNR values are calculated.

To compare the ECPE results with the previous EC testbed results, we follow these steps for each measure-image pair:

- We get the prioritized packet rates (PPRs) incurred as the result of ECPE. Note that, according to the transmission scheme employed in ECPE tests, PPR is equal to PRR.
- We query the testbed results database for the tests which are five per cent close to the PRR values obtained from the previous step. As a result of the query, we come up with the real image loss patterns. The amount of the patterns changes according to the measure used.
- We attain resulting images by projecting the loss patterns to the image individually. Thus, we have several transmission results for the image.
- We calculate the PSNR of the resulting images and get the mean of them as the result of the measure-image pair.

These operations are illustrated in Figure 4.26. An example image transmitted with both EC and ECDP is also presented in Figure 4.27.

4.4.2. ECPE Results

The results of ECPE scheme for each priority measure in terms of PSNR are shown in Figure 4.28 and Figure 4.29 as two parts. As a success criterion, the PSNR differences for each image are calculated and the means of the PSNR differences for each measure are obtained. In Table 4.4, these values with associated success rates are depicted. Most of the measures are successful in terms of PSNR but delta-entropy. The most successful one is entropy for this scheme with a 18.93 per cent gain in PSNR. Entropy measure succeeds because entropy weighs simply the amount of information included in a dataset; and in EC scheme, the amount of information in a macro-block is increased by embedding the downsized replicas of the image.

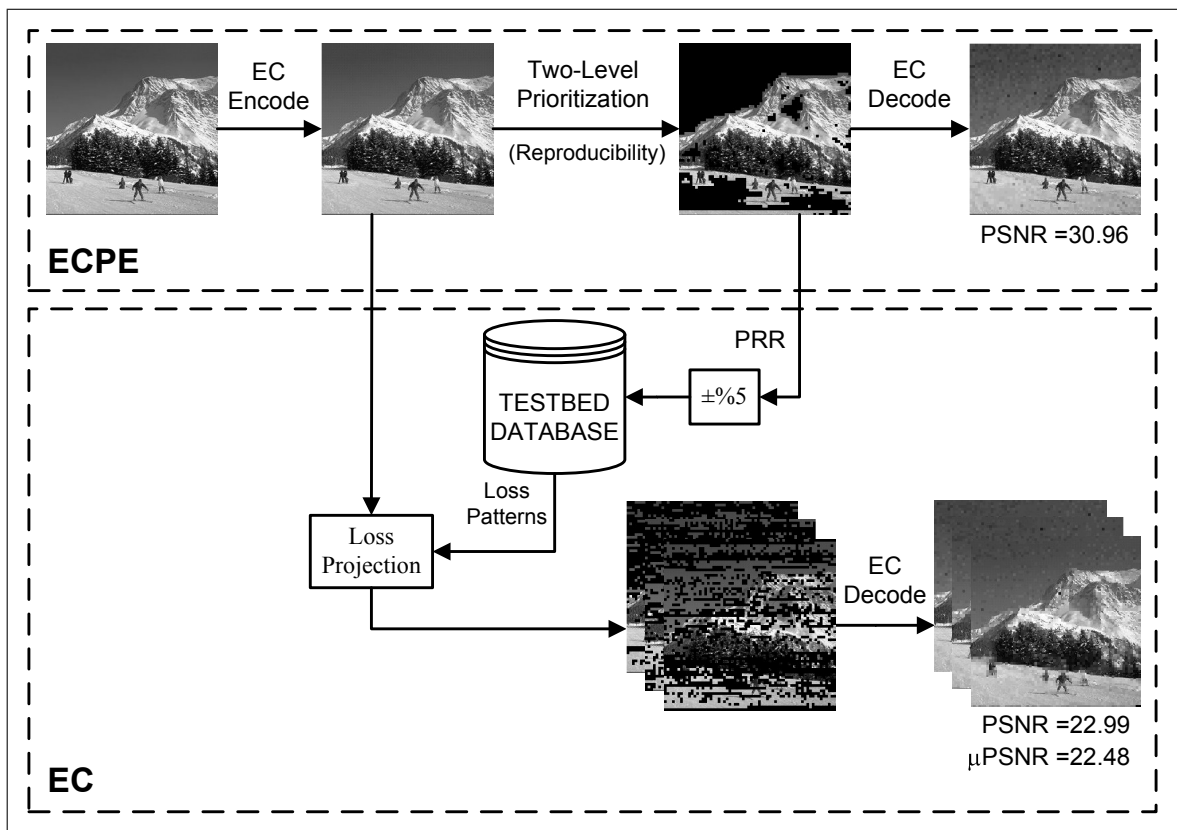


Figure 4.26. Operations to compare ECPE with EC

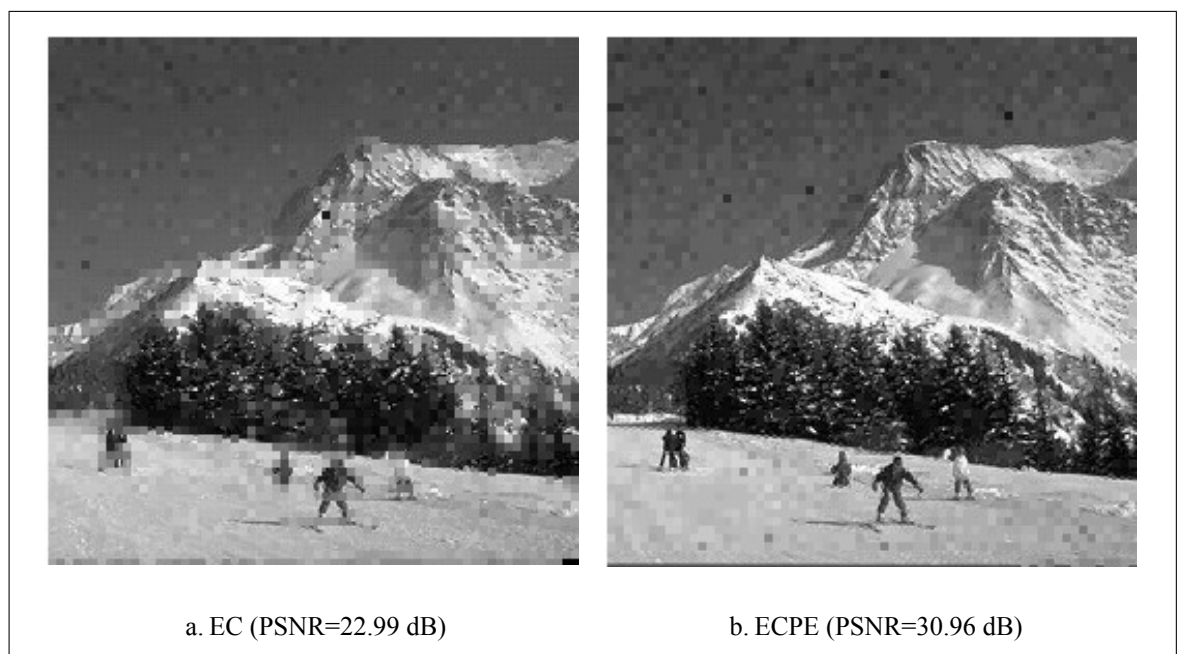


Figure 4.27. EC vs. ECPE

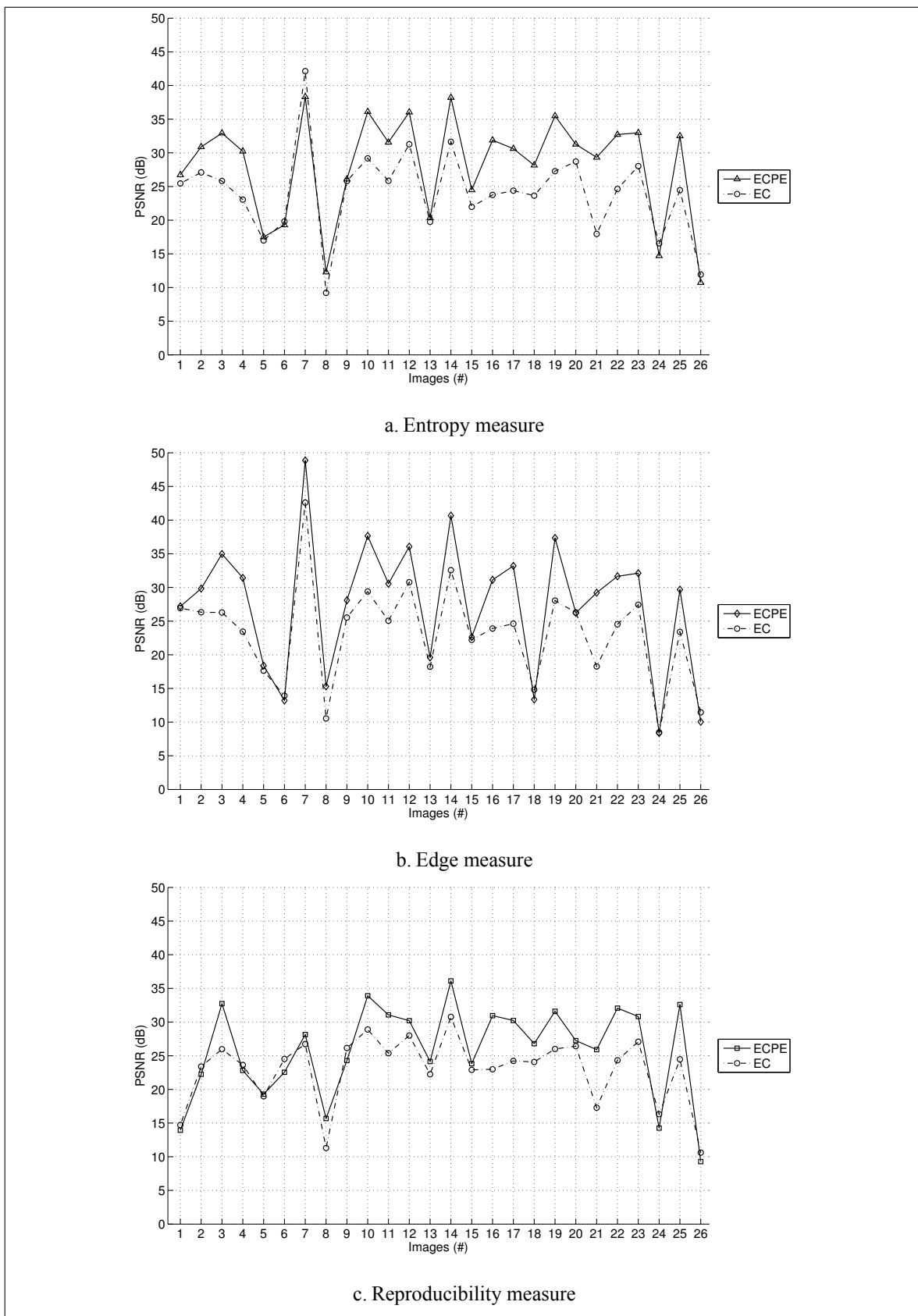


Figure 4.28. PSNR values for all measures, for EC and ECPE schemes (Part 1 of 2)

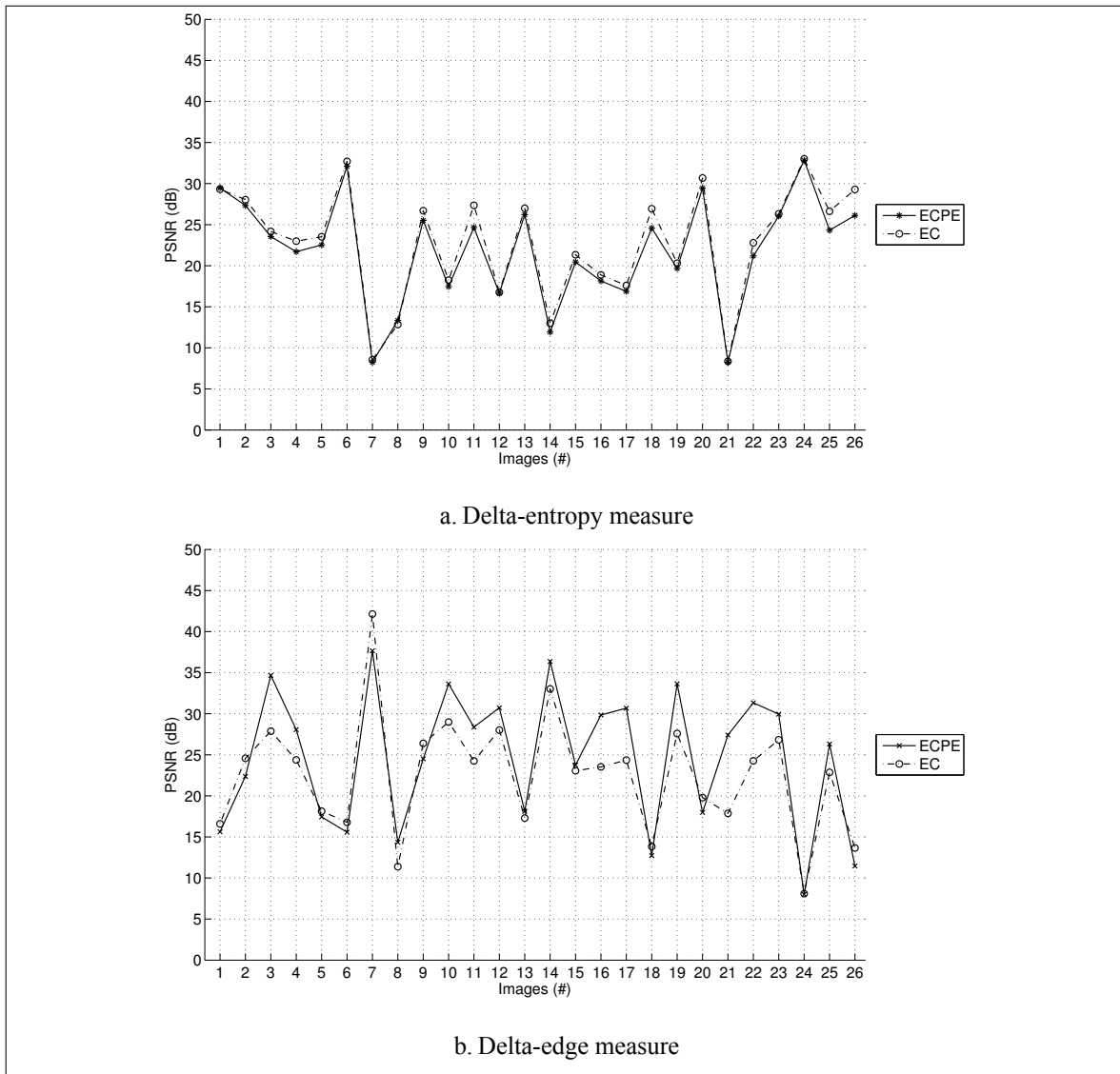


Figure 4.29. PSNR values for all measures, for EC and ECPE schemes (Part 2 of 2)

Table 4.4. ECPE analysis

Measures	$\mu(\Delta PSNR_j)$	Success (%)
Entropy	4.39	18.93
Edge	4.04	16.78
Reproducibility	2.90	12.61
Delta-entropy	-0.95	-4.16
Delta-edge	2.12	9.40

4.4.3. Discussion

In ECPE method, prioritization, erasure code injection and reconstruction are employed together. Utilizing EC over MBPE increases the robustness of important parts of the image. First, the region of interest (ROI) of the application, is extracted simply making use of MBPE. Then, it is transmitted without any reliability mechanisms owing to EC. Thus, the important data survived from source to sink without additional delay and with balanced traffic. It also makes it possible to have an idea about the whole scene. When using this method, the requirement of more computationally capable nodes at the source for EC should be considered.

5. CONCLUSION AND FUTURE WORK

By the addition of multimedia data, the capability and the accuracy of the current applications in WSNs are highly improved along with new applications. Majority of the WMSN applications include still-image transmission, since lots of valuable information can be extracted from images. This thesis mainly focuses on image coding and transmission. With the motivation that the challenges and problems in image transmission can be addressed by natural properties of wireless medium and image data, several proposals are made with their performance evaluations.

A new self-adaptive, priority-based coding scheme (MBPE) is proposed which utilizes a set of novel priority measures on image partitions rather than a full image. The performance of the measures is evaluated in an application scenario based on border surveillance. Hybrid usage of the measures is also analyzed. All performance results are compared with Monte Carlo simulations. All of the measures are implemented on real sensor nodes and their processing cost in CPU cycles are presented. For the performance measurements, a new metric called Object Transmission Rate (OTR) is proposed.

The results show that each measure has achieved better performance than the simulations, except delta-entropy measure. However, the measures have advantages in different respects. Edge measure has minimum memory demand, whereas reproducibility measure requires the least processing time. Delta-edge measure is the most efficient one, since it achieves high OTRs with minimum number of transmitted packets.

This scheme also makes it possible to extract information from the area of interest without acquiring the whole scene. Using MBPE with two-level prioritization, approximately half of the bandwidth is saved; hence, approximately half of the energy consumption of the whole system is reduced. This superior performance is achieved in a much simpler and computationally efficient manner than traditional compression methods.

To examine the effect of real erratic channels on image transmission, a real testbed is

established and the performance of an existing error concealment (EC) algorithm is examined with it. Thousands of image transmissions are realized. In the testbed, an orthogonal backchannel mechanism is employed for gathering the image loss patterns and link qualities occurred in each hop, at the same time. By projecting the patterns to different images, the accuracy of the results is justified. The test results are also stored in a database to make use of for future experiments.

The result of the extensive tests revealed that the EC algorithm is robust to packet losses in WSN. Thus, it removes the delay and additional bandwidth requirements introduced by the reliability and error correction mechanisms i.e. ARQ and FEC. Another advantage of the algorithm is that it does not require additional processes and capabilities at the intermediate nodes. However, the utilization of this algorithm can be possible only by using more capable nodes at the source, because of the complexity of the algorithm. To decrease the computational burden on the source nodes, the algorithm should be optimized and improved.

Hybrid usage of EC with MBPE (ECPE) is also promising. Since, conceptually, both of them are related with different aspects of reconstruction of image data. The result of their synergy is studied in detail by using previously stored real testbed results. The results indicate that some performance gain is attained by employing MBPE over EC. Another hybrid approach may be coupling MBPE with compression algorithms. This can be done in different ways. One of them is to compress only the most prioritized parts of the images. Another way is to adjust the compression parameters according to the priority level.

Another contribution of this work is a new image transmission framework which utilizes MBPE. This framework addresses several problems faced in multimedia transmission such as, delay, delay-jitter, additional bandwidth, congestions caused by streaming data, and QoS support. The transmission mechanism included in it, which is based on the bursty and regulated transmission of large image partitions with prioritization via multiple paths, makes it possible to address the mentioned problems. Another advantage of this framework is scalability in terms of available memory and bandwidth.

Finally, following objectives are accomplished in this thesis. A lightweight coding scheme, which significantly decreases the energy consumption of the network by minimizing the required bandwidth, is devised. The need for computationally more capable nodes at the source is eliminated. A database is created including thousands of real image transmission loss patterns which can be used in future works, instead of unrealistic simulations. Additionally, an image transmission framework considering the shortcomings and needs of WMSN is devised.

There are many works in the literature which are based on prioritization of different entities. The measures proposed for MBPE can be employed in almost any of those works. For instance, it can be easily adopted to packet dropping schemes. In those schemes, relatively low priority packets can be dropped in case of congestion or energy deficiency.

In the proposed MBPE scheme, determination of priority levels and corresponding thresholds is done prior to deployment by statistical methods. However, adaptive determination of them can increase ease of deployment add additional flexibility to applications. This is a highly challenging goal. Interdisciplinary approaches inspired by information theory and image processing will be beneficial.

The proposed image transmission framework should be tailored and evaluated within a real testbed in which cameras suitable for WMSNs are used. A detailed infrastructure for determining link qualities by using the broadcast nature of the medium, and mapping the priority levels to them, should be suggested.

An extensive survey about applicable compression algorithms, accompanied with real tests, will be enlightening. The use of compression algorithms together with our coding and transmission scheme should be examined as a future work.

REFERENCES

1. Akyildiz, I., W. Su, Y. Sankarasubramaniam and E. Cayirci, “Wireless sensor networks: a survey”, *Computer networks*, vol. 38, no. 4, pp. 393–422, 2002.
2. Yick, J., B. Mukherjee and D. Ghosal, “Wireless sensor network survey”, *Computer Networks*, vol. 52, no. 12, pp. 2292–2330, 2008.
3. Gurses, E. and O. Akan, “Multimedia communication in wireless sensor networks”, in *Annales des Télécommunications*, vol. 60, p. 872, Presses Polytechniques Romandes, 2005.
4. Culurciello, E. and A. Andreou, “CMOS image sensors for sensor networks”, *Analog Integrated Circuits and Signal Processing*, vol. 49, no. 1, pp. 39–51, 2006.
5. Akyildiz, I., T. Melodia and K. Chowdhury, “A survey on wireless multimedia sensor networks”, *Computer Networks*, vol. 51, no. 4, pp. 921–960, 2007.
6. Chiasserini, C.-F. and E. Magli, “Energy consumption and image quality in wireless video-surveillance networks”, in *Personal, Indoor and Mobile Radio Communications, 2002. The 13th IEEE International Symposium on*, vol. 5, pp. 2357 – 2361 vol.5, 15-18 2002.
7. Lee, D., H. Kim, M. Rahimi, D. Estrin and J. D. Villasenor, “Energy-efficient image compression for resource-constrained platforms.”, *IEEE transactions on image processing : a publication of the IEEE Signal Processing Society*, vol. 18, no. 9, pp. 2100–13, September 2009.
8. Soro, S. and W. Heinzelman, “A Survey of Visual Sensor Networks”, *Advances in Multimedia*, vol. 2009, pp. 1–22, 2009.
9. Wallace, G., “The JPEG still picture compression standard”, *IEEE Transactions on*

Consumer Electronics, vol. 38, no. 1, 1992.

10. Christopoulos, C., A. Skodras and T. Ebrahimi, “The JPEG2000 still image coding system: an overview”, *IEEE Transactions on Consumer Electronics*, vol. 46, no. 4, pp. 1103–1127, 2000.
11. Pearlman, W., *An embedded wavelet video coder using three-dimensional set partitioning in hierarchical trees (SPIHT)*, IEEE Computer Soc. Press, 1997, ISBN 0-8186-7761-9.
12. Pekhteryev, G., Z. Sahinoglu, P. Orlik and G. Bhatti, “Image transmission over IEEE 802.15.4 and ZigBee networks”, in *Circuits and Systems, 2005. ISCAS 2005. IEEE International Symposium on*, pp. 3539 – 3542 Vol. 4, 23-26 2005.
13. Lin, S. and D. J. Costello, *Error control coding: fundamentals and applications*, Prentice-hall Englewood Cliffs, NJ, 1983.
14. Zorzi, M., “Performance of FEC and ARQ error control in bursty channels under delay constraints”, in *48th IEEE Vehicular Technology Conference, 1998. VTC 98*, vol. 2, 1998.
15. Sarisaray, P., G. Gur, S. Baydere and E. Harmanci, “Performance Comparison of Error Compensation Techniques with Multipath Transmission in Wireless Multimedia Sensor Networks”, *15th International Symposium on Modeling, Analysis, and Simulation of Computer and Telecommunication Systems*, pp. 73–86, October 2007.
16. Zhu, Q. F. and Y. Wang, *Error Control and Concealment for Video Communication*, p. 163, Marcel Dekker, Inc., New York, 1999, ISBN 9780824719289.
17. Sheikh, H., M. Sabir and A. Bovik, “A statistical evaluation of recent full reference image quality assessment algorithms”, *IEEE Transactions on Image Processing*, vol. 15, no. 11, pp. 3440–3451, 2006.
18. Akyildiz, I., T. Melodia and K. Chowdhury, “Wireless Multimedia Sensor Networks:

- Applications and Testbeds”, *Proceedings of the IEEE*, vol. 96, no. 10, pp. 1588–1605, 2008.
19. Polastre, J., R. Szewczyk and D. Culler, “Telos: enabling ultra-low power wireless research”, in *IPSN 2005. Fourth International Symposium on Information Processing in Sensor Networks, 2005.*, vol. 00, pp. 364–369, IEEE, 2005.
 20. Irgan, K., C. Unsalan and S. Baydere, “Priority Encoding of Image Data in Wireless Multimedia Sensor Networks for Border Surveillance”, in *Proceedings of the 25th International Symposium on Computer and Information Sciences (ISCIS)*, Springer, LNCS, 2010.
 21. Gur, G., Y. Altug, E. Anarim and F. Alagoz, “Image error concealment using watermarking with subbands for wireless channels”, *IEEE Communications Letters*, vol. 11, no. 2, pp. 179–181, 2007.
 22. Sarisaray, P., K. Irgan, S. Baydere and E. Harmanci, “Image Quality Estimation in Wireless Multimedia Sensor Networks : An Experimental Study”, in *(under review)*, 2010.
 23. Misra, S., M. Reisslein and G. Xue, “A survey of multimedia streaming in wireless sensor networks”, *IEEE Communications Surveys & Tutorials*, vol. 10, no. 4, pp. 18–39, 2008.
 24. Lu, Q., W. Luo, J. Wang and B. Chen, “Low-complexity and energy efficient image compression scheme for wireless sensor networks”, *Computer Networks*, vol. 52, no. 13, pp. 2594–2603, 2008.
 25. Malvar, H., “Biorthogonal and nonuniform lapped transforms for transform coding with reduced blocking and ringing artifacts”, *IEEE Transactions on Signal Processing*, vol. 46, no. 4, pp. 1043–1053, April 1998.
 26. Chiasserini, C.-F. and E. Magli, “Energy-Efficient Coding and Error Control for

- Wireless Video-Surveillance Networks”, *Telecommunication Systems*, vol. 26, no. 2-4, pp. 369–387, 2004.
27. Xiong, Z., A. Liveris and S. Cheng, “Distributed source coding for sensor networks”, *Signal Processing Magazine, IEEE*, vol. 21, no. 5, pp. 80 – 94, sept. 2004.
 28. Wang, W., D. Peng, H. Wang, H. Sharif and H.-H. Chen, “Energy Efficient Multirate Interaction in Distributed Source Coding and Wireless Sensor Network”, *2007 IEEE Wireless Communications and Networking Conference*, pp. 4091–4095, March 2007.
 29. Xue, Z., K. K. Loo, J. Cosmas and P. Y. Yip, “Distributed Video Coding in Wireless Multimedia Sensor Network for Multimedia Broadcasting”, *Wseas Transactions On Communications*, vol. 7, no. 5, pp. 418–427, 2008.
 30. Wu, M. and C. W. Chen, “Collaborative Image Coding and Transmission over Wireless Sensor Networks”, *EURASIP Journal on Advances in Signal Processing*, vol. 2007, pp. 1–10, 2007.
 31. Girod, B., A. Aaron, S. Rane and D. Rebollo-Monedero, “Distributed video coding”, *Proceedings of the IEEE*, vol. 93, no. 1, pp. 71–83, 2005.
 32. Slepian, D. and J. Wolf, “Noiseless coding of correlated information sources”, *IEEE Transactions on information Theory*, vol. pp, pp. 471–490, 1973.
 33. Wyner, A., “The rate-distortion function for source coding with side information at the decoder”, *Information Theory, IEEE Transactions on*, vol. 22, pp. 1–10, 1976.
 34. Shannon, C., “A mathematical theory of communication”, *ACM SIGMOBILE Mobile Computing and Communications Review*, vol. 5, no. 1, p. 55, 2001.
 35. Wang, Y. and Q. Zhu, “Error control and concealment for video communication: a review”, *Proceedings of the IEEE*, vol. 86, no. 5, pp. 974–997, May 1998.
 36. Gur, G., F. Alagoz and M. AbdelHafez, “A Novel Error Concealment Method for

- Images Using Watermarking in Error-Prone Channels”, in *2005 IEEE 16th International Symposium on Personal, Indoor and Mobile Radio Communications*, pp. 2637–2641, IEEE, 2005.
37. Adsumilli, C., M. Farias, S. Mitra and M. Carli, “A robust error concealment technique using data hiding for image and video transmission over lossy channels”, *IEEE Transactions on Circuits and Systems for Video Technology*, vol. 15, no. 11, pp. 1394–1406, 2005.
 38. Bashiri, D., A. Aghagolzadeh, J. Museviniya and M. Nooshyar, “A novel still image error concealment using fragile watermarking in wireless image transmission and packet-switched networks”, *2008 International Symposium on Telecommunications*, pp. 792–797, August 2008.
 39. Hemami, S., “Digital image coding for robust multimedia transmission”, in *Symposium on Multimedia Communications and Video Coding*, 1995.
 40. Rane, S., J. Remus and G. Sapiro, “Wavelet-domain reconstruction of lost blocks in wireless image transmission and packet-switched networks”, in *Proceedings. International Conference on Image Processing*, pp. I–309–I–312, IEEE, 2002.
 41. Rane, S. D., G. Sapiro and M. Bertalmio, “Structure and texture filling-in of missing image blocks in wireless transmission and compression applications.”, *IEEE transactions on image processing : a publication of the IEEE Signal Processing Society*, vol. 12, no. 3, pp. 296–303, January 2003.
 42. Akkaya, K. and M. Younis, “Energy and QoS aware routing in wireless sensor networks”, *Cluster Computing*, vol. 8, no. 2, pp. 179–188, 2005.
 43. Yuan, Y., Z. Yang, Z. He and J. He, “An integrated energy aware wireless transmission system for QoS provisioning in wireless sensor network”, *Computer Communications*, vol. 29, no. 2, pp. 162–172, 2006.

44. Felemban, E. and E. Ekici, “MMSPEED: multipath Multi-SPEED protocol for QoS guarantee of reliability and. Timeliness in wireless sensor networks”, *IEEE Transactions on Mobile Computing*, vol. 5, no. 6, pp. 738–754, June 2006.
45. Hamid, A., M. M. Alam and C. S. Hong, “Design of a QoS-aware Routing Mechanism for Wireless Multimedia Sensor Networks”, *Communications Society*, pp. 1–6, 2008.
46. Dong, W., Z. Ke, N. Chen and Q. Sun, “QoS Routing Algorithm for Wireless Multimedia Sensor Networks”, in *Proceedings of the 4th International Symposium on Advances in Computation and Intelligence*, pp. 517–524, Springer-Verlag, 2009.
47. Kandris, D., M. Tsagkaropoulos, I. Politis, A. Tzes and S. Kotsopoulos, “A hybrid scheme for video transmission over wireless multimedia sensor networks”, in *Control and Automation, 2009. MED '09. 17th Mediterranean Conference on*, pp. 964 –969, 24-26 2009.
48. Politis, I., M. Tsagkaropoulos, T. Dagiuklas and S. Kotsopoulos, “Power Efficient Video Multipath Transmission over Wireless Multimedia Sensor Networks”, *Mobile Networks and Applications*, pp. 274–284, 2008.
49. Maimour, M., C. Pham and J. Amelot, “Load repartition for congestion control in multimedia wireless sensor networks with multipath routing”, in *Wireless Pervasive Computing, 2008. ISWPC 2008. 3rd International Symposium on*, pp. 11 –15, 7-9 2008.
50. Wu, H. and a. Abouzeid, “Error resilient image transport in wireless sensor networks”, *Computer Networks*, vol. 50, no. 15, pp. 2873–2887, 2006.
51. Albanese, A., J. Blomer, J. Edmonds, M. Luby and M. Sudan, “Priority encoding transmission”, *Information Theory, IEEE Transactions on*, vol. 42, no. 6, pp. 1737 –1744, nov 1996.
52. Zhang, L., M. Hauswirth, L. Shu, Z. Zhou, V. Reynolds and G. Han, “Multi-priority Multi-path Selection for Video Streaming in Wireless Multimedia Sensor Networks”,

- in *Proceedings of the 5th international conference on Ubiquitous Intelligence and Computing*, pp. 439–452, Springer-Verlag, Berlin, Heidelberg, 2008.
53. Lecuire, V., C. Duran-Faundez and N. Krommenacker, “Energy-Efficient Transmission of Wavelet-Based Images in Wireless Sensor Networks”, *EURASIP Journal on Image and Video Processing*, vol. 2007, pp. 1–12, 2007.
 54. Zilan, R., J. M. Barceló-Ordinas and B. Tavli, “Image Recognition Traffic Patterns for Wireless Multimedia Sensor Networks”, pp. 49–59, Springer-Verlag, 2008.
 55. Rahimi, M., R. Baer, O. Iroezi, J. Garcia, J. Warrior, D. Estrin and M. Srivastava, “Cyclops: in situ image sensing and interpretation in wireless sensor networks”, in *Proceedings of the 3rd international conference on Embedded networked sensor systems*, p. 204, ACM, 2005.
 56. Boice, J., X. Lu, C. Margi, G. Stanek, G. Zhang, R. Manduchi and K. Obraczka, “Meerkats: A power-aware, self-managing wireless camera network for wide area monitoring”, in *Workshop on Distributed Smart Cameras (DSC 2006)*, Boulder, CO, pp. 1–13, Citeseer, 2006.
 57. Culurciello, E. and A. G. Andreou, “CMOS image sensors for sensor networks”, *Analog Integrated Circuits and Signal Processing*, vol. 49, no. 1, pp. 39–51, June 2006.
 58. Park, C. and P. H. Chou, “eCAM: ultra compact, high data-rate wireless sensor node with a miniature camera”, in *Proceedings of the 4th international conference on Embedded networked sensor systems*, SenSys '06, pp. 359–360, ACM, New York, NY, USA, 2006.
 59. Rowe, A., A. Goode, D. Goel and I. Nourbakhsh, “CMUcam3: an open programmable embedded vision sensor”, Tech. Rep. CMU-RI-TR-07-13, Robotics Institute, Carnegie Mellon University, 2007.
 60. Ferrigno, L., S. Marano, V. Paciello and A. Pietrosanto, “Balancing computational and transmission power consumption in wireless image sensor networks”, in *Virtual*

- Environments, Human-Computer Interfaces and Measurement Systems, 2005. VECIMS 2005. Proceedings of the 2005 IEEE International Conference on*, pp. 61–66, 2005.
61. Simoncelli, E., “Translation Insensitive Image Similarity in Complex Wavelet Domain”, in *Proceedings. (ICASSP '05). IEEE International Conference on Acoustics, Speech, and Signal Processing, 2005.*, vol. X, pp. 573–576, IEEE, 2005.
 62. Dosselmann, R. and X. D. Yang, “Existing and emerging image quality metrics”, in *Electrical and Computer Engineering, 2005. Canadian Conference on*, pp. 1906 –1913, 1-4 2005.
 63. Martínez-Rach, M. O., O. López, P. Piñol, M. P. Malumbres, J. Oliver and C. T. Calafate, “Quality assessment metrics vs. PSNR under packet loss scenarios in manet wireless networks”, in *Proceedings of the international workshop on Workshop on mobile video - MV '07*, p. 31, ACM Press, New York, New York, USA, 2007.
 64. Wang, Z., A. C. Bovik, H. R. Sheikh and E. P. Simoncelli, “Image quality assessment: from error visibility to structural similarity.”, *IEEE transactions on image processing : a publication of the IEEE Signal Processing Society*, vol. 13, no. 4, pp. 600–12, April 2004.
 65. Engelke, U., M. Kusuma, H.-J. Zepernick and M. Caldera, “Reduced-reference metric design for objective perceptual quality assessment in wireless imaging”, *Signal Processing: Image Communication*, vol. 24, no. 7, pp. 525–547, 2009.
 66. Li, X., “Blind image quality assessment”, *Proceedings. International Conference on Image Processing*, pp. I-449–I-452, 2002.
 67. Caviedes, J. and S. Gurbuz, “No-reference sharpness metric based on local edge kurtosis”, in *Proc. of IEEE Int. Conf. on Image Processing*, vol. 3, pp. 53–56, 2002.
 68. Wang, Z. and E. Simoncelli, “Reduced-reference image quality assessment using a wavelet-domain natural image statistic model”, in *Proc. of SPIE Human Vision and*

- Electronic Imaging*, vol. 5666, pp. 149–159, SPIE, San Jose, CA, 2005.
69. Wang, Z., G. Wu, H. R. Sheikh, E. P. Simoncelli, E.-H. Yang and A. C. Bovik, “Quality-aware images.”, *IEEE transactions on image processing : a publication of the IEEE Signal Processing Society*, vol. 15, no. 6, pp. 1680–9, June 2006.
 70. Eskicioglu, A. and P. Fisher, “Image quality measures and their performance”, *IEEE Transactions on Communications*, vol. 43, no. 12, pp. 2959–2965, 1995.
 71. Avcıbaşı, I., B. Sankur and K. Sayood, “Statistical evaluation of image quality measures”, *Journal of Electronic Imaging*, vol. 11, no. 2, p. 206, 2002.
 72. de Freitas Zampolo, R. and R. Seara, “A comparison of image quality metric performances under practical conditions”, in *IEEE International Conference on Image Processing, 2005. ICIP 2005*, vol. 3, 2005.
 73. Miyahara, M., K. Kotani and V. Algazi, “Objective picture quality scale (PQS) for image coding”, *Communications, IEEE Transactions on*, vol. 46, no. 9, pp. 1215 –1226, sep 1998.
 74. Yaghmaee, M. H. and D. A. Adjeroh, “Priority-based rate control for service differentiation and congestion control in wireless multimedia sensor networks”, *Computer Networks*, vol. 53, no. 11, pp. 1798–1811, 2009.
 75. Lathi, B., *Modern digital and analog communication systems*, Oxford University Press, 4. edn., 1995.
 76. Sonka, M., V. Hlavac and R. Boyle, *Image Processing, Analysis and Machine Vision*, CL Engineering, 3. edn., 2007.
 77. Ballester, C., M. Bertalmio, V. Caselles, G. Sapiro and J. Verdera, “Filling-In by Joint Interpolation of Vector Fields and Gray Levels”, *IEEE Transactions on Image Processing*, pp. 1200–1211, 2001.

78. Kundur, D. and D. Hatzinakos, “Digital watermarking for telltale tamper proofing and authentication”, *Proceedings of the IEEE*, vol. 87, no. 7, pp. 1167–1180, July 1999.
79. Kundur, D. and D. Hatzinakos, “Toward Robust Logo Watermarking Using Multiresolution Image Fusion Principles”, *IEEE Transactions on Multimedia*, vol. 6, no. 1, pp. 185–198, February 2004.
80. PASCAL NoE, *The PASCAL Object Recognition Database Collection*, http://pascallin.ecs.soton.ac.uk/challenges/VOC/databases.html\#VOC2005_1, 2010.
81. Olivia, A. and A. Torralba, “Modeling the shape of the scene: a holistic representation of the spatial envelope”, *Int. Journal of Computer Vision*, vol. 42, pp. 145–175, 2001.
82. U.C. Berkeley EECS Department, *TinyOS: An operating system for sensor networks.*, <http://www.tinyos.net/>.